Isotopic Signatures of Precipitation and Streams along the North Shore of Lake Superior

A Thesis
SUBMITTED TO THE FACULTY OF THE
UNIVERSITY OF MINNESOTA
BY

Kinzey Stoll

IN PARTIAL FULFILLMENT OF THE REQUIREMENTS
FOR THE DEGREE OF
MASTER OF SCIENCE

Dr. Salli Dymond

June 2019

ACKNOWLEDGEMENTS

This project would not have been possible without professors Dr. Salli Dymond and Dr. John Swenson. Dr. Salli Dymond provided support and feedback consistently throughout the project. She was actively involved with planning, field work, data analysis, and editing. Dr. John Swenson worked actively on planning and data analysis as well as providing useful feedback for the direction of the project.

I would like to thank the Minnesota Pollution Control Agency (MPCA), specifically Jenny Jasperson, for technical guidance of the project and field equipment support providing temperature loggers for the stream. Jenny was influential in the initial planning and implementation of the field work done to complete this project.

I would like to thank Julia Halbur for her help working the Picarro L2130-i cavity ring down mass spectrometer at UMD-LLO. Peter Bouchard for help in the field over the summer of 2018. He helped provide support, entertainment, and an extra set of hands for data collection. I would also like to thank the other member of Dr. Dymond's lab: Hannah Behar, Emma Burgeson, and Shelby Hammerschmidt. These women helped to discuss scientific concepts related to the project to increase understanding and to help with communication.

Finally, I would like to thank my roommates and friends in Duluth for being supportive through the process. I would like to specifically thank Zorina Anderson for field support when possible. I would like to thank my family for their constant support and love through the process as well. Despite living in a different state, they have believed in my abilities and helped me to stay confident in my project.

Table of Contents

List of Tables

List of Figures

Chapter 1: Introduction

The Great Lakes Region covers 245,000 km^2 in east-central North America and consists of five of the earth's largest freshwater lakes: Superior, Huron, Erie, Michigan, and Ontario. The lakes contain 80% of the continent's freshwater yet cover only 1% of the total landmass (Jasechko et al., 2014). The largest of the Great Lakes, Lake Superior, is surrounded by landscapes and soils that have been heavily influenced by regional glaciations along with geology from periods of volcanic activity (Sims, et al., 1972). Interlayered volcanic, sedimentary, and metamorphic rocks are found along the shores. Volcanic rocks in the region include basalts, gabbros, diabases, anorthosites, granites, and rhyolites. Many of these volcanic rocks have been transformed into metamorphic rocks, mostly greenstone. Sedimentary rocks include sandstones, shales, and conglomerates known for their distinct red color (Van Hise and Leith, 1909; Minnesota Department of Natural Resources, 2018). The terrain in the region comes from the failed-rift system which eroded over time via weather and glaciers. The glaciers influenced regional topography by leaving behind tills, moraines, drumlins, eskers, lakes, and rivers. One glacial moraine runs parallel to the northern shore of Lake Superior, creating a steep change in topography. On top of this moraine and the surrounding region lies till consisting of clays and sands left behind by glaciers. These relatively thin soils are classified as Orthents, Ochrepts, and Boralfs (Minnesota Department of Natural Resources, 2018). The climate of the region is considered humid continental climate (Arnfield, 2019). Vegetation in the region includes eastern white pine (Pinus strobus L.), red pine (Pinus resinosa Aiton), jack pine (Pinus banksiana Lamb.), balsam fir (Abies balsamea (L.) Mill.), white spruce (Picea glauca Moench), quaking and bigtooth aspen

(Populus tremuloides Michx. and Populus granidentata Michx., respectively), and paper birch (Betula papyrifera Marsh.). It is ecologically classified as the Laurentian Mixed Forest Province by the Minnesota Department of Natural Resources (2018).

Lake Superior covers 33% of the Great Lakes Region (82,000 km^2) and impacts the precipitation and temperature regimes of the surrounding coastal landmass (Jasechko, et al., 2014). The land closest to the lake remains warmer in the winter and colder in the summer. The temperature of the air has been shown to change by as much as 6°C when moving 50 km inland along the northern shore (Scott and Huff, 1996). One of the most notable effects of Lake Superior on precipitation patterns is Lake-Effect Snow (LES). LES forms when a cold air mass moves over a lake, collects warm moisture from the surface, and precipitates out upon reaching land. While both the north and south shores of Lake Superior can experience LES, the downwind side often receives more (Neff and Nicholas, 2005). This has been shown in other lakes in the Great Lakes region, including areas in New York and Michigan (Burnett, et al, 2003; Burnett, et al, 2004).

Precipitation is a major input into the lake systems, whether through overland flow, streamflow, or direct interception via the lake surface (Neff and Nicholas, 2005). Lake Superior has four major source areas for precipitation: the Gulf of Mexico, Pacific Ocean, Arctic regions, and the Atlantic Seashore (Gat, et al, 1994). Each source area produces different types of storms, some of which are impacted by the lake more than others. Using the isotopic values of hydrogen and oxygen, scientists have traced precipitation through the water cycle into groundwater, streamflow, and lakes (Dansgaard, 1964). Jasechko, et al. (2014) studied the isotopic signature of each of the Great Lakes and compared the values to the Global Meteoric Water Line (GMWL). Their

results plotted away from the line, which they attributed as the effects of evaporation and the new inputs of precipitation and runoff into the lakes. Stable isotopes have also been used to study the interaction of groundwater and streams. Sklash and Farvolden (1979) studied two watersheds in Canada and, by examining isotopic values, showed groundwater as a major component of streamflow following snowmelt and storm runoff events. While the fate of precipitation after it falls differs for each catchment, isotopes have been shown to be a successful tracer of environmental processes such as evaporation, sublimation, and runoff (Klaus and McDonnell, 2013). Comparing regional isotopes to global standards elucidates underlying mechanics of hydrological processes in a region, such as the importance and magnitude of groundwater recharge and evaporation (Gat, et al., 1994; Massone, et al., 2016).

While isotopic patterns of precipitation in the Great Lakes region have been well-studied (Bowen, et al., 2012; Burnett, et al, 2003; Burnett, et al, 2004; Jasechko, et al., 2014; Neff and Nicholas, 2005), less work on isotopes has been conducted specifically around Lake Superior. Kendall and Coplen (2001) studied the isotopic signatures of rivers across the United States. The rivers around the Great Lakes had a heavier isotopic signature than expected, but the north shore of Lake Superior lacked enough sampling locations to provide good resolution. They interpreted the differences in signatures to be connected to the mixing of evaporated waters from the lakes with atmospheric waters (Kendall and Coplen, 2001). Thus, this study investigates the isotopic signatures found in precipitation and streams along the north shore of Lake Superior. Snow samples were collected over the course of one winter and stream samples were collected monthly across five watersheds along the north shore. The Lester River Watershed, which is

located closest to Duluth, MN, was studied further for more spatial and temporal information. Klaus and McDonnell's (2013) research suggest that collecting higher frequency of samples spatially and temporally can remove gaps in isotopic data, especially for studies utilizing hydrograph separation. Knowing the isotopic signatures in the streams and precipitation around Lake Superior will help future research focused on tracing the precipitation through overland flow into the lake itself or via groundwater recharge.

Chapter 2: Background

Isotopes

Stable isotopes of water (i.e., oxygen and hydrogen) can be used to track its movement through the hydrologic cycle. To do this, the rarer form of each element is compared to its more common form. For oxygen, the common isotope is ^{16}O and the rarer forms are either ^{17}O or ^{18}O. For hydrogen, the rare forms are ^{2}H, also known as deuterium or D, and ^{3}H, also known as tritium. The common forms of both elements comprise roughly 99% of the total isotope abundance, with the rarer forms make up the remaining 1%. Because it is challenging to determine absolute abundance of each isotope, values are reported as relative abundance using the ratio of rare to common isotopes. Furthermore, isotope ratios of water samples are then compared to a global standard for water, known as the Vienna Standard Mean Ocean Water (VSMOW). VSMOW values are created and maintained by the International Atomic Energy Agency (IAEA). For hydrogen, the abundance ratio of $^{2}H/^{1}H$ is 1.5575×10^{-4}. For oxygen, the abundance ratio of $^{18}O/^{16}O$ is 2.0052×10^{-3} (Clark and Fritz, 1997; Kendall and McDonnell, 1998).

The variations of isotopes within a system can be used to better understand the movement and storage of water across landscapes. Water samples collected from one location in the form of rain, snow, streamflow, groundwater, etc. are compared to the international standard (VSMOW) using the following equation:

$$\delta\ ^{18}O_{sample} = ((^{18}O/^{16}O)_{sample}/((^{18}O/^{16}O)_{reference})-1) * 1000\ ^{0}/_{00} \quad \text{(Eqn. 1)}$$

where the sample indicates a sample of water from a known location and the reference is VSMOW or a similar known standard. Equation 1 reports values in “delta notation”, where delta values are presented in parts per thousand, per mil ($^{0}/_{00}$).

Water isotopes are sensitive to changes in climatic conditions, especially changes in temperatures that result in phase changes. The oceans contain a uniform isotopic signature with variations found near the poles or other large masses of ice and cold water. This is different from isotopic signatures of freshwaters. Research on the isotopic signatures of freshwaters depend on the history of a region and incoming sources which have been found to have a wide range of $\delta^{18}O$ and $\delta^{2}H$ (Dansgaard, 1964; Epstein and Mayeda, 1953). The isotopic signature of a freshwater sample at a particular point is also influenced by amount, altitude, continental, and latitude effects (Dansgaard, 1964; Kendall and McDonnell, 1998). The amount effect refers to the amount of precipitation or rain that a specific area receives, which is impacted by the amount of regional evaporation that occurs. More rain in a region generally produces lower δ values, while less rain results in higher δ values (Dansgaard,1964). Altitude effect relates to changes in the isotopic signature as rainout occurs over changing altitudes. Higher altitudes with cooler temperatures tend to have lighter isotopic signatures in precipitation, as rain has already precipitated and the subsequent air mass is depleted (Clark and Fritz, 1997: Kendall and McDonnell, 1998). Snowmelt isotopes were studied in a catchment with altitudes ranging from 6300 to 1300 masl across 20 km. Their results showed higher altitude samples to be lighter in $\delta^{2}H$ and the lower altitude samples to be heavier in $\delta^{2}H$ (Massone, et al., 2016). The continental effect is driven by latitudes and temperatures and results from clouds moving across large land masses. The farther a cloud is from its point of formation, the lighter the isotopic signature of the precipitation will be. Coastal regions receiving rain first will have heavier isotopic signatures than inland regions. Lastly, the latitude effect shows that increases in latitude are linked to decreasing (lighter) δ values-

the poles thus are the lightest and equatorial regions have heavier values (Jouzel et al., 2013). This arises because colder temperatures result in increased fractionation at higher latitudes (Clark and Fritz, 1997; Kendall and McDonnell, 1998).

Evaporation and condensation processes lead to variations of isotopes found in clouds and precipitation. The mass ratio between ^{2}H and ^{1}H is greater than the mass ratio between ^{16}O and ^{18}O. Because of this, each element fractionates at different speeds, with hydrogen atoms being able to move between phases with less energy required. Under non-equilibrium conditions, water vapor contains more ^{2}H than ^{18}O, resulting in excess ^{2}H (deuterium) to be found and leading to what is known as a deuterium -excess (*d*-excess) present in precipitation. The global average of $\delta^{2}H$ found in precipitation is $10^{0}/_{00,}$ but this varies regionally due to changes in humidity, wind speed, and sea surface temperatures. Global d-excess generally ranges between $0^{0}/_{00}$ and $20^{0}/_{00,}$ where anything above $10^{0}/_{00}$ is from enhanced moisture recycling and anything below $10^{0}/_{00}$ is from enhanced evaporative loss (Clark and Fritz, 1997; Kendall and McDonnell, 1998; Frohlich, et al., 2001).

The relationship between hydrogen and oxygen isotopes in global precipitation have been shown to vary systematically in a linear fashion along a Global Meteoric Water Line (Eqn. 2) (Rozanski, et al., 1993):

$$\delta\ ^{2}H=8*\ \delta^{18}O + 10 \qquad \text{(Eqn. 2)}$$

where $\delta^{2}H$ and $\delta^{18}O$ are values from the same sample of water given in $^{0}/_{00}$. Comparing a water sample to the GMWL reveals trends in evaporation or condensation and can provide insight into the hydrological processes that partition precipitation into streams or groundwater (Brooks, et al, 2013; Clark and Fritz, 1997; Kendall and McDonnell, 1998).

Deviations from the GMWL can be used to show the local patterns of a region forming the Local Meteoric Water Line (LMWL) and Local Evaporation Line (LEL). A LMWL is formed by fitting a linear regression to precipitation data collected in a specific region. A LEL is formed by fitting a linear regression to data from surface waters that plot below the GMWL (Figure 2-1). When discussing isotopic data, four terminologies are common: enriched vs. depleted, heavier vs. lighter, higher vs. lower, and more/less positive vs. more/less negative (Kendall and McDonnell, 1998).

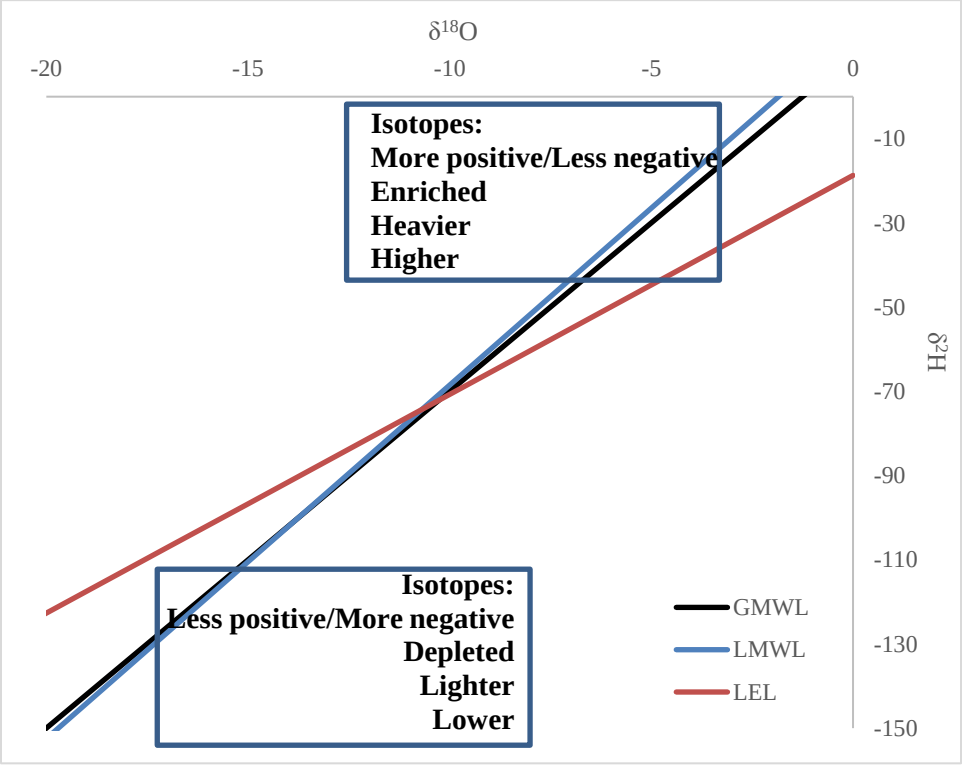

Figure 2-1) Plot of the GMWL (Rozanski, et al., 1993) and the LMWL and LEL for Lake Superior (Jasperson, et al., 2018).

Snow Hydrology

Water stored in a snowpack can provide hydropower, drinking water, and irrigation for downstream regions but natural variation in snowpack depth can also lead

to droughts and floods. The storage and release of winter snowpack water is increasingly important given climate change projections (Schmieder, et al, 2016). Lake Superior receives substantial amounts of snow on the north shore (7.5-10 cm) and the south shore (greater than 20 cm) annually (Scott and Huff, 1996). Freezing, refreezing, rain-on-snow events, wind redistribution, and melting will change the isotopic signature of a snowpack from its initial signature (Ala-aho, et al., 2017; DeWalle and Rango, 2011; Jouzel, et al., 2013). The melting and refreezing of a snowpack homogenize the isotopic signature, resulting in a combined signal of all the snowstorms that have fallen throughout the winter (Ala-aho, et al., 2017; Zhou, et al., 2008). Such melting and refreezing can occur within the snowpack and fluctuate on microscopic to macroscopic scales that vary in space and time (Schweizer, et al., 2008). In a study investigating the effects of refreezing snow on isotopic signatures in the liquid and solid phase, it was found that isotopic fractionation occurs between the liquid-solid phase changes (Zhou, et al., 2008). Microscopic changes within a snowpack include sublimation, melting, and the movement of meltwater laterally or vertically through the snowpack. Macroscopic changes across a snowpack include variability in the distribution of snow across a landscape due to topography, wind, temperature, shelter, and snowstorm duration and trajectory. Understanding the complexity and variability of snowpack dynamics is critical for identifying weak layers which can trigger avalanches (Schweizer, et al., 2008; DeWalle and Rango, 2011) and in determining spring floods (Zhou, et al., 2008). The complications of metamorphism within the snowpack leads some research on snow isotopes to be addressed through models (Ala-aho, et al., 2017; Jouzel, et al., 2013).

Snow is isotopically lighter than rainfall due to the colder temperatures at which it forms (Dansgaard, 1964; Ala-aho, et al., 2017). Each snowfall event is isotopically different owing to the combined amount, altitude, continental, and latitude effects (Ala-aho, et al., 2017). In Argentina, variations in snow isotope values occur over years and through different sampling techniques from snow core, snowpack, and composite samples. Snowmelt in the region was connected to downstream recharge and the high-altitude headwaters were concentrated with the majority of snowmelt in the catchment (Massone, et al., 2016).

Sublimation removes lighter isotopes from the surface of a snowpack, resulting in a heavier snowpack during the time of snowmelt (Ala-aho, et al., 2017). The effects of sublimation occur within the top seven cm of a snowpack and depend upon temperature, relative humidity, and wind speed (Zhou, et al., 2008). In forested systems, interception of snowfall by the canopy can impact the isotopic signature of the snowpack, as trees can hold large amounts of snow via canopy interception. Intercepted snow is altered by sublimation before falling into the snowpack, therefore snow found underneath the canopy may not represent the original isotopic signature of the storm. (Ala-aho, et al., 2017; DeWalle and Rango, 2011). Variations are found in the isotopic signature of snowmelt as well, often leading to difficulties separating streamflow and spring floods on hydrographs (Zhou, et al., 2008). The isotopic signature of snow on north and south facing slopes can also vary during the snowmelt season due to the differences in insolation and timing of melt (Schmieder, et al., 2016).

The region around Lake Superior is subject to a variety of winter storms, most notably Lake-Effect Snow (LES) from November through February (Kunkel, et al, 2000).

LES occurs when cold air masses move over warm, open waters of a lake, resulting in convection due to temperature differences (Wright, et al., 2013). The added moisture to the clouds precipitates out shortly after the air mass reaches land. LES is felt most heavily on the downwind side of the lake (Scott and Huff, 1996; Wright, et al., 2013). The strength of LES is related to lake-air temperature differences, wind speed, wind direction, fetch, air temperatures, ice-surface coverage, and residence times of the air mass over the lake (Kunkel, et al, 2000; Wright, et al., 2013). Two other types of storms produce snowfall around Lake Superior: Alberta Clippers and Colorado Lows or Panhandle Hooks. An Alberta Clipper is a low-pressure system moving across Canada and the Great Lakes Region towards the southeast. Generally, these storms come from the Arctic Ocean and bring colder temperatures, strong winds, and shallower snows (5-10 cm) (NWS, 2018). Colorado Lows or Panhandle Hooks are low-pressure systems that originate in the central plains region of the United States. Their source waters come from the Pacific Ocean along the west coast and sometimes moisture from the Gulf of Mexico as they move towards the northeast. These storms produce deeper snowfalls (12-15 cm) (NWS, 2018).

Hydrograph Separation

Hydrographs graphically display the changes in discharge of a watershed over time, thereby showing a stream's response to snowmelt and rainfall (Brooks, et al, 2013; Clark and Fritz, 1997). Information from hydrographs can deepen knowledge regarding the recharge and storage of a watershed and assist with reservoir routing and hydrologic planning (Clark and Fritz, 1997). The two main components often noted in a hydrograph

are baseflow and stormflow. The baseflow is considered groundwater or other subsurface water present in the watershed used to sustain the streamflow during long periods of time without rainfall or snowmelt. Stormflow is water entering a stream following snowmelt or rainfall events. Three main pathways by which precipitation can become stormflow include channel interception, overland flow, and shallow subsurface flow. Channel interception is precipitation falling directly onto the stream channel. Overland flow, or runoff, occurs either when rainfall intensity exceeds infiltration rates or when the ground is saturated. Shallow subsurface flow, or interflow, occurs when precipitation infiltrates into the ground. It then moves quickly through the soils or through macropores into the stream. The response of a stream through these pathways changes the peak and magnitude seen on hydrographs for different watersheds (Brooks, et al, 2013).

Two methods of separating hydrographs into its different components include graphical and chemical approaches. Graphical separation faces limitations because it only shows water considered a part of baseflow (slow) or a part of stormflow (fast). Groundwater is depicted as decreasing during storm events which contradicts evidence found in chemical hydrograph separation (Clark and Fritz, 1997; Klaus and McDonnell, 2013). Chemical hydrograph separation can more specifically trace the components of water through different pathways using ions or stable isotopes as tracers. It can be calculated using two-component (Eqn. 2) or three component separations (Eqn. 3) solved using mass balance equations:

$$Q_t = Q_{gw} + Q_r \text{ (Eqn. 2)}$$

$$Q_t = Q_{gw} + Q_r + Q_s \text{ (Eqn. 3)}$$

where Q is discharge, and the subscripts relate to the component being examined (t= total, gw= groundwater, r= runoff, and s= soil water) (Clark and Fritz, 1997). Isotopic values of streamflow should plot near the line when connecting two components or within the triangle when connecting three.

Common ions used as tracers are dissolved silica and chlorine. Dissolved silica is useful when absent in one component of the water (i.e. groundwater) and present in the others (i.e. soil water and runoff). It is often a label of waters flowing through areas of elevated silicas and can be linked to geographic sources (Klaus and McDonnell, 2013). Difficulties arise from silica dissolved during brief contact with new water in the system or biological uptake (Hooper and Shoemaker, 1986). Chlorine is used to account for time source separations between pre-event water (groundwater and soil water) and event water (stormflow/runoff). Other tracers that have been used in studies include sodium (reactive tracer), electric conductivity, and dissolved organic carbon (DOC), although these are not considered conservative and can create challenges in linking to specific components (Clark and Fritz, 1997; Klaus and McDonnell, 2013).

Stable isotopes have been found to be one of the best tracers due to their conservative nature leading to isotope-based hydrograph separation (Klaus and McDonnell, 2013). Using $\delta^{18}O$ and $\delta^{2}H$ isotopes, numerous studies have found event water contributing less to the hydrographs and pre-event water often contributing more than 50% (Hooper and Shoemaker, 1986; Klaus and McDonnell, 2013; Sklash and Farvolden, 1979). These studies should be conducted with an understanding of 5 basic assumptions (Klaus and McDonnell, 2013; Sklash and Farvolden, 1979): (1) there must be a distinction between the isotopic signature of event and pre-event waters; (2) the

isotopic signature in waters from an event remain constant or spatial and temporal variations are accounted for; (3) the isotopic signature in pre-event waters remain constant or spatial and temporal variations are accounted for; (4) groundwater and soil water have similar isotopic signatures or soil water contributes minimally to pre-event waters; and (5) contributions of surface storage to streamflow are minimal.

While these assumptions are critical, they reflect an ideal system. Research is being done on how to move past violated assumptions. This often involves greater spatial sampling or greater temporal sampling to understand variations in isotopic signatures more clearly. More work is being done to identify trends of deflection off the meteoric water line of at least one component in a system as well (Klaus and McDonnell, 2013). Early work began by comparing discharge and $\delta^{18}O$ from streams and groundwater to determine groundwater input to streams during storms (Sklash and Farvolden, 1979). Hooper and Shoemaker (1986) examined challenges to interpreting isotopic hydrograph separations when examining $\delta^{2}H$ values for multiple water components (i.e., rain water, stream water, and meltwater). Their research has informed work conducted in complex systems such as determining the percentage of ice-melt in glacial rivers (Kong and Pang, 2012). Research is still being conducted seeking an understanding of the mechanism for moving groundwater into streams during storm events (Pearce, et al., 1986). Klaus and McDonnell (2013) address various laboratory techniques and how higher- resolution and higher frequency of monitoring could affect future research in the field.

Groundwater Isotopes

Groundwater is an important source of water for agricultural practices and residential uses (Jasechko, et. al., 2014). Stable isotopes can be used to characterize both groundwater recharge and age. Recharge to groundwater comes from precipitation or streams (Yeh, et al., 2014). Comparisons of isotopic signatures from each of the sources to the groundwater itself can be used to estimate percentages of recharge into the aquifer as well as determine where water leaves the aquifer. Groundwater is lost through discharge into streams, transpiration, evaporation, and pumping (Jasechko, et. al., 2014, Yeh, et al., 2014). A study conducted in Taiwan showed groundwater in the Huanlin river basin receives 83% recharge from mountain streams and 17% from precipitation through examining the significantly different isotopic signatures (Yeh, et al., 2014). Taiwan's climate is classified as humid subtropical (Arnfield, 2019). Meanwhile, in the British Isle with a marine west coast climate, groundwater recharge is greatest in the winter because summer conditions result in more evaporation and transpiration of precipitation (Arnfield, 2019; Darling et al., 2003). Groundwater isotope composition in this study resulted from the mixing of rainfall across years and seasons, with winter values being more prominent in the isotopic signature (Darling et al., 2003). In general, arid and temperate climates experience more groundwater recharge in the winter, compared to the summer (Jasechko et al., 2014).

The age of groundwater is used to refer to the residence time water has spent in an aquifer underground. It is split into two divisions, young groundwater or old groundwater, depending on residence time. Tritium, a radioactive element with a half-life of 12.32 years, is used to determine young groundwater. Although tritium is produced

naturally, there was a spike in abundance due to nuclear bomb testing around the 1960s. The detection of tritium in groundwater provides the interpretation that a portion of the groundwater is young and was introduced into the system after the 1950s (Plummer, 2005). The use of tritium has become common method in determining relative groundwater age. Scholl, et. al. (1996) in their study around the Kilauea volcanic area divided the samples in their study area into three categories using tritium concentrations. The three groups involved old water (greater than 35year residence time or higher inputs of freshwater), intermediate-age waters (18-25year residence time), and recent waters (0-17year residence time). The values of tritium ranged from 0 to 5.4 TU. Krypton-85, Argon-39, Silicon-32, Sulphur-35, Chlorofluorocarbons, and Sulphur Hexafluoride have also been used to determine the age of groundwater. Each of these methods experiences some limitations, either from practicality, complicated environmental interactions, or complex interpretations (Plummer, 2005). Older groundwater, lacking traceable tritium, is often dated using radiocarbon(C^{14}). C^{14} measurements are collected from dissolved inorganic carbon (DIC) and corrected for hydrochemical and physical changes (Strauch, 2014). A study conducted in France used 40 boreholes to sample groundwater and test radiocarbon to determine the ages of groundwater in the region and create isochrons covering it. The samples contained no traces of tritium and ages ranged from around 3,000 up to almost 800,000 years (Blavoux and Olive, 1981). Other methods of dating old groundwater include Kr-81, Cl-36, U-234/238, and He-4 (Strauch, 2014).

Chapter 3: North shore- Snow Sampling

Introduction

The Great Lakes Basin produces over $438 billion through commerce and industry in the US (Neff and Nicholas, 2005). Communities in the region contain over 33 million people who benefit economically from proximity to the large freshwater source (Magnuson, et al., 1997; Neff and Nicholas, 2005). Lake Superior, the largest freshwater lake in the basin, covers an area of 82,000 km^2 and contributes to hydroelectric power, fishing, tourism, and shipping (Jasechko, et al., 2014). This valuable resource is sensitive to changes in climate and influences the climate of the surrounding region (Magnuson, et al., 1997; Neff and Nicholas, 2005; Scott and Huff, 1996; Wright, et al., 2013).

Precipitation is one of the major water inputs into Lake Superior (Neff and Nicholas, 2005). While precipitation around the lake often originates in one of four regions: the Gulf of Mexico, the Pacific Ocean, Arctic Regions, and the Atlantic Seashore, the lake itself can also impact precipitation (Gat, et al., 1994; Wright, et al., 2013). The most common impact of the large water body is known as Lake-Effect Snow (LES), which occurs between late fall and winter due to large temperature gradients that generate evaporation off the lake (Jasechko, et al., 2014; Wright, et al., 2013). LES is known for precipitating on the downwind, or leeward, side of the lake, producing between 10-50% of the total regional winter precipitation (Scott and Huff, 1996). As ice cover on the lake increases in February and March, the interaction between the atmosphere and the lake surface becomes limited, lowering LES as the spring progresses (Wright, et al, 2013). Summer and spring are characterized by minimal evaporation from all the Great Lakes, minimizing the lake impact on regional precipitation during these time periods (Neff and Nicholas, 2005).

Precipitation falling from the sky is subject to many possible pathways in the hydrologic cycle. Water may flow directly into streams or open water bodies through overland flow or infiltrate into the ground becoming subsurface flow. Subsurface flow can recharge groundwater or become shallow subsurface water used to nourish plant life and streams (Brooks, et al, 2013). Water may evaporate or sublimate back into the atmosphere as well. Precipitation accounts for 27% of the annual lake water budget for Lake Superior and enters the lake either when it falls directly onto the lake or through stream discharge into the lake (Neff and Nicholas, 2005).

Stable isotopes of hydrogen and oxygen can be used as conservative tracers to follow the movement of water through the water cycle. Storm events fingerprint the isotopic signature of the source waters where the storm originated, which is modified by effects such as distance from the source, amount to rain out, and altitude changes (Clark and Fritz, 1997; Dansgaard, 1964; Kendall and McDonnell, 1998). Precipitation isotopes from rain events are often used to separate hydrographs of streams into event water and pre-event water (Pearce, et al., 1986). As the study of stable isotopes in hydrographs expanded, research extended to studying the impact of the snowmelt and snowpack (Klaus and McDonnell, 2013). The study of snow was found to be crucial in cold climate regions where streams were sustained by snowmelt and avalanches commonly occur (Ala-aho, et al., 2017; Schweizer, et al., 2008). Snow isotopes are more complex than rain due to added metamorphism that can occur to a snowpack before it melts and enters other portions of the hydrologic cycle (Ala-aho, et al., 2017; Dansgaard, 1964). Ala-aho, et al., (2017) highlight complexities such as fractionation from sublimation leaving the snowpack with heavier bulk isotopic compositions. Their work also discusses the cycles

of freeze/thaw occurring over winter altering the stratigraphy of the snow from different storm events. Due to these on-going changes, early snowmelt often carries different isotopic signatures than the peak of the melt, which comes from more homogenized snow (Ala-aho, et al., 2017; Schmieder, et al., 2016).

Communities around the Great Lakes may be impacted by increased variability in winter snowfall events due to climate change (Kunkel, et al., 2000). Periods of low snowfall generally result in lost revenue due to decreased participation in winter snow sports (Kunkel, et al., 2000). Meanwhile, higher snowfall can be difficult to municipalities which are faced with increased costs of snow removal and more freeze damage to roads and buildings (Kunkel, et al., 2000). While LES affecting the south shore of Lake Superior contains 52% of the evaporated moisture from the lake, the rest of the lake moisture remains as water vapor (Scott and Huff, 1996). Changing climates may lead to changes in ice cover and surface temperatures, which can change the timing and amount of evaporation occurring off the lakes in winter (Wright, et al, 2013). Many studies have been conducted on the downwind side of the Great Lakes and the impacts of snow in these regions, however little research has been conducted on the upwind side of the lakes. For Lake Superior, the north shore has little detailed regional information regarding the effects of snow on watersheds and communities. Evaporation from Lake Superior is likely to impact precipitation along the north shore, even if not to the same extent of influence along the south shore. The goal of this study was to examine spatial variability of snowstorms and to understand the impact of Lake Superior on snow along the north shore. The five study watersheds run northward along the northwest shore of

Lake Superior from Duluth, MN to just beyond Grand Marais, MN, and were chosen to cover a large spatial region (Figure 3-1).

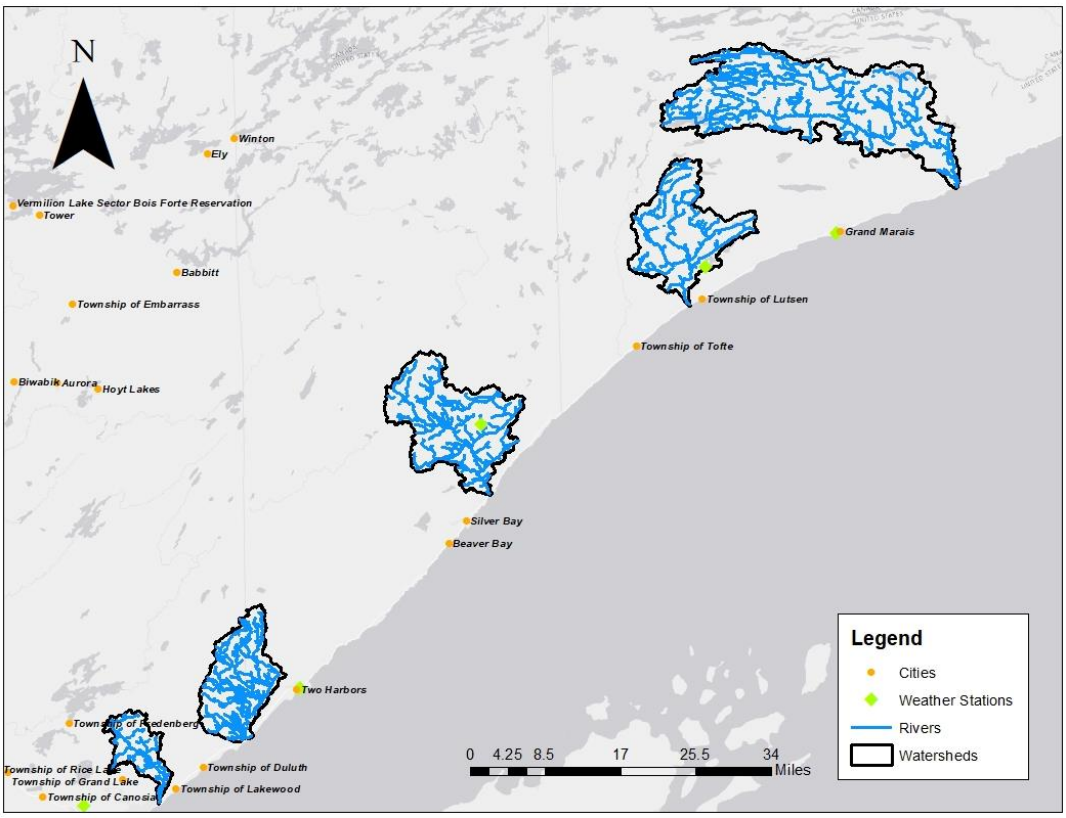

Figure 3-1) The five watersheds sampled along the north shore. The order of the watersheds starting with the farthest left is the Lester River, Knife River, Baptism River, Poplar River, and Brule River.

Study Site Descriptions

Lake Superior is the largest of the Great Lakes and drains through the St. Lawrence Seaway (Jasechko, et al., 2014). The lake's surface area (82,103 km^2) covers 39% of the 245,000 km^2 basin (Neff and Nicholas, 2005). Water enters the lake via precipitation, streamflow, groundwater seepage, and water diversions. The two major diversions are hydroelectric plants Ogoki and Long Lac, which redirect water into Lake Superior's basin rather than the Hudson Bay. Most of the water in Lake Superior discharges through St. Mary's River and into Lake Huron (Neff and Nicholas, 2005).

Neff and Nicholas (2005) show that in the yearly water budget for Lake Superior, evaporation accounts for a loss of 1536 $m^3 s^{-1}$ or 20.75%. The largest water loss from evaporation or sublimation occurs between September and February (Jasechko, et.al., 2014; Scott and Huff, 1996). Mean summer temperatures are 21°C and winter temperatures average around -16°C. Mean annual precipitation is between 48 to 89 cm across the state of Minnesota, while average annual snowfall around Lake Superior is 178 cm (NOAA, 2018). The study area encompasses the north shore of Lake Superior, with the focus on five study watersheds: Lester River, Knife River, Baptism River, Poplar River, and the Brule River.

Lester River Watershed

The Lester River Watershed is located near the city of Duluth, MN (Figure 3-). The watershed drainage area is 96 km^2 before the river combines with Amity Creek and discharges into Lake Superior. The underlying geology of the watershed is 25% anorthosite, 15% basalts, 48% troctolite, 10% gabbros, and 2% granites, while the soils are primarily Typic

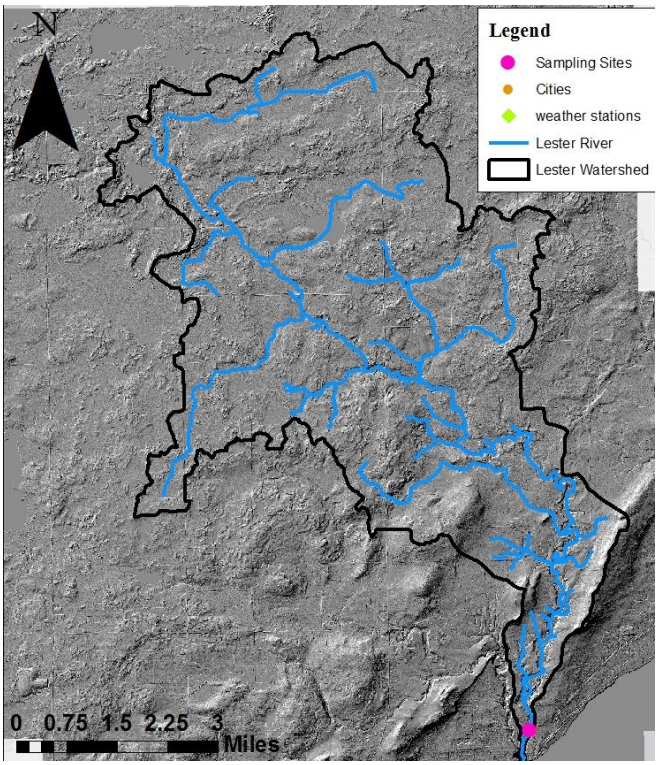

Figure 3-2) The Lester River watershed outline and main stream network.

Epiaquepts with a coarse-loamy texture (Soil Survey Staff, 2018). The watershed is predominately forested, with almost half of the land area comprised of mixed hardwood and coniferous vegetation. The remaining land area is divided between wetlands, grasslands, agricultural lands, urban and impervious surfaces, and open water (U.S. Geological Survey, 2016; Lakesuperiorstreams, 2009). Annual average temperature is 4.3°C and annual precipitation is 78 cm (NOAA, 2018).

Knife River Watershed

The Knife River Watershed is located near the city of Knife River, MN and covers 223 km^2 (Figure 3-3-3). The underlying geology is 67% basalt and 33% gabbros. The soils in the watershed are classified as coarse-loamy Dystric or Oxyaquic Eutrudepts (Soil Survey Staff, 2018). The Knife River Watershed is 72% covered by forests, 16% wetlands, 11% agricultural lands and grasslands, 1% urban areas and other surface waters (U.S. Geological Survey, 2016; Lakesuperiorstreams, 2009). Annual average temperature is 5.2°C and annual precipitation is 79 cm (NOAA, 2018).

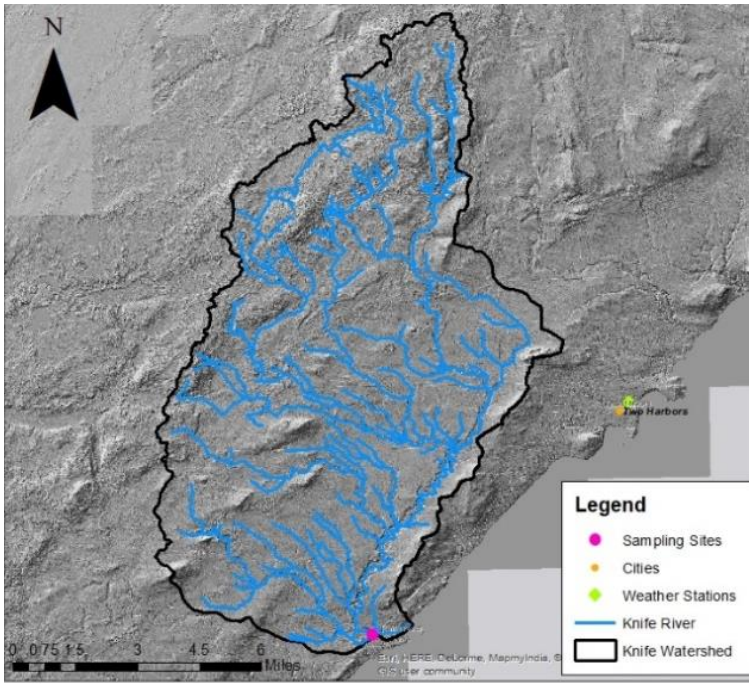

Figure 3-3) The Knife River Watershed's outline and main stream network.

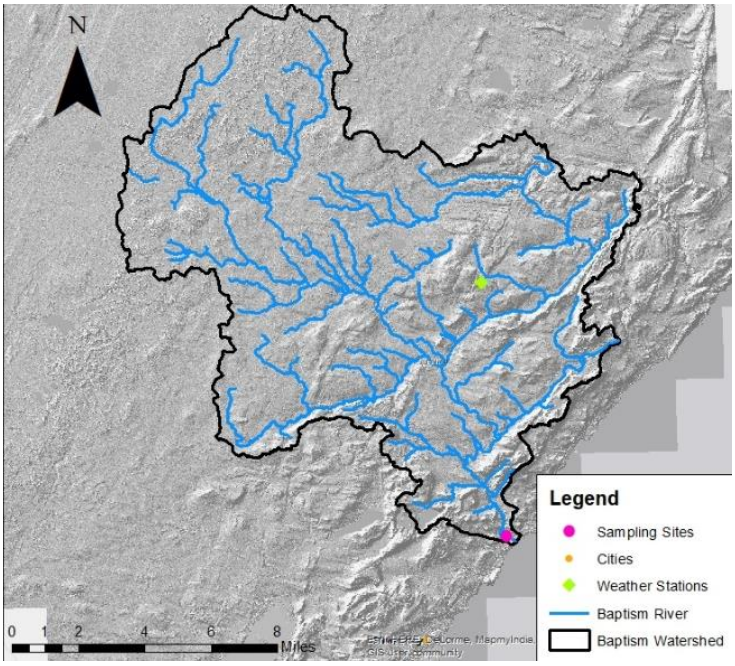

Figure 3-4) The Baptism River watershed is outlined with the stream network throughout.

Baptism River Watershed

The Baptism River Watershed is located near Ilgen City, MN and discharges to Lake Superior through Tettegouche State Park (Figure 3-4). The watershed basin covers 218 km^2 with geology consisting of 10% anorthosite, 14% basalts, 53% gabbros, and 23% granite. Like the Knife River, soils are either coarse-loamy Dystric Eutrudepts or coarse-loamy Oxyaquic Eutrudepts (Soil Survey Staff, 2018). The Baptism River Watershed has 84% forest cover, 13% shrubs, and the remaining 3% is divided among agricultural lands, urban areas, and surface water sources (U.S. Geological Survey, 2016; Lakesuperiorstreams, 2009). Annual average temperature is 4.0°C and annual precipitation is 81 cm (NOAA, 2018).

Poplar River Watershed

The Poplar River Watershed covers an area of 295 km^2 near the city of Lutsen, MN, which contains the Lutsen Mountain ski resort (Figure 3-5). This ski resort produces its own snow which could change the nature of the snow found in this area. The geology

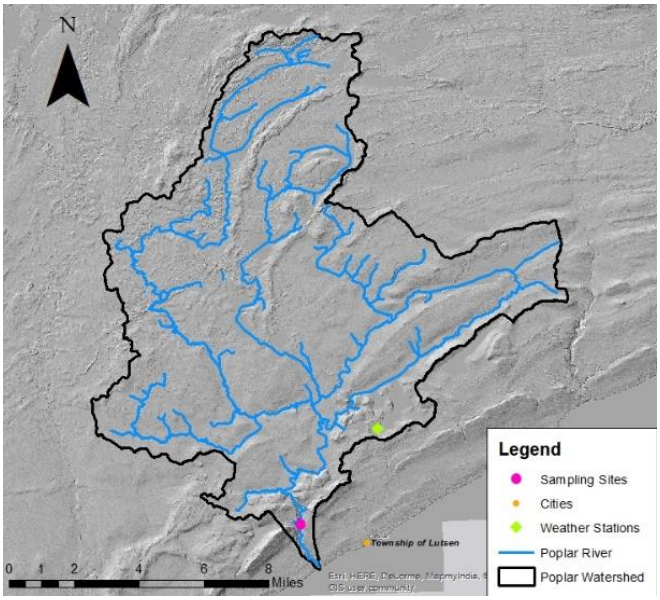

Figure 3-5) The Poplar River Watershed outline and

consists of 65% basalts and 35% gabbros and the soils consist of coarse-loamy, Oxyaquic Eutrudepts, although a large portion of data are still missing (Soil Survey Staff, 2018). The Poplar River Watershed has 70% forests, 19% wetlands, 7% lakes and ponds, and 4% grasslands, agricultural lands, and urban areas (U.S. Geological Survey, 2016; Lakesuperiorstreams, 2009). Annual average temperature is 2.6°C and annual precipitation is 85 cm (NOAA, 2018).

Brule River Watershed

The Brule River Watershed is located north of Grand Marais, MN with the outlet found in CR Judge Magney State Park (Figure 3-6). It covers an area of 686 km^2. Forests cover almost 74% of the watershed, open waters and wetlands cover 20%, and the remaining 5% is split into

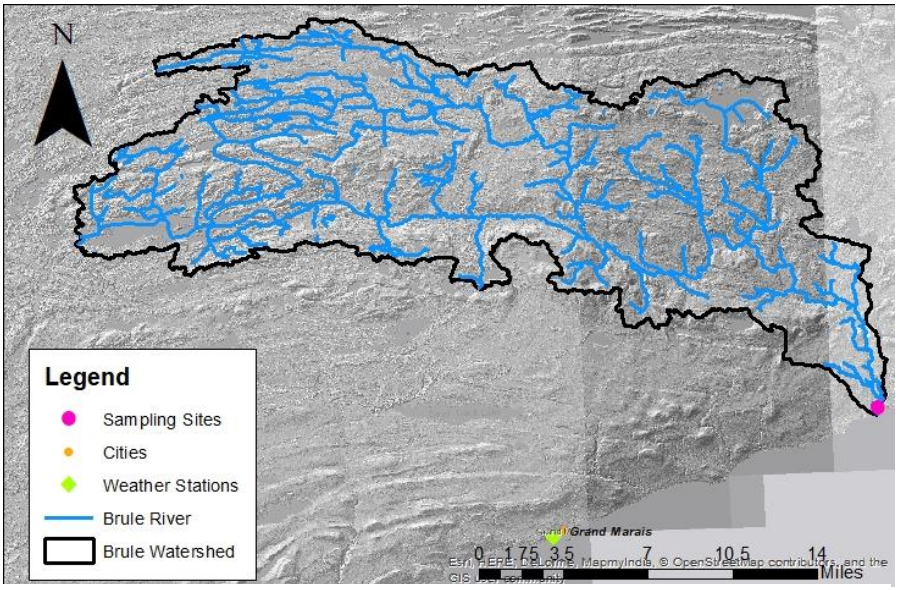

Figure 3-6) The Brule River watershed outline and streams.

agricultural lands, grasslands, and little to no urban lands (U.S. Geological Survey, 2016; Lakesuperiorstreams, 2009). The underlying geology of the region is composed of 5% anorthosite, 35% basalts, 34% gabbros, and 26% granites. Soils of the region are mostly still unknown but have been classified as Aeric Glossaqualfs and coarse-loamy, Typic Dystrudepts (Soil Survey Staff, 2018). Annual average temperature is 3.8°C and annual precipitation is 68 cm (NOAA, 2018).

North shore Sampling Methods

Streamflow, snowfall, and snowmelt water were collected at five sampling locations selected along the north shore of Lake Superior. These water samples were used to trace the movement of water and differences between snowstorms in the region by comparing isotopic values of δ^2H and $\delta^{18}O$. Data collection for snow samples was event-based, occurring after significant snowfall (> 2.5 cm from approximately October – April, 2017-2018) across each of the five study watersheds (Figure 3-1). Fresh snow from each event was collected in 500 mL Nalgene bottles and melted at room temperature. Melted snow was then transferred into 20 mL glass scintillation vials and covered with Parafilm to ensure no evaporative loss. Samples were collected on flat, relatively open ground close to the outlet of each watershed. All snow samples were collected within 48 hours of snowfall to avoid major changes in the isotopic signature due to fractionation from wind, sublimation, or melting. Snowmelt samples were collected directly from the flowing water in the streams during April 2018. There were 23 snow samples collected from these five north shore sites during five different storms. The storms were classified as Alberta Clippers, system storms, or complex storms. Alberta Clippers are low-pressure

systems originating in the Arctic Ocean and moving across Canada to the Great Lakes. System storms are low-pressure storms from the central plains of the United States considered either a Colorado low or a Panhandle hook. Complex storms are a combination of different storm types or could not be discerned. One storm on March 31, 2018, only spanned three of the sites so samples were only collected from the Lester, Knife and Baptism watersheds following this storm. Storms were classified by the amount of snowfall and wind direction. Five snowmelt samples were collected on April 28th, 2018 (Table 3-1).

Streamflow samples were collected directly from the streams at each of the five watersheds, in September 2017 as well as May, June, July, and August 2018. Samples were collected in flowing water using 20 mL glass scintillation vials near the outlet of each watershed leading into Lake Superior. There were 25 samples collected from the five streams altogether. All snow and stream samples collected were analyzed using a Picarro L2130-i cavity ring down mass spectrometer to test for values of δ^2H and $\delta^{18}O$ (Appendix 1). Water samples were compared to the international standard (VSMOW) using the following equation:

$$\delta\ ^{18}O_{sample} = (((^{18}O/^{16}O)_{sample}/((^{18}O/^{16}O)_{reference})-1) * 1000\ ^{0}/_{00} \quad \text{(Eqn. 1)}$$

where the sample indicates a sample of water from a known location and the reference is VSMOW or a similar known standard. Equation 1 reports values in "delta notation", where delta values are presented in parts per thousand, per mil ($^{0}/_{00}$) and is used for both hydrogen and oxygen isotopes.

ANOVA tests were run to compare mean values across site locations and to compare mean values across sampling dates using *stats* package in R. An $\alpha = 0.05$ was used to determine statistically significant differences between the sample sites and dates. Tukey's HSD (honestly significant differenced) tests were used to perform pairwise comparisons across the sites and dates, controlling for multiple tests to produce adjusted p-values with 95% familywise confidence (Tukey, 1949). δ^2H and $\delta^{18}O$ values were plotted against the Global Meteoric Water Line (GMWL: $\delta^2H = 8*\delta^{18}O + 10$) and the Local Meteoric Water Line (LMWL: $\delta^2H = 8.4*\delta^{18}O + 15.5$) (Rozanski et al., 1993; Jasperson, et al., 2018).

Table 3-1: Summary of the samples collected along the north shore of Lake Superior.

Date	Number of Samples	Type of sample	Type of storm	Snowfall (cm)
9/25/2017	5	stream	n/a	n/a
12/9/2017	5	snow	clipper	2.5 to 5
12/15/2017	5	snow	clipper	8 to 15
1/12/2018	5	snow	system	4.6 to 8
2/21/2018	5	snow	complex	6.6 to 12.7
3/31/2018	3	snow	system	< 3.8
4/28/2018	5	snowmelt	n/a	n/a
5/24/2018	5	stream	n/a	n/a
6/25/2018	5	stream	n/a	n/a
7/25/2018	5	stream	n/a	n/a
8/22/2018	5	stream	n/a	n/a

Results

Overall, there were seasonal trends apparent in the data (Figure 3-7). However, there was no significant difference between the mean isotopic composition of site locations along the north shore (Appendix 2). The isotopic signatures from the streams and snowmelt plot in small clusters along the LMWL and GMWL (Figure 3-8). Data collected from snowstorms showed more range in δ^2H and $\delta^{18}O$ values, plotting lighter

on the graph (Figure 3-8). Using snow and snowmelt data collected from the sites located on the north shore, the LMWL created with my data for winter precipitation is $\delta^2H = 8.0 * \delta^{18}O + 14.8$.

Mean $\delta^{18}O$ values across sites for snow and snowmelt samples plotted between -22 and -20 $^{0}/_{00}$ (Figure 3-7). Mean values across the dates showed differences when grouping dates into seasons. The data were divided into three seasons: winter (October through March), snowmelt in April, and summer (May through August) (Appendix 2). April snowmelt values were significantly different than winter values but were isotopically similar to summer streamflow. Snow samples collected over winter were isotopically similar and streamflow samples collected over summer were isotopically similar. There is an observable seasonal trend in the data, which was lighter in the winter months and heavier during the summer months (Figure 3-9). Streamflow collected during the fall and summer showed low variance in isotopic values for both δ^2H and $\delta^{18}O$ (Table 3-2).

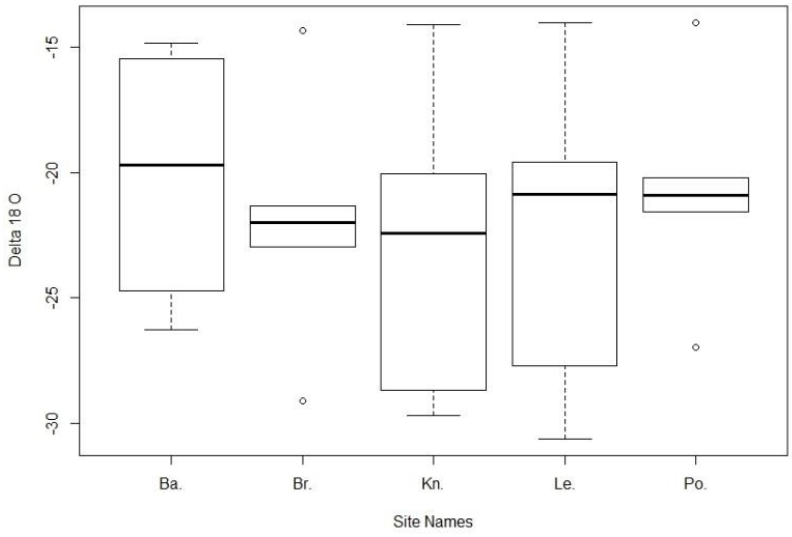

Figure 3-7) Mean and variance in $\delta^{18}O$ across each of the five watershed sites. The names of the sites were abbreviated to the first two letters of each name, i.e. Baptism = Ba., Brule = Br., Knife = Kn., Lester = Le., and Poplar =Po. The data plotted are from winter storms and snowmelt (12/9/2017 through 4/28/2018).

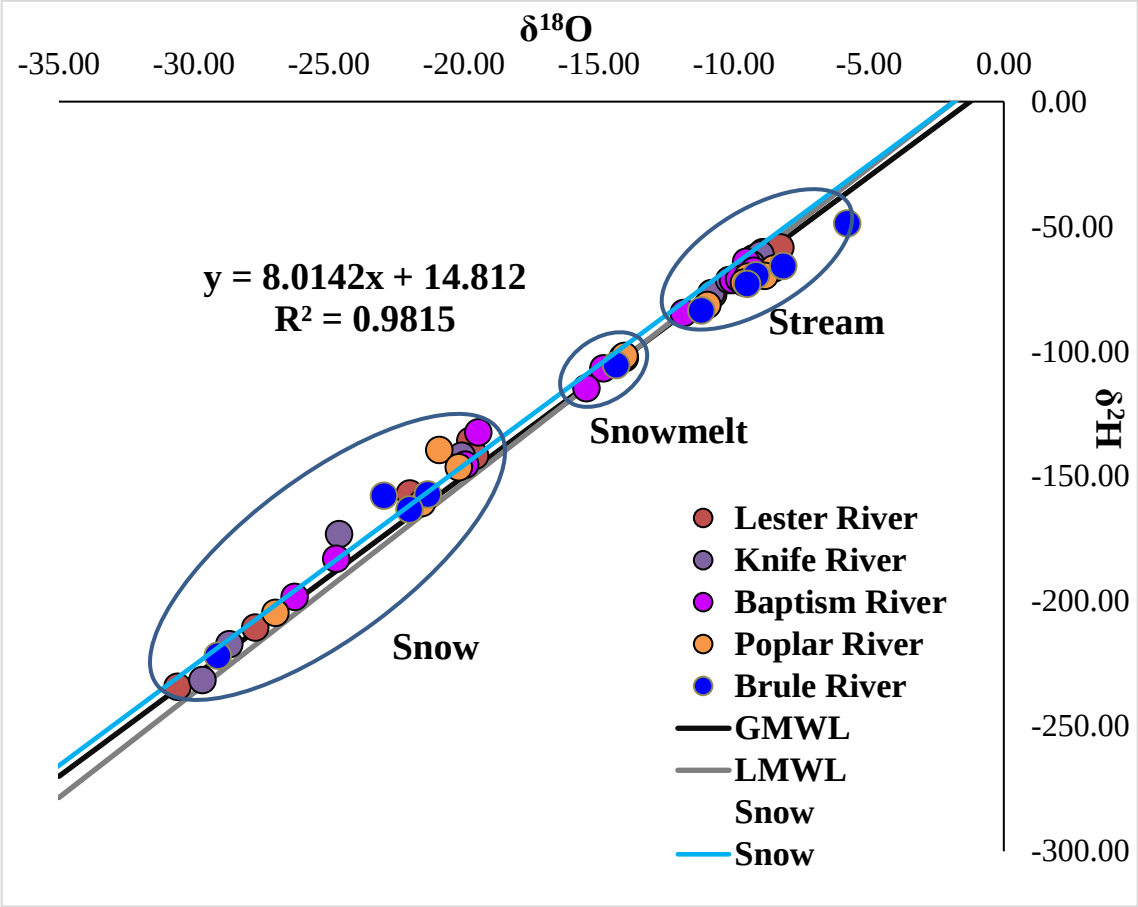

Figure 3-8) Fall (stream), winter (snow), early spring (snowmelt), and summer (stream) plotted against the GMWL and LMWL (Rozanski, et al, 1993; Jasperson, et al, 2018). Data are plotted according to the watershed site that it was collected from: Lester, Knife, Baptism, Poplar, or Brule River.

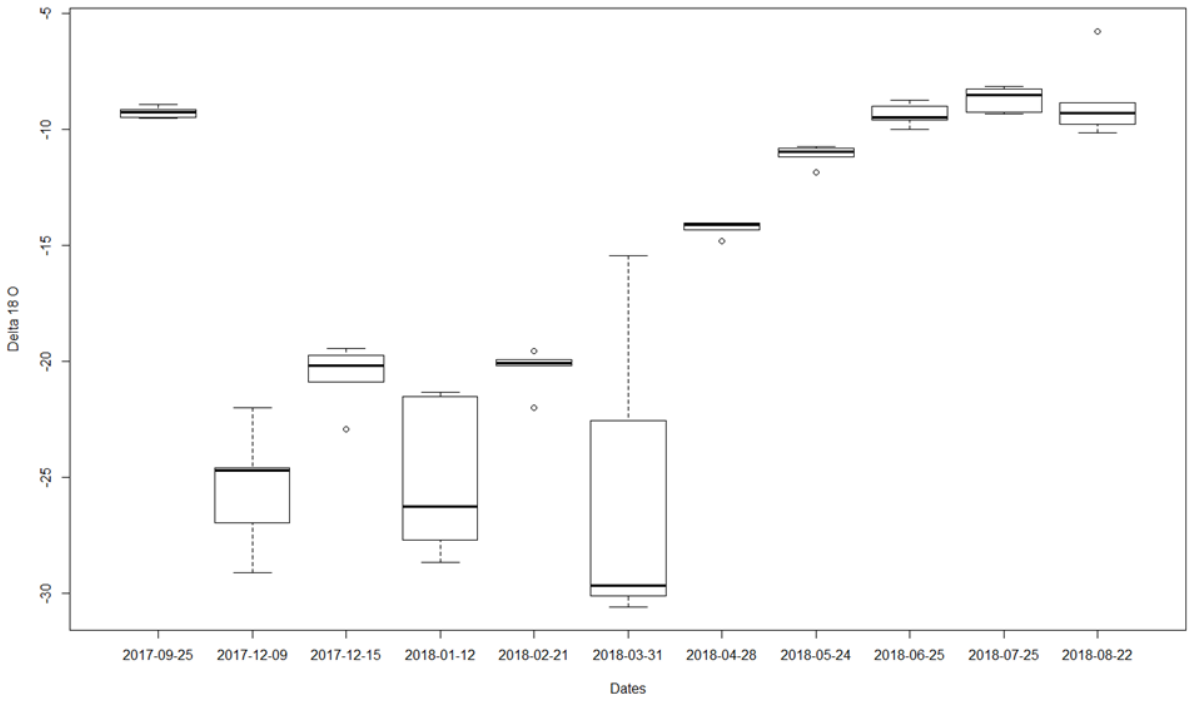

Figure 3-9) Mean and variation of $\delta^{18}O$ from samples collected on each of the given dates. All dates show data for five samples, except for March 31, 2018 due to the lack of fresh snow at two of the five sites.

Table 3-2) Mean values (μ) and one standard deviation (σ) of the $\delta^{18}O$ and $\delta^{2}H$ across the five study sites for each sample date during the study period.

	$\delta^{2}H$		$\delta^{18}O$	
Dates	**μ**	**σ**	**μ**	**σ**
9/25/2017	-65.35	4.30	-9.27	0.25
12/9/2017	-187.90	25.63	-25.48	2.69
12/15/2017	-141.58	9.81	-20.65	1.40
1/12/2018	-188.77	28.04	-25.11	3.46
2/21/2018	-148.75	8.35	-20.36	0.95
3/31/2018	-193.45	68.22	-25.24	8.49
4/28/2018	-103.84	2.15	-14.27	0.34
5/24/2018	-80.73	3.59	-11.12	0.44
6/25/2018	-68.10	5.78	-9.38	0.51
7/25/2018	-64.78	3.71	-8.71	0.56
8/22/2018	-65.52	9.54	-8.78	1.74

Discussion

Along the north shore, the five watersheds sampled span over 1500 km^2 and show no significant difference in isotopic values of δ^2H and $\delta^{18}O$. Isotopic signatures found in precipitation and snow are often variable throughout large areas (Harper and Bradford, 2003). Across 4200 km^2 in Kilauea, HI, precipitation samples showed large spatial variations. The area was divided into different regions based on the microclimates and changes in topography present (Scholl, et al., 1996). Spatial variability in snowmelt and snow isotopes was found in a 98 km^2 catchment due to the direction of the slope faces (Schmieder, et al., 2016). Furthermore, within one storm event spatial variability has been found across three cities along the east coast that were 20 to 30km apart (Gedzelman, et al., 1989). In contrast to these, my data show little variability across sampling sites due to similarities in elevations and slope directions. The results suggest that there is little to no change in the climate conditions along the north shore as well. While each watershed varies in size and location, they show the same general isotopic trends indicating that understanding the climate processes of one watershed should be applicable to the other watersheds.

Lawrence, et al. (1982), identified the importance of a storm's path, structure, and evolution on the resulting isotopic composition of its precipitation. From my five sampling sites along the north shore, the snowstorms were separated into three categories: clipper, system (Colorado Low or Panhandle Hook), and complex (Table 3-1). There were no trends in variance across the types of storms and there were no observable differences across the mean values of $\delta^{18}O$ from each storm (Figure 3-9). In contrast to my study, sites on the leeward side of Lake Erie and Lake Ontario found noticeable

differences in isotopic signatures of four different storm types (Burnett, et al., 2004). A study conducted in Mohonk Lake, New York, also found significant variability in the isotopic signatures of storms. During the two-year study, values of δ^2H ranged from $-7^0/_{00}$ to $-170^0/_{00}$ due to the time of year and trajectories of each storm sampled (Lawrence, et al, 1982). It would be anticipated that data collected from storms in the region of my study would show different isotopic signatures because of differences in sources and trajectories. My data does not show these distinct differences indicating that something else is impacting the region. The contribution of Lake Superior to the atmospheric moisture of storms could account for similarities between the isotopic means across all 5 sites. The lake is said to affect the moisture of the air around it, with 52% of the added moisture deposited on the south shore as LES (Scott and Huff, 1996; Wright, et al, 2013). It is possible that the proximity of the lake to each site location has contributed moisture to incoming storms and precipitates out almost immediately. Further data collection from snow storms affecting the north shore would be necessary to identify any moisture input from Lake Superior.

Across my study sites, snow samples were isotopically lighter than the snowmelt and stream values. Similar trends have been found in the Austrian Alps (Schmieder, et al., 2016), which are consistent with patterns described in early work on isotopes (Dansgaard, 1964). My data represent the seasonality in the streams and precipitation along the north shore of Lake Superior characterized by heavier isotopes in the summer and fall compared to lighter isotopes found in the winter. Seasonality within the study watersheds will impact groundwater recharge, water availability for plants, as well as the

amount of overland flow and snowmelt entering stream systems leading directly into Lake Superior (Jasechko, et al., 2014).

Overall, my data demonstrate the seasonality and spatial similarity among the site locations. This suggests that changes to the climate conditions within one watershed along the north shore are likely to impact the other watersheds as well. Changes in climate will lead to changes in precipitation by impacting ice cover and temperatures around Lake Superior (Wright, et al., 2013). These data are a useful starting point in collecting a longer record of snow along the north shore of Lake Superior. With more data collected over time, the dynamics and differences between snowstorms in the region may become clearer. A larger snowpack dataset covering a range in elevation in each watershed would help determine the impact that Lake Superior has on atmospheric recycling of moisture on the upwind side of the lake.

Chapter 4: Lester River Watershed

Introduction

Across the globe, people are concerned with the storage and movement of water resources. Changes to climate conditions such as temperature and precipitation alters the amount of incoming freshwater to many regions. Understanding the storage and movement of water in locations facing changes is becoming more important as more people face water stress and demand issues (Oki and Kanae, 2006; Kunkel, et al., 2000).

Rivers play an important role in the hydrologic cycle, transporting around 45,500 km^3/yr of water into the oceans (Oki and Kanae, 2006). While studying the isotopic signatures of rivers across the United States, the region around the Great Lakes showed unique trends of heavier $\delta^{18}O$ values than anticipated at higher latitudes. The heavier $\delta^{18}O$ values were attributed to evaporated moisture from the lakes joining with atmospheric moisture (Kendall and Coplen, 2001). The Great Lakes region contains five of the largest freshwater lakes in the world, which altogether contains 80% of the freshwater in continental North America (Jasechko, et al., 2014). Hydrologic and isotopic studies around the Great Lakes have focused on the region rather than individual lakes or on the downwind side of the lakes due to Lake-Effect Snow (LES) (Jasechko, et al., 2014; Neff and Nicholas, 2005; Bowen, et al., 2012; Burnett, et al., 2004). The focus of these studies has left a lack of knowledge regarding the movement and storage of water on the upwind side of the Great Lakes especially the largest, Lake Superior.

Groundwater is a key component in many streams during times of baseflow and is influential in maintaining cold stream temperatures during typically warm summer months (Sklash and Farvolden, 1979; Lakesuperiorstreams, 2009). Along the north shore of Lake Superior, groundwater is often shallower because of the high exposure of

bedrock and thin glacial tills. Flooding causes streams to incise into the tills and creates more mixing and recharge between surface waters and groundwaters (Jasperson, et al., 2018). Additionally, to study changes to groundwater and streams in a specific location or region, a baseline of data is needed for future comparisons (Darling, et al., 2003). Along the north shore, the study conducted in Amity Creek was the first to collect isotopic data of streams, groundwater, and precipitation. This data was used to create a Local Meteoric Water Line (LMWL, $\delta^2H = 8.4 * \delta^{18}O + 15.5$) and Local Evaporation Line (LEL, $\delta^2H = 5.21 * \delta^{18}O + 18.72$) which is useful for comparisons of future studies within this region (Jasperson, et al., 2018).

Isotopes have been found to be useful in tracing sources of incoming precipitation, recharge and discharge of groundwater, and highlighting evaporation in the systems using deuterium-excess (d-excess) (Dansgaard, 1964; Gat, 1994; Klaus and McDonnell, 2013; Sklash and Farvolden, 1979; Darling, et al., 2003; Jasperson, et al., 2018; Wu, et al., 2019; Scholl, et al., 1996; Schmieder, et al., 2016). D-excess has been shown to correlate well to humidity, air temperatures, and sea surface temperatures, providing a useful tool when seeking to understand changes to the climate of a region (Frohlich, et al, 2001). D-excess values change in a seasonal pattern, reaching maximum values during the winter and minimum values over the summer within the northern hemisphere. Higher d-excess values can also be linked to evaporation from lake systems combining with water vapor from oceanic sources in precipitation (Machavaram and Krishnamurthy, 1995). In Japan, d-excess within streams shares a similar seasonal pattern to that found in precipitation, however d-excess within the streams can dampen the

effects of precipitation and become biased towards winter isotopic values (Katsuyama, et al., 2015).

Lake Superior impacts the climate of the surrounding region by altering precipitation and temperatures. Over the winter, air temperatures remain warmer near the lake and precipitation downwind increases substantially. During the summer, air temperatures remain cooler and thunderstorms are impacted by the presence of the lake (Scott and Huff, 1996). Between 1950 and 1995, Lake-Effect Snow (LES) events on the leeward side of Lake Erie occurred roughly 17 times per decade. The favorable conditions were found to strongly correlate with air temperature, lake-air temperature differences, wind speed, and wind direction. Changes to any of these conditions will affect the timing, intensity, and frequency of precipitation events around the Great Lakes in the future (Kunkel, et al., 2000). Between 1910 and 1996, there has been a 10% increase in precipitation across Minnesota. The increase of precipitation is noticeable in the increase in frequency and intensity of storms during the summer across the state, leading to longer and higher discharge in the streams (Novotny and Stefan, 2007).

Along the north shore of Lake Superior, the discharge of the streams remained relatively stable because the mean annual precipitation has remained constant thus far (Novotny and Stefan, 2007). Streams along the north shore could experience changing temperatures and flows if changes to precipitation or other climate conditions were to occur in the region. Understanding changes to streams along the north shore of Lake Superior is important to the surrounding communities because they are involved in fishing in the cold-water streams for recreation. The Lester River, which is located on the north shore of Lake Superior, is a designated trout stream that is important for the local

economy (Lakesuperiorstreams, 2009). While increases to stream discharge could benefit aquatic habitat in the streams, it may also lead to increasing incision and more soil erosion in the region (Novotny and Stefan, 2007). In order to more clearly understand changes to stream systems along the north shore of Lake Superior, it is important to understand the starting isotopic composition of the streams and how they respond to precipitation events and seasonal changes. Therefore, the goal of this study was to examine stream water and precipitation in the Lester River watershed. The research conducted was done to provide information regarding the spatial and temporal distribution of isotopes in the stream.

Methods

Study Site

The Lester River Watershed is located on the northwest corner of Lake Superior (Figure 4-1). It covers 96 km^2 before combining with Amity Creek and discharging into Lake Superior near the city of Duluth, MN. The soils consist of clay rich glacial tills with a coarse-loamy texture classified as Typic Epiaquepts (Soil Survey Staff, 2018). The underlying geology of igneous rocks includes anorthosite, basalts, troctolite, gabbros, and granites. The watershed is predominately covered in mixed hardwood forests and coniferous vegetation. The remaining land area is divided between wetlands, grasslands, agricultural lands, urban and impervious surfaces, and open water (U.S. Geological Survey, 2016; Lakesuperiorstreams, 2009). Annual average temperature is 4.3°C and annual precipitation is 78 cm (NOAA, 2018). There were fifteen sampling sites in the watershed spread across different areas characterized geomorphologically (Figure 4-2).

The sites were picked to spatially cover the watershed as well as collect information on tributaries and wetlands or ponds.

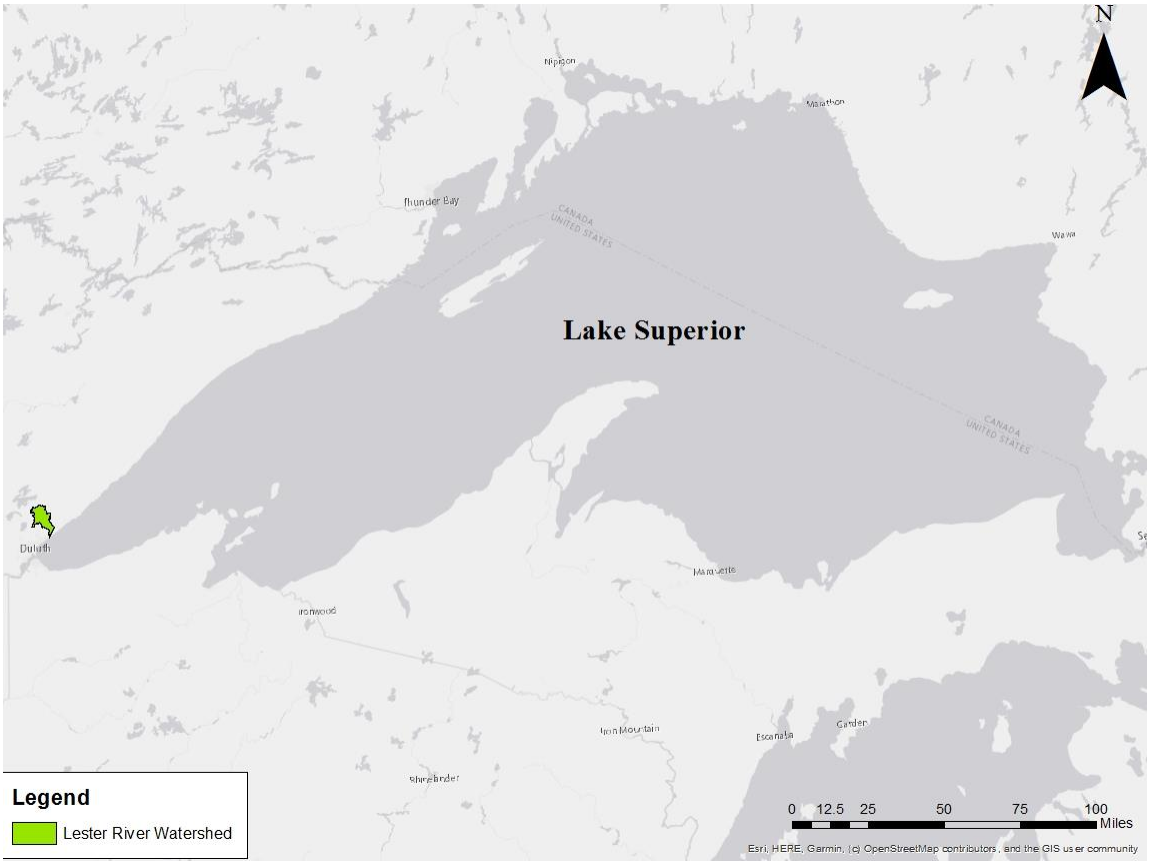

Figure 4-1) A map of Lake Superior with the location of the Lester River watershed.

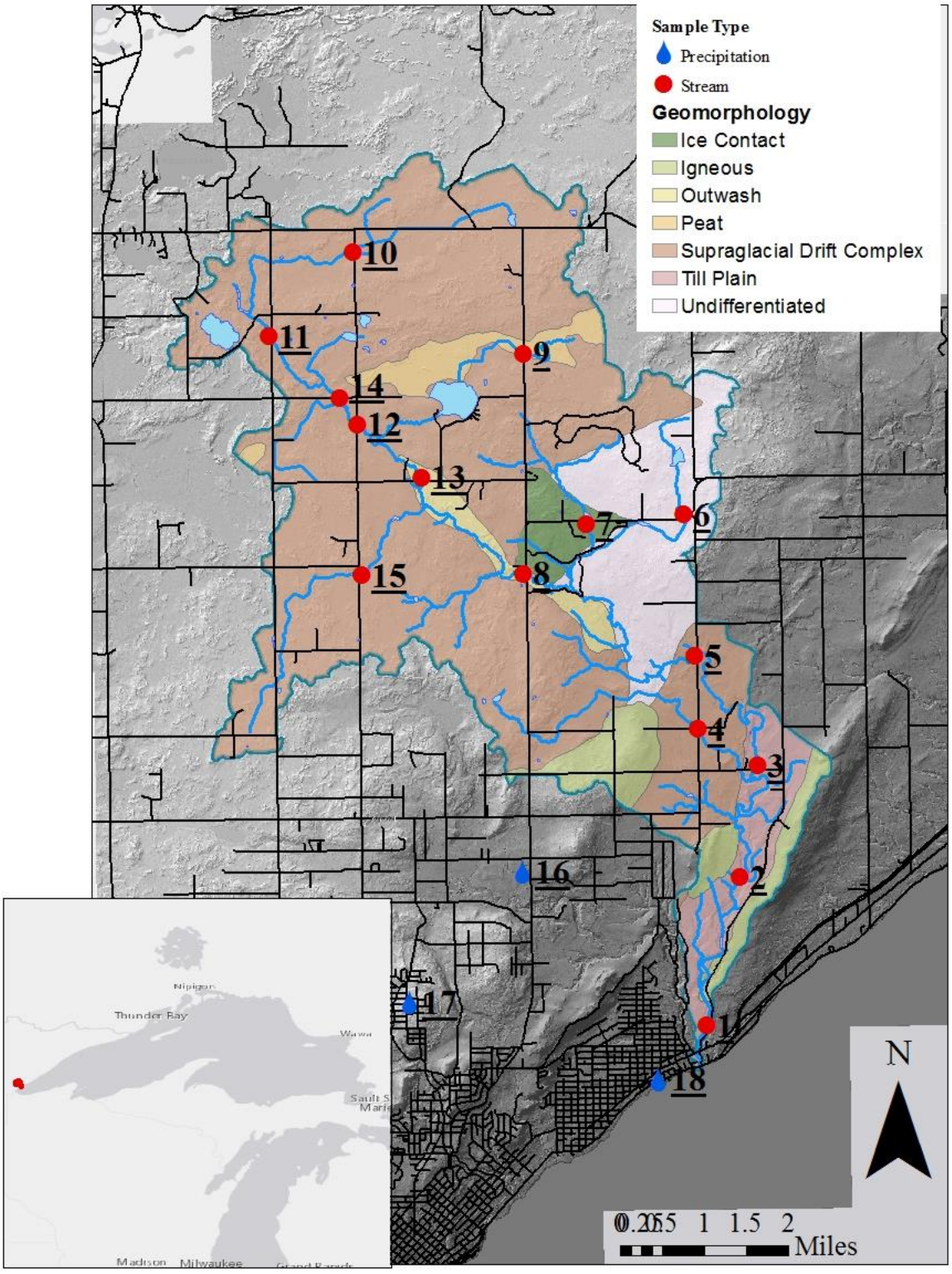

Figure 4-2) The Lester River Watershed contains 15 stream sampling sites distributed amongst different geomorphologies left behind by the last glaciation. Three sites outside the watershed were used to collect precipitation.

Field Sampling Methods

Streamflow samples were collected from 15 sites in the Lester River watershed on a weekly basis from May to December 2018 (Figure 4-2). Sites were chosen to represent underlying geology, topography, and distinctive landscape features in the watershed such as wetlands. Samples were collected from flowing water in the middle of the stream using a telescopic pole and cup. Stream water was stored in 20 mL glass scintillation vials with no headspace and sealed with Parafilm until analysis. Additionally, Onset HOBO tidbit v2 Water Temperature Data Loggers were placed in the stream channel at eight sampling sites to measure *in situ* water temperature (Table 4-1, Appendices 3 and 4). Snapshot temperatures were taken weekly at all sites using an HI-9811-5 pH/EC/TDS/°C Portable Meter alongside the water samples. Overall, 543 stream samples were collected throughout the study period.

Precipitation samples were collected using an evaporation free rain gauge located within the watershed (Site 16, Figure 4-2). Precipitation samples were collected from two additional locations in the city of Duluth, one closer to the mouth of the Lester River (and thus Lake Superior), and one farther inland (Sites 17 and 18, Figure 4-2). 24 rainfall samples were collected from July through early November. One sample of groundwater was collected from a residential well at a depth of 185 ft with 180 feet of clay and 5 feet of sand and gravel on September 21st, 2018.

Table 4-1) Summary of site locations and number of samples collected from the Lester River watershed. Multiple samples were taken at a wetland site (6), spring (9), headwaters (10), and an old meander channel (12).

Site ID	# of samples collected weekly	Total Sample Number	Subwatershed Area (km^2)	Geomorphology	Temp. Logger
1	1	30	91.12	Igneous	n/a
2	1	27	88.05	Till plain	yes
3	1	27	73.9	Till plain	n/a
4	1	30	6.77	SDC	yes
5	1	29	71	SDC	yes
6	3	73	3.04	Undifferentiated	yes
7	1	30	8.39	Ice Contact	n/a
8	1	26	48.02	Ice Contact	yes
9	2	47	2.6	SDC	n/a
10	2	54	6.82	SDC	yes
11	1	25	12.54	SDC	yes
12	2	46	19.96	SDC	n/a
13	1	29	28.54	Outwash	n/a
14	1	25	17.56	SDC	n/a
15	1	22	5.82	SDC	yes

Laboratory Analysis

All water samples were stored in a cool, dark location until analysis and wrapped with Parafilm to prevent any leaking. 23 samples collected in October showed anomalous values and were removed due to possible instrument error (Appendix 6). Samples were transferred from 20 mL glass scintillation vials into even smaller vials to be run through the machine. Samples were analyzed for δ^2H and $\delta^{18}O$ using a Picarro L2130-i cavity ring-down mass spectrometer. δ^2H and $\delta^{18}O$ values were converted by the analyzer to per mil (‰) notation relative to VSMOW using this equation:

$$\delta\ ^{18}O_{sample} = (((^{18}O/^{16}O)_{sample}/((^{18}O/^{16}O)_{reference})-1) * 1000\ ^{0}/_{00} \quad \text{(Eqn. 1)}$$

where the reference is VSMOW and the sample is collected at a specific location (Gonfiantini, 1978). The guaranteed analytical precision of the water isotope analyzer is $0.025^{0}/_{00}$ for $\delta^{18}O$ and 0.1‰ for δ^2H. The analyzer had standards run during the

beginning, end, and intermittently to account for any shifts in the machine through each runtime (Appendix 3).

Modeling Stream Discharge

Discharge data from the Lester River were not collected during the summer of 2018, so a linear regression was developed between precipitation and discharge collected from April 20, 2011 to December 31, 2016 by the Minnesota Department of Natural Resources (DNR) and Minnesota Pollution Control Agency (MPCA) (Minnesota Department of Natural Resources, 2019). To create the model, a linear regression was plotted through the precipitation and discharge data. The model examined the response time of the watershed by testing the precipitation on the same day as discharge, and with a time-lag of one, two, or three days. The two best response times (same day and one-day lag time) were then used with a threshold value of precipitation (1.8 inches) to further refine the model. This regression was used to determine discharge near the stream outlet (Site 3) using precipitation measured by the National Weather Service for the watershed over the study period. Stream discharge was then scaled to each site location based on watershed contributing area.

Statistical Analysis

R statistical software was used to create a linear regression model for temperature (°C) and $\delta^{18}O$ values. ANOVA tests were used to compare mean $\delta^{18}O$ values across sampling dates and sampling locations as well as temperatures across site locations (α=0.05). Tukey's HSD tests were used to perform pairwise comparisons, controlling for

multiple tests to produce adjusted p-values with 95% familywise confidence (Tukey, 1949). δ^2H and $\delta^{18}O$ were plotted against the Global Meteoric Water Line (GMWL, $\delta^2H=8*\delta^{18}O + 10$) and Local Meteoric Water Line (LMWL, $\delta^2H=8.4*\delta^{18}O + 15.5$) by sampling dates and by site location (Rozanski, et al, 1993; Jasperson, et al., 2018).

Table 4-2) Summary of samples collected in the Lester River Watershed from May 21, 2018 to December 18, 2018. Mean values (μ) and one standard deviation (σ) of the $\delta^{18}O$ and $\delta^{2}H$ across all fifteen study sites for each sample date during the study period.

Date	# of samples	Precip. (cm)	Mean Air Temp (°C)	μ ($\delta^{2}H$)	σ ($\delta^{2}H$)	μ ($\delta^{18}O$)	σ ($\delta^{18}O$)	Snapshot Temps (°C)	d-excess
5/21/2018	20	0.0508	12.6	-78.13	1.54	-10.79	0.21	12.46	8.12
5/29/2018	20	3.5306	20.7	-74.45	4.12	-10.36	0.28	n/a	8.49
6/4/2018	20	3.7592	12.4	-70.94	1.27	-10.17	0.20	n/a	10.40
6/12/2018	20	0.9652	15.2	-70.15	1.48	-9.88	0.21	n/a	8.94
6/19/2018	20	6.0198	18.6	-57.55	1.27	-8.58	0.14	17.74	11.08
6/26/2018	20	0.1524	16.9	-60.86	2.65	-8.76	0.25	15.81	9.22
7/2/2018	20	6.1214	20.7	-61.10	1.07	-9.01	0.15	n/a	10.98
7/10/2018	20	2.7432	22.1	-49.70	1.74	-7.70	0.18	19.43	11.92
7/16/2018	20	1.016	22.3	-53.39	3.07	-7.97	0.29	19.58	10.47
7/24/2018	20	0.254	19.3	-55.38	3.33	-8.05	0.35	19.34	9.05
7/31/2018	20	0.1778	19.2	-56.48	4.54	-8.03	0.60	18.68	7.75
8/7/2018	20	4.1402	18.1	-58.09	5.03	-8.30	0.65	17.18	8.29
8/13/2018	19	0	24.2	-59.45	5.49	-8.38	0.79	21.26	7.58
8/21/2018	20	0.0762	19.8	-60.80	5.88	-8.50	0.95	18.49	7.17
8/28/2018	20	3.81	18.5	-59.63	6.19	-8.36	0.96	n/a	7.25
9/3/2018	20	2.3876	18.2	-58.11	4.73	-8.30	0.60	15.95	8.27
9/11/2018	20	0.4064	17.0	-58.72	4.90	-8.35	0.62	18.05	7.92
9/18/2018	20	4.445	20.1	-56.17	1.97	-8.36	0.28	16.21	10.78
9/25/2018	20	2.667	11.7	-57.52	1.33	-8.59	0.17	n/a	11.16
10/2/2018	20	0.9398	7.4	-59.81	2.32	-8.78	0.28	n/a	10.44
10/9/2018	20	6.2992	6.9	-62.74	2.02	-9.42	0.24	7.4	12.59
10/18/2018	10	2.6416	2.8	-65.17	1.18	-9.61	0.19	4.77	11.67
10/24/2018	10	0.254	5.2	-65.22	1.83	-9.52	0.26	4.25	10.99
10/31/2018	15	2.5146	5.9	-69.22	1.84	-10.08	0.27	4.39	11.48
11/7/2018	20	1.5748	1.7	-73.30	1.87	-10.71	0.32	2.28	12.40
11/13/2018	10	0.3556	-7.8	-71.76	1.53	-10.43	0.32	n/a	11.72
11/20/2018	8	0.5334	-6.6	-71.91	1.39	-10.46	0.33	n/a	11.77
11/27/2018	8	1.4732	-5.2	-75.54	1.58	-11.01	0.30	n/a	12.51
12/4/2018	8	0.3048	-4.5	-73.92	1.30	-10.79	0.26	n/a	12.37
12/11/2018	7	0.0254	-7.9	-73.90	1.19	-10.75	0.29	n/a	12.10
12/18/2018	4	0	-1.6	-74.38	1.38	-10.85	0.34	n/a	12.41

Results

Temporal Variability in Isotopic Signatures

Data collected from all sites in the Lester River watershed show an observable sinusoidal seasonal trend (Figure 4-3). Mean $\delta^{18}O$ values from July, August, and September varied from -7.70$^{0}/_{00}$ and -9.01$^{0}/_{00}$. The maximum summer value from all sites was -6.54$^{0}/_{00}$ and the minimum summer value was -9.86$^{0}/_{00}$ These mean values were significantly different from data collected during May, October, November and December. The mean $\delta^{18}O$ values from these months ranged from -9.42$^{0}/_{00}$ to -11.01$^{0}/_{00}$ (Table 4-2, Appendix 5). The maximum value across all sites from October to December was -8.39 $^{0}/_{00}$ and the minimum value was -11.51$^{0}/_{00}$. Early June showed similar patterns of the isotopic mean $\delta^{18}O$ values of May, the middle and end of October, and the middle and end of November and December. While on the other hand, the end of June showed similar mean $\delta^{18}O$ values to the month of August, the month of September, and the beginning of October. The isotopic data generally grew heavier during the summer (July), with more evaporation in late summer and early fall (August and September). Streamflow signatures then grew lighter as late fall progressed into winter (October, November, and December) (Figure 4-4).

Spatial Variability in Isotopic Signatures

Across all site locations, the mean $\delta^{18}O$ values varied between -8.62 $^{0}/_{00}$ and -9.43 $^{0}/_{00}$. There was no significant difference between the mean $\delta^{18}O$ values across the different sites (Figure 4-5, Appendix 5). Site 4 had the lightest $\delta^{18}O$ value of -11.51$^{0}/_{00}$, while site 6 had the heaviest $\delta^{18}O$ value of -6.53$^{0}/_{00}$. During the summer months of July

and August, the $\delta^{18}O$ values exhibited greater variation than other months (Figure 4-5, Table 4-2).

Specific sites within the watershed showed trends. The sites with the largest variance were sites 6, 7, and 10. Site 10 is the headwaters of the watershed and had a mean $\delta^{18}O$ value of -9.14$^{0}/_{00}$, and most samples plotted along the LMWL (Figure 4-6, Table 4-3). Site 6 and 7 are wetlands and exposed to more evaporation. These sites had mean $\delta^{18}O$ values of -8.62$^{0}/_{00}$ and -9.2$^{0}/_{00}$ respectively. These sites plotted lower than the GMWL and LMWL and closer to the local evaporation line (LEL, $\delta^{2}H=5.2*\delta^{18}O - 18.7$) (Jasperson, et al., 2018). Site 1 was at the mouth of the Lester River, and plotted in between the LWML and the data affected by evaporation (Figure 4-6). It had a mean $\delta^{18}O$ value of -9.39 $^{0}/_{00}$ with the variance of the data in the middle of the values. The lowest variance was found at sites 8, 11 and 14. Each of these sites are located along the main stem of the stream.

Stream Discharge

The Lester River watershed responds quickly to precipitation events (Figure 4-7). Discharge data collected at Site 3 from 2011 to 2016 was used with precipitation data from the same time period to model discharge in the stream across all sites during the sampling period in 2018 (NOAA 2018; Minnesota Department of Natural Resources, 2019). The best modeled response of the stream was found to occur within one-day of the rain event and used the threshold precipitation (model 5, $R^2 = 0.77$) (Table 4-4). The data were used to determine baseflow conditions at the mouth of the stream (Site 1) to be 0.39 cms (Figure 4-8).

Table 4-3) Mean values (μ) and one standard deviation (σ) of the $\delta^{18}O$ and $\delta^{2}H$ across the fifteen sampling sites for each sample date during the study period.

	$\delta^{2}H$		$\delta^{18}O$	
Site ID	**μ**	**σ**	**μ**	**σ**
1	-65.35	7.1	-9.39	0.95
2	-65.44	7.22	-9.43	0.95
3	-65.63	7.03	-9.42	0.9
4	-65.29	7.24	-9.42	1.01
5	-65.46	6.95	-9.43	0.91
6	-59.9	8.85	-8.62	1.32
7	-63.62	9.71	-9.2	1.47
8	-63.69	6.68	-9.08	0.84
9	-60.17	7.92	-8.83	1.03
10	-61.07	9.52	-9.14	1.19
11	-64.05	7.19	-9.21	0.84
12	-62.57	7.61	-9.02	0.97
13	-64.77	7.3	-9.19	0.96
14	-64.43	6.69	-9.26	0.77
15	-60.69	7.44	-8.82	1.01

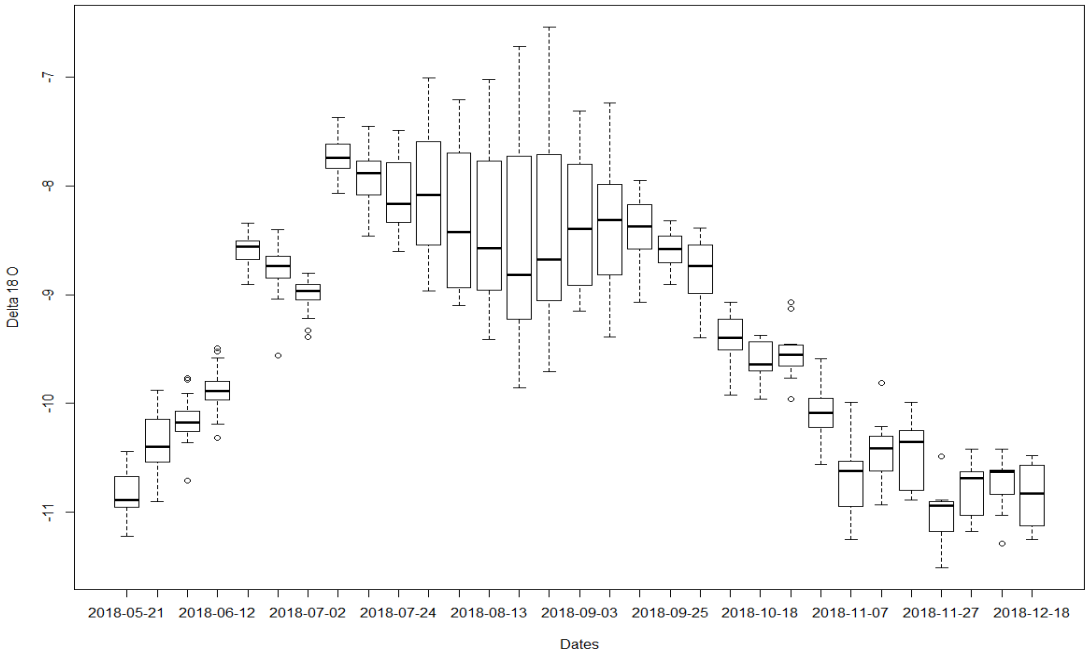

Figure 4-3) Samples collected from all sites in the Lester River watershed across the dates collected. Mean values and variance in the data are shown.

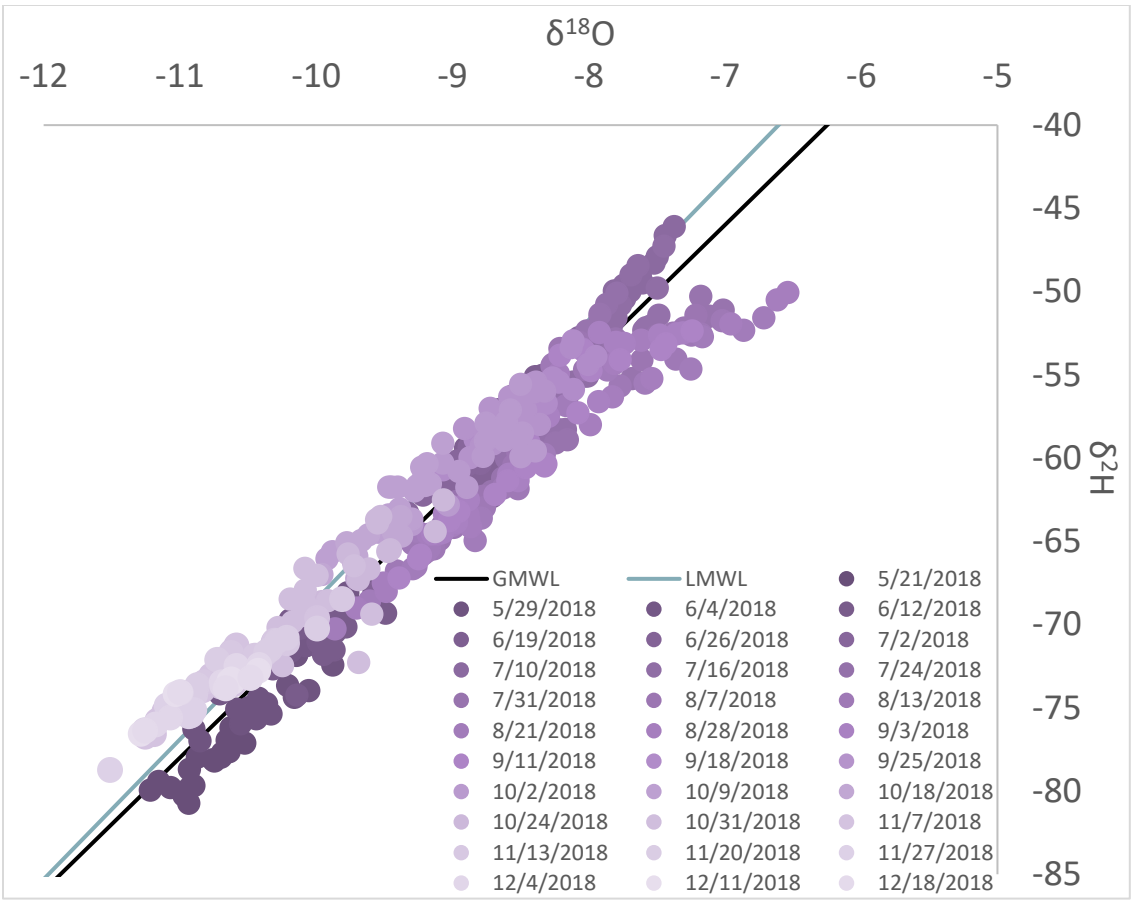

Figure 4-4) All data collected in the Lester River watershed presented by the sampling collection date.

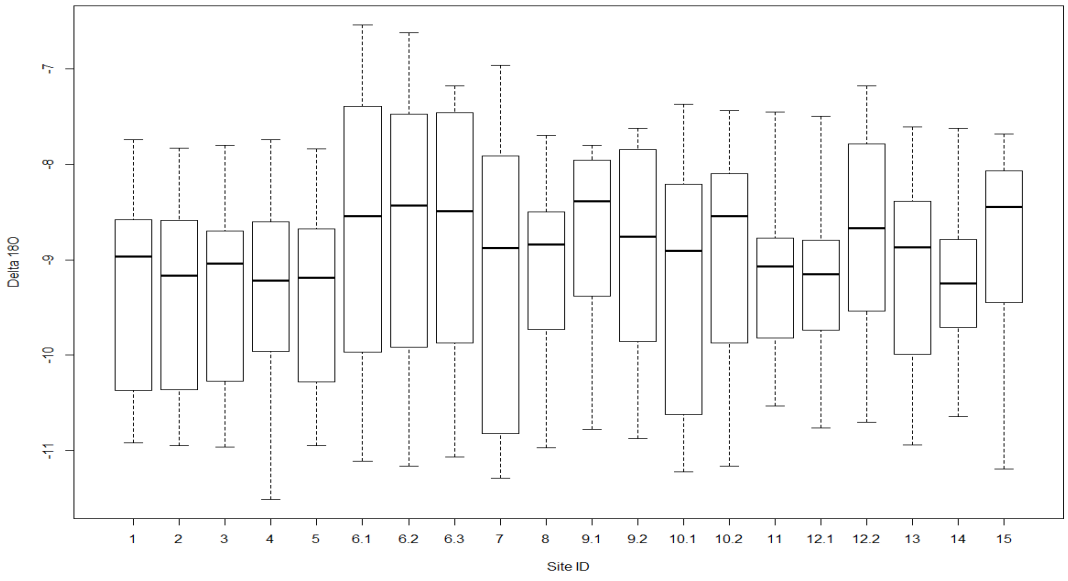

Figure 4-5) Mean $\delta^{18}O$ values for each site location.

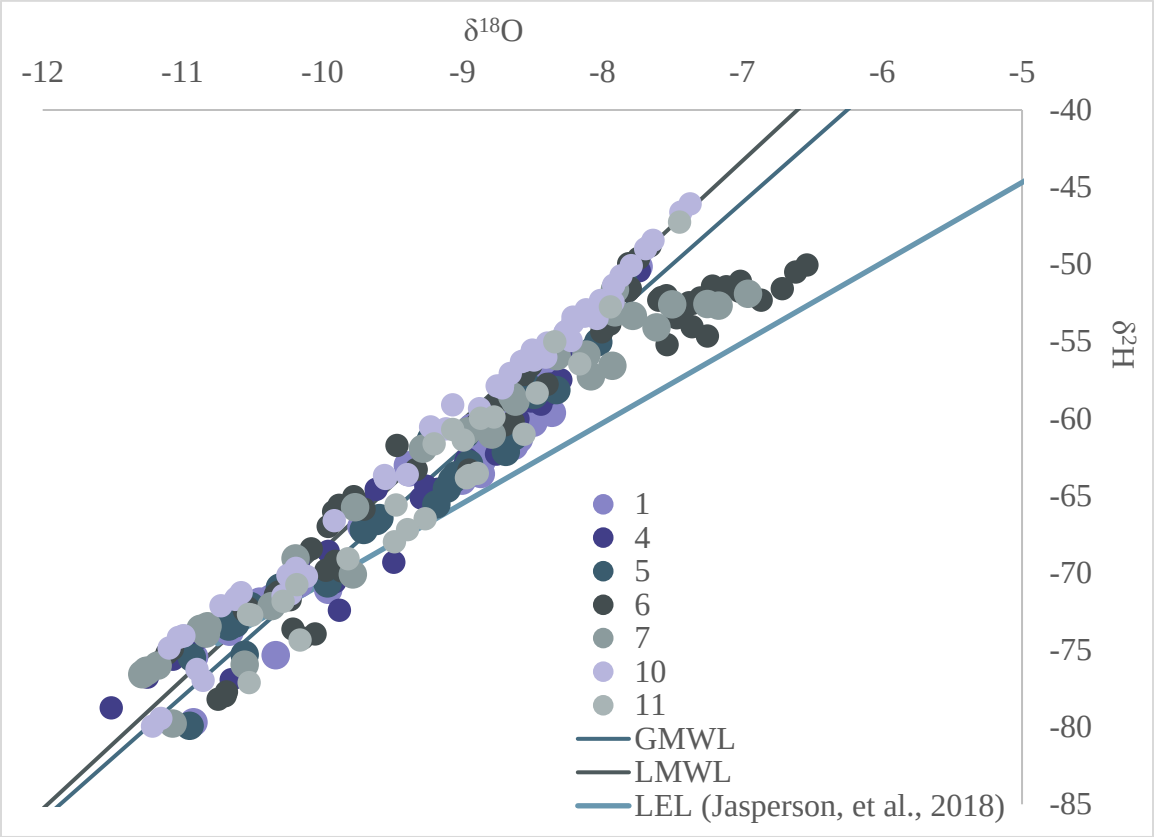

Figure 4-6) Data across all the dates presented by the site locations for seven of the fifteen sites. Data plotted against the GMWL, LMWL, and LEL (Rozanski, et al, 1993; Jasperson, et al, 2018).

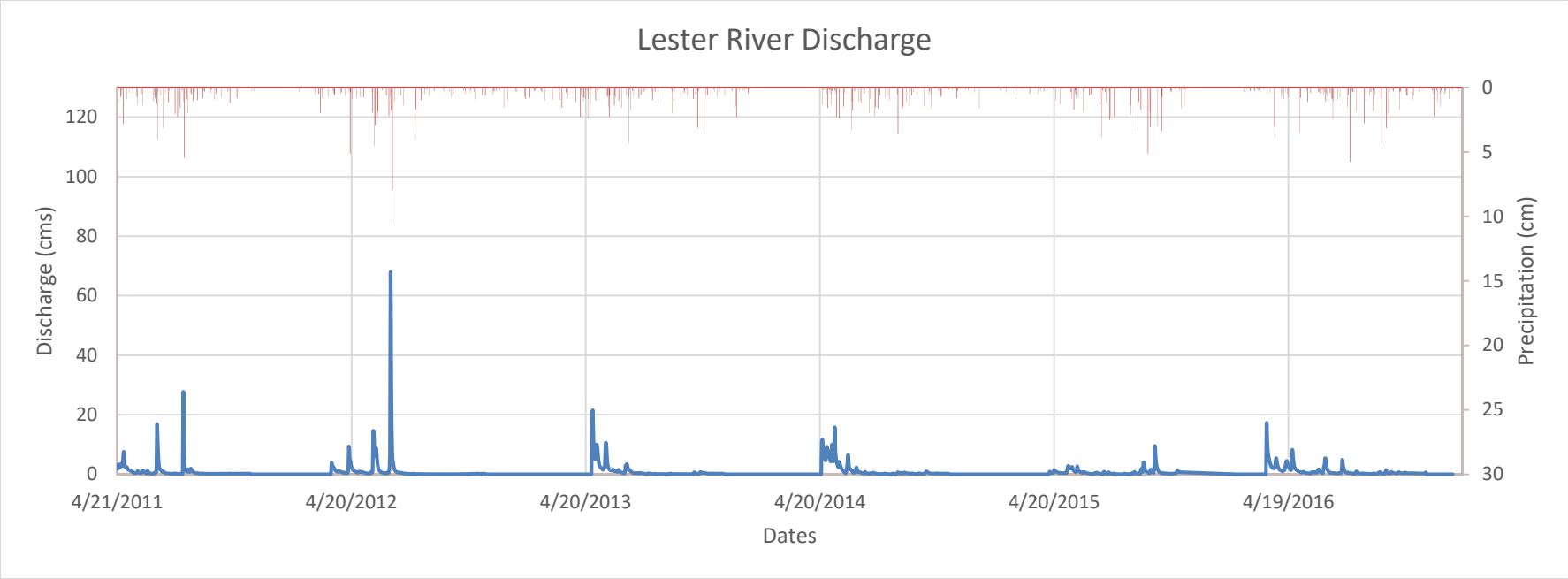

Figure 4-7) Hydrograph of stream discharge and precipitation data from April 2011 to December 2016 (NOAA, 2018; Minnesota Department of Natural Resources, 2019).

Table 4-4) Comparisons of linear models between Discharge and Precipitation using R statistical software.

	Model	Lag in Time	R^2 Value	p-value	F-statistic	DF		Estimate Std.	p-value
All data used	1	none	0.1092	<2.2e-16	222.6	1806	Intercept	18.271	2.00E-16
							Slope	114.875	2.00E-16
	2	1 day	0.2777	<2.2e-16	695.6	1806	Intercept	11.942	9.90E-10
							Slope	182.865	2.00E-16
	3	2 day	0.07354	<2.2e-16	144.4	1806	Intercept	20.184	2.00E-16
							Slope	94.371	2.00E-16
Data using precipitation above 1.8 cm.	4	none	0.2227	9.56E-05	17.62	57	Intercept	-204.06	0.0282
							Slope	279.6	9.56E-05
	5	1 day	0.7751	<2.2e-16	200.9	57	Intercept	11.21	0.633
							slope	499.08	2E-16

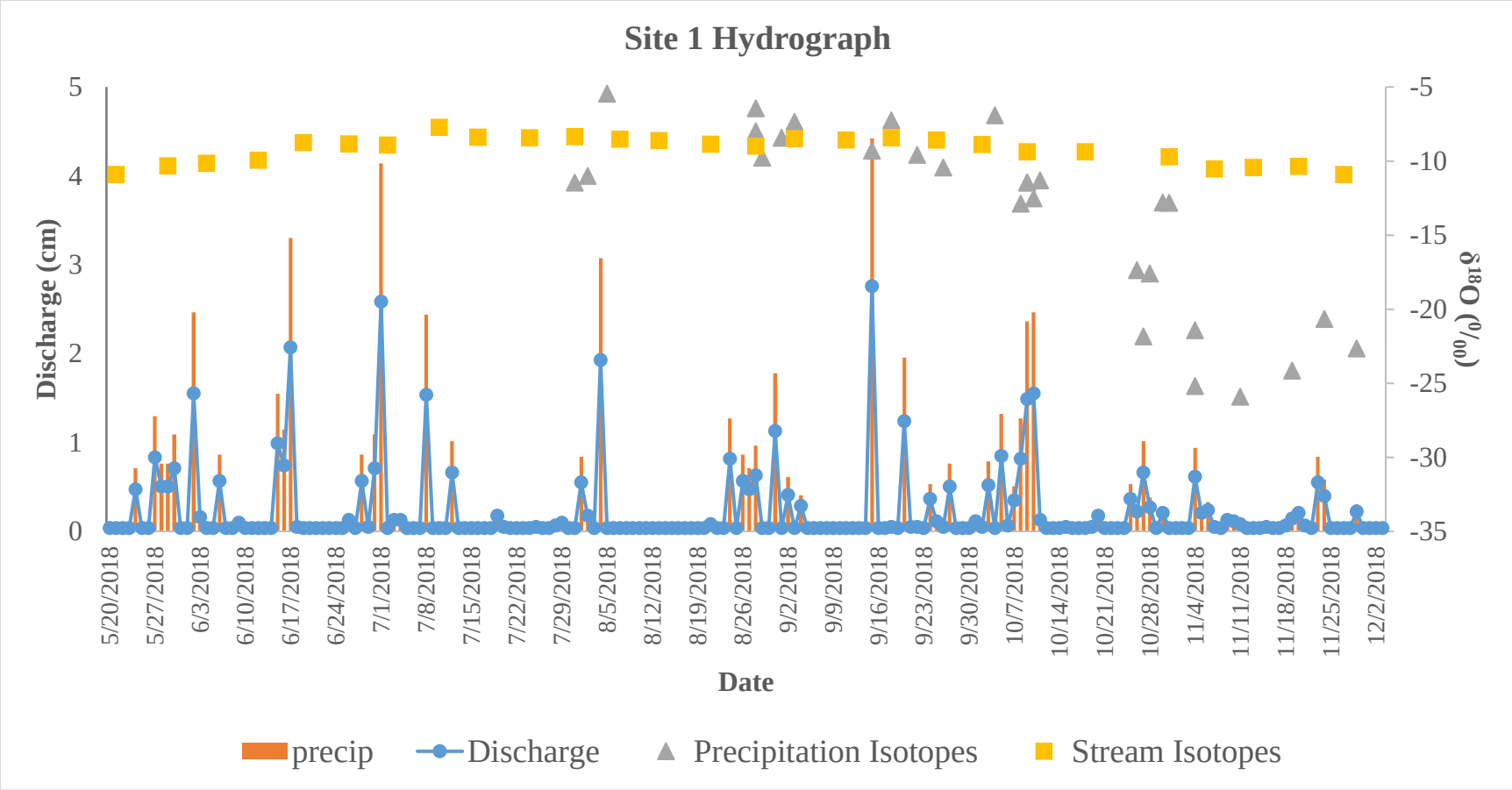

Figure 4- 8) Hydrograph for Site 1, the mouth of the Lester River, over the sampling period (5/2018-12/2018) using modeled discharge data from model 5 (Table4-4).

D-excess

The deuterium excess values across space and time shows the opposite trend than the isotope data from the stream. The values become lower in the summer months of July and August, falling from 10 to 7 indicating evaporative loss before increasing into September, October, November, and December from 10 to 12 indicating moisture recycling (Table 4-2) (Frohlich, et al., 2001). The lowest d-excess of 2.15 occurred in August at site 6, a wetland area which is often isotopically heavier due to evaporation. The highest d-excess value was 14.05 at site 10, the headwaters, in December. Overall, there was no consistent trend in d-excess across the sites relating to the average global d-excess of 10. The variance in the d-excess changes seasonally with greater variance in the summer and early fall months and less variance in winter and spring (Figure 4-9).

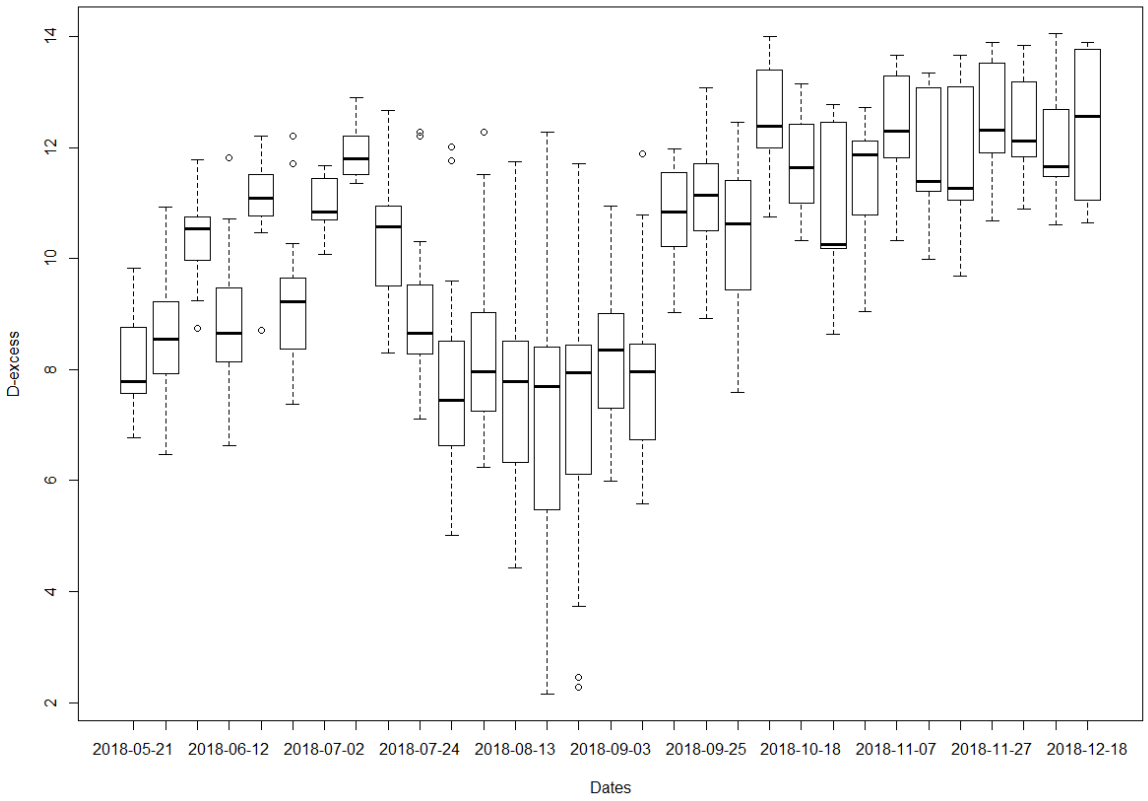

Figure 4-9) D-excess of stream isotopic values plotted against sampling dates.

Temperatures

Stream temperature was positively correlated with stream $\delta^{18}O$ values (R^2 = 0.526, p-value = 2.2E-16). Stream $\delta^{18}O$ became heavier with warming stream temperatures (Figure 4-10). Temperatures showed the same seasonal trend as the isotopes, with temperature increasing in the summer months and then decreasing into the fall. Likewise, the variability in temperature both within and across sites was greater in the summer than in the fall. The mean stream temperatures ranged from 12.6 to 16.5 °C. Despite the temporal trends, mean stream temperatures at each site across the study period were not significantly different from one another (Figure 4-11, 4-12).

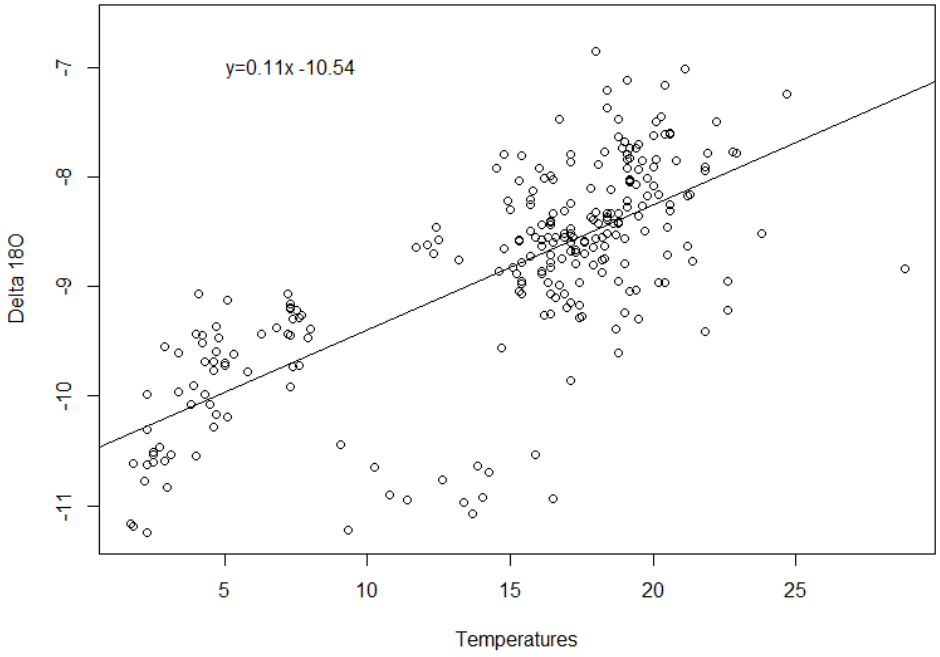

Figure 4-10) Linear regression between temperatures (°C) and $\delta^{18}O$ values collected at the same time. The regression equation is $\delta^{18}O$=0.11 T-10.54.*

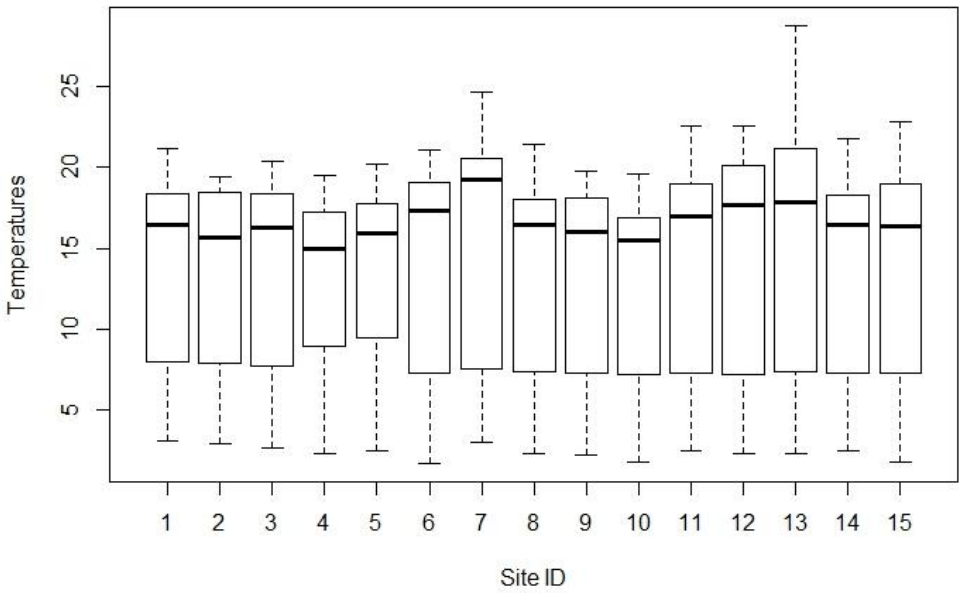

Figure 4-11) Mean values of Temperature (°C) across site locations.

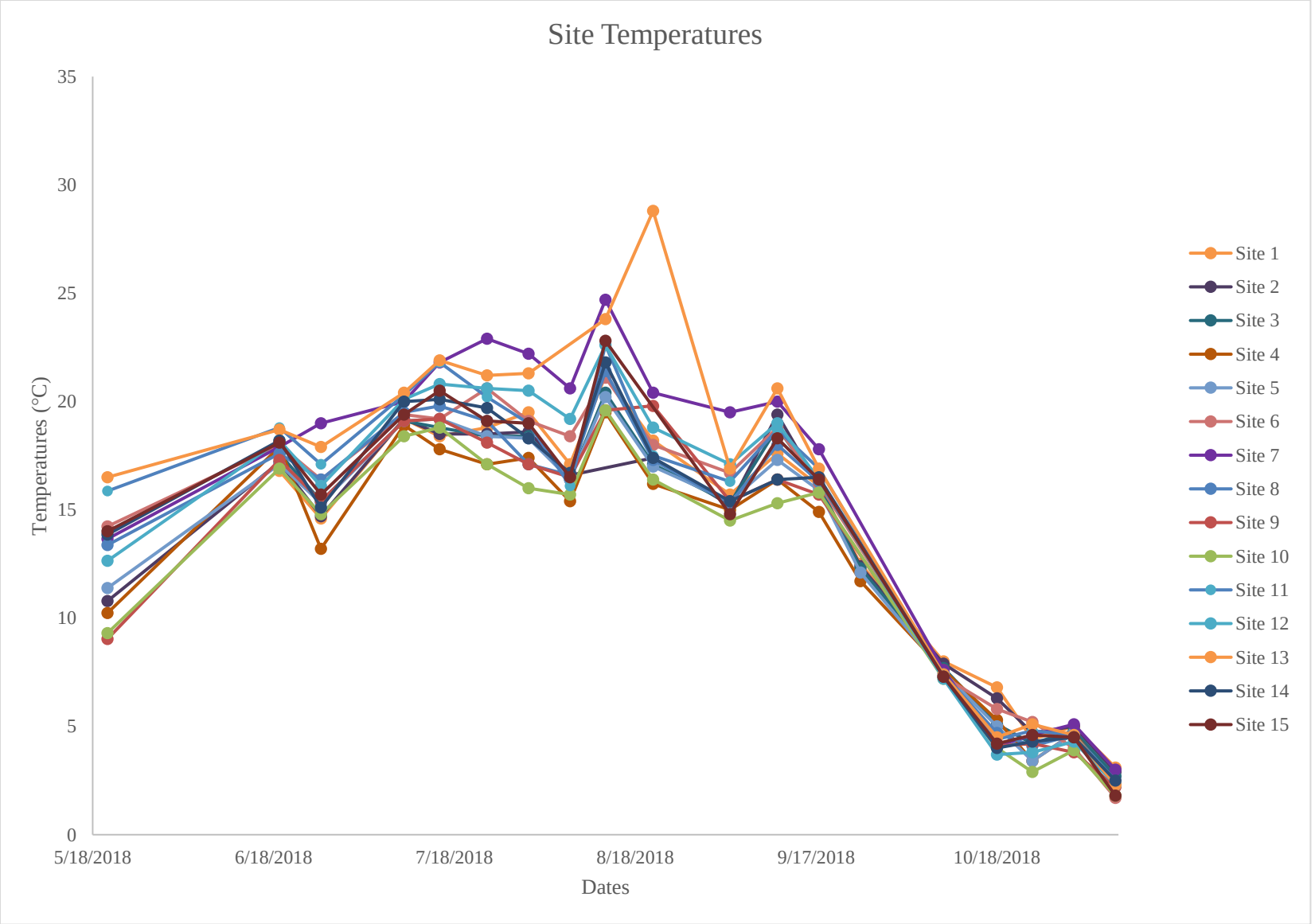

Figure 4-12) Snapshot temperature data collected at each site location.

Discussion

Temporal Variability in Isotopic Signatures

The Lester River shows a clear temporal trend in the isotopic signature across all sites in the stream. $\delta^{2}H$ and $\delta^{18}O$ values are heavier in the summer months (July and August) and lighter in spring and winter months (May, October, November, and December) (Figures 4-3, 4-4). The response of the watershed to precipitation events is seen more clearly on a spatial scale or through changes in variance. Isotopic signatures at the mouth of the river are consistent through time and are mostly impacted by seasonal changes (Figure 4-8) (Kendall and Coplen, 2001). There is a consistent pattern across the globe where snowmelt in the spring produces lighter isotopes and precipitation events over the summer produce heavier isotope values in streams. Precipitation events become a mixture of snow and rain during the fall and winter months, overall producing lighter isotopic values. This pattern occurs due to the relationship between temperature and isotope fractionation and only changes due to unique storm events (Clark and Fritz, 1997; Scholl, et al., 1996). Any changes to the precipitation patterns of the Lester River will result in changes to the stream itself and water movement throughout the watershed. Storm-driven precipitation isotopes have been noted to control the seasonality present in water near the Kilauea volcanic area of Hawaii rather than temperature seasonality due to the frequency of storms (Scholl, et al., 1996).

Within the Lester River, temporal data provide an understanding of how the stream responds to storm events as well as droughts. This information can be used to investigate groundwater recharge in the watershed as well as groundwater inputs into the stream. Groundwater recharge would likely occur during snowmelt (April and May) or

during the fall (September and October) due to the higher precipitation inputs during these times. The precipitation into the stream caused less variance in the isotopic values of stream water and would provide an incoming source of water that can infiltrate through soil to recharge groundwater. During the summer months (July and August), the amount of precipitation was low, while variance in isotopic values increased (Figure 4-3). The warmer temperatures of summer and evapotranspiration of plants slows the process of precipitation infiltrating into groundwater. During these months, stream discharge contains greater portions of baseflow in parts of the British Isles (Darling, et al., 2003). To understand groundwater recharge into Lake Superior, it would be useful to understand the timing and amount of recharge in watersheds and groundwater inputs into the streams around the lake.

Spatial Variability in Isotopic Signatures

The mean $\delta^{18}O$ in streamflow across all sites and dates was $-9.11^{0}/_{00}$ with $\sigma = 1.08$ (Figure 4-5). Temperature data across all sites and dates averaged 14.67 °C with a $\sigma =$ 5.23 (Figure 4-11). Spatially, the isotopic values across the watershed change due to environmental conditions. During times of greater precipitation inputs (May, June, September, October), the system shows less variability in both isotopic values and temperatures (Figures 4-3, 4-12; Appendix 5). During times of lower precipitation (July and August), the isotopic values and temperatures show greater variability (Table 4-2).

Departures from the GMWL and LMWL highlight different hydrological processes in the watershed at specific site locations. Sites 1, 6, 7, 10, and 11 are the most notable. Sites 6 and 7 are exposed wetlands and ponds resulting in more evaporation and

together cover 12.5% (11.5 km^2) of the total watershed area. The signatures at these sites fall below the GMWL and LMWL. Jasperson, et al. (2018) produced a LEL (δ^2H = 5.21* $\delta^{18}O$ – 18.72, R^2=0.98) from data collected during the month of September in a nearby watershed. Evaporation leaves water with an enriched isotopic signature plotting along LELs with slopes around 4-7. The slope of the line is related to humidity with steeper slopes being found in more humid conditions (Clark and Fritz, 1997). Isotopic data from sites 6 and 7 indicate evaporation occurs in these locations, but the data do not fall on the LEL (Figure 4-6). Wu, et al. (2019) examined spatial and temporal variations in river water and precipitation throughout Kyrgyzstan. The data collected were used to produce a LMWL from monthly average-weighted precipitation values and a River Water Line (RWL). The RWL was developed using stream water samples across multiple years and seasons including: autumn 2012, summer 2013, and spring 2014. The study compared RWLs from each season as well noting differences in the slopes and intercepts from changes to climatic conditions and water supply. The LMWL and RWL in their study area produced similar lines leading to the conclusion that the river water did not experience substantial evaporation. From the stream samples collected in the Lester River watershed, the RWL is $\delta^2H = 7*\delta^{18}O +0.82$ (R^2= 0.96). The slope and the intercept for the RWL fall between the values of the LEL and LMWL, indicating that the Lester River watershed experienced noticeable evaporation to some degree.

Sites 10 and 11 are located near the headwaters of the stream and cover 13.7% (12.5 km^2) of the total watershed area. Isotopic values from these sites plot along the LMWL created from precipitation values in the area (Figure 4-6) (Jasperson, et al., 2018). Groundwater often carries a similar isotopic signature to average annual isotopic

precipitation values. This comes from precipitation being the main source of groundwater recharge over time (Kendall and Coplen, 2001; Sklash and Farvolden, 1976). Because sites 10 and 11 plot along the LMWL, these sites are possible sources of groundwater input during times of little to no precipitation. Site 1 is located at the mouth of the river and plots in the middle of all the values and closer to the RWL. This indicates that the sample at the mouth of the river aggregates evaporation and groundwater signals occurring across the watershed in times of low precipitation. Samples collected here could be an accurate representation of the average isotopic values in the watershed over time.

D-excess

D-excess has been shown to correlate well with climatic conditions and is often used to estimate secondary processes occurring to the contents of atmospheric vapor (Frohlich, et al., 2001; Machavaram and Krishnamurthy, 1995). D-excess has a global average of $10^{0}/_{00}$ from the equation:

$$d=\delta^{2}H - 8*\delta^{18}O \quad \text{(Eqn. 1)}$$

where d= deuterium excess and $\delta^{2}H$/ $\delta^{18}O$ are the isotopic ratios of hydrogen and oxygen from a sample compared with a standard and written in per mil notation (Dansgaard, 1964). D-excess shows clear geographical and seasonal trends. The trend within the northern hemisphere shows maximum values of d-excess in winter and minimum values during the summer. This is related to the relative humidity and evaporation conditions, where more evaporation leads to higher d-excess values (Frohlich, et al., 2001). The data collected from the Lester River show a similar trend in

the d-excess values, with minimum values found in July and August and maximum values found in October, November, and December. As summer months warm, relative humidity rises, resulting in lower evaporation rates. This decreases d-excess values (Frohlich, et al., 2001; Machavaram and Krishnamurthy, 1995). The seasonal trend found across multiple study regions in Japan was accounted for by incoming moisture from multiple sources to each location (Katsuyama, et al., 2015). While the Great Lakes region receives precipitation from multiple sources, evaporation from the lake itself accounts for the seasonal trends found in the Lester River (Gat, et al., 1994; Jasechko, et al., 2014). Within the Lester River watershed, d-excess values ranged from 2.2 to 18.2 $^{0}/_{00}$(mean = 10.1$^{0}/_{00}$), with the mean aligning well to the global average. Machavaram and Krishnamurthy (1995) have noted how understanding d-excess can further inform processes regarding changes to atmospheric conditions directly around the Great Lakes, including LES. When examining the United States as a whole, the eastern states have d-excess values from 10-15$^{0}/_{00}$. The western states have d-excess values less than 6$^{0}/_{00}$ with greater overall spatial heterogeneity. D-excess values along the north shore of Lake Superior were modeled to be between 2 -10$^{0}/_{00}$ (Kendall and Coplen, 2001). Katsuyama, et al. (2015) stated that the stream values in Japan collected over the summer were biased towards winter precipitation in snowy regions, highlighting the need for collecting information over a long-time scale. Due to the influence of snow on the Lester River watershed, future work should consider collecting data over long periods of time to examine any seasonal biases.

Temperatures

Streams with colder waters are important to the communities along the north shore of Lake Superior involved in fishing. In the Duluth area, brook trout (*Salvelinus fontinalis*) are a native species that thrive in colder waters. Brook trout prefer to live in waters with temperatures between 7.8 and 20°C. They reach stress levels when stream temperatures rise above 20 to 25°C and cannot survive in these conditions for long periods of time (Lakesuperiorstreams, 2009). Stream temperatures are controlled by the amount of light, depth of water, air temperatures, and groundwater inputs to the stream (Lakesuperiorstreams, 2009; Leach and Moore, 2011). Across the Lester River, the temperatures rose above the 20°C threshold during the study period at eleven different site locations. Site 13 had the highest temperature that went to 28.8°C (Figure 4-12). The temperatures went above 20°C from July 10th to September 11th, 2018. Overall, this shows that the Lester River would be okay for brook trout spawning and growth, although not optimal (Appendix 4).

Deep groundwater discharge into streams subdues changes in stream chemistry and temperatures. Water from directly below the bed of the stream includes more mixing of source waters. This shallower ground water would still follow seasonal patterns shown in both temperatures and stream chemistry (Leach and Moore, 2011). In the Lester River, four sites (Site 2, 4, 9, and 10) showed less variability and had generally colder stream temperatures overall. These sites followed the seasonal patterns but could be the result of groundwater input into the stream when input from precipitation is lower. Due to the amount of variation still present in stream temperatures at these sites, it is likely that any groundwater input into the stream came from a shallow source. Understanding the

groundwater input into streams along the north shore is important for maintaining fisheries and protecting fish habitats (Jasperson, et al., 2018).

Air temperatures have been found to correlate well with $\delta^{18}O$ in precipitation. Within the United States, eastern states follow a regression line of $y=0.51x+13.09$ ($R^2= 0.85$) and western states follow the line $y=0.58x-18.46$ ($R^2= 0.44$) where $y= \delta^{18}O$ and x=temperatures (°C) (Kendall and Coplen, 2001). The smaller correlation in the western states is attributed to irregular topography and seasonal differences in sources of moisture in the air (Kendall and Coplen, 2001). A study in Japan also correlated the $\delta^{18}O$ in stream waters with mean air temperatures, showing a regression line $y=0.44x-13.5$ ($R^2=0.77$) (Katsuyama, et al., 2015). Stream temperatures are often correlated with mean air temperatures (Leach and Moore, 2011). The regression line created through my data compares stream temperatures and $\delta^{18}O$ values, $\delta^{18}O=0.11* T-10.54$, resulting in a different slope and intercept than the other correlations made within the United States (Figure 4-10, $R^2=0.526$). The Lester River watershed shows some topographic changes and is subjected to moisture from multiple sources over the course of the year explaining the lower correlation. The regression produced for this region identifies another reason to consider the Great Lakes Region unique.

Chapter 5: Conclusion

Overall, the two projects have provided information to guide future research in watersheds along the north shore of Lake Superior. The data collected from the five sites along the north shore showed a seasonal trend in precipitation and stream water isotopes. Storms traveling over the distance of the shore would be expected to have changing isotopic signatures. However, there was no clear trend in changes across the sites within a specific storm. Different types of storms start with different source waters, leading to the expectation of isotopically different precipitation. My data do not demonstrate this distinction between storms. In order to see trends in specific storm types clearly, more data over a longer time period would be needed. It is also possible that Lake Superior acts as another major source of atmospheric moisture along the north shore. The influence of the lake has been noted along the south shore due to LES, but the effect that it has in snow storms along the north shore is still unknown.

Within the Lester River watershed, a more extensive spatial and temporal dataset was collected. These data showed seasonal trends in the isotopic signatures and temperatures of the stream across all site locations. Over the course of the study period, the impact of precipitation on stream signatures showed lower variability than times of drought. During long stretches of time without precipitation, the effects of evaporation at different sites in the stream became noticeable. At certain sites with lower variance in temperatures and isotopic signatures, groundwater input into the stream is possible during droughts. While there were clear spatial trends across the watershed, the isotopic values across all sites reached a common average value of $-9.11^{0}/_{00}$. The samples collected at the mouth of the river often resembled the average values, combining the effects of precipitation, evaporation, and groundwater inputs across the watershed overall.

There have been noticeable differences in storms around the Great Lakes region, including along the north shore of Lake Superior. The frequency and intensity of storms has increased, impacting the streams along the north shore which respond quickly to precipitation events. As more and larger storm events begin impacting the streams, there could be changes to stream morphology and increases in sediment erosion. These changes along with changes in discharge levels could also impact fish habitat. The Lester River showed temperature conditions suitable for trout habitation. Maintaining the ability of the streams along the north shore to support fish is important to the surrounding communities. Changing the timing and magnitude of different seasonal events, such as snowmelt, could also lead to changes in the functioning of the stream and possibly groundwater recharge as well. These changes would be seen in isotopic signatures outside of the seasonal pattern established through the data. Overall, the data show that changes to seasonal processes in the region would lead to changes in the streams. In order to notice changes, data would need to be collected on a long-term scale. Future work should focus on sampling snow from a variety of storms at different along the north shore over time as well as identifying the timing of groundwater input and recharge in watersheds. The information of the hydrologic processes in the Lester River watershed could be applied to other watersheds along the north shore as well to see if any microclimate changes occur.

References

Ala-aho, P., Tetzlaff, D., McNamara, J. P., Laudon, H., Kormos, P., and Soulsby, C. (2017). Modeling the Isotopic Evolution of Snowpack and Snowmelt: Testing a spatially distributed parsimonious approach. *Water Resources Research*, 53, 5813–5830.

Arnfield, A. J. (2019), Köppen climate classification. Encyclopædia Britannica, inc.

Blavoux, B., & Olive, P. (1981). Radiocarbon dating of groundwater of the aquifer confined in the Lower Triassic sandstones of the Lorraine region, France. *Journal of Hydrology*, *54*, 167–183.

Brooks, K. N., Ffolliott, P. F., and Magner, J. A. (2013). Hydrology and the Management of Watersheds (Fourth). John Wiley and Sons, Inc.

Bowen, G. J., Kennedy, C. D., Henne, P. D., & Zhang, T. (2012). Footprint of recycled water subsidies downwind of Lake Michigan. *Ecosphere*, *3*(6).

Burnett, A. W., Kirby, M. E., Mullins, H. T., and Patterson, W. P. (2003). Increasing Great Lake-effect snowfall during the twentieth century: A regional response to global warming? *Journal of Climate*, *16*(21), 3535–3542.

Burnett, A. W., Mullins, H. T., and Patterson, W. P. (2004). Relationship between atmospheric circulation and winter precipitation $\delta^{18}O$ in central New York State. *Geophysical Research Letters*, *31*(22).

Clark, I. D., and Fritz, P. (1997). Environmental Isotopes in Hydrogeology. New York: Lewis Publishers.

Dansgaard, W. (1964). Stable isotopes in precipitation. *Tellus*, *16*(4), 436–468.

Darling, W. G., Bath, A. H., & Talbot, J. C. (2003). The O and H stable isotope composition of freshwaters in the British Isles. 2. Surface waters and groundwater. *Hydrology and Earth System Sciences*, *7*(2), 183–195.

DeWalle, D. R., & Rango, A. (2011). Principles of Snow Hydrology. New York: Cambridge University Press.

Epstein, S., & Mayeda, T. (1953). Variation of O^{18} content of waters from natural sources. *Geochimica et Cosmochimica Acta*, *4*, 213–224.

Frohlich, K., Gibson, J. J., & Aggarwal, P. K. (2001). Deuterium Excess in Precipitation and Its Climatological Significance. *International Atomic Energy Agency*, 54–66.

Gat, J. R., Bowser, C. J., & Kendall, C. (1994). The contribution of evaporation from the Great Lakes to the continental atmosphere: estimate based on stable isotope data. *Geophysical Research Letters*, *21*(7), 557–560.

Gedzelman, S. D., Rosenbaum, J. M., & Lawrence, J. R. (1989). The Megalopolitan Snowstorm of 11-12 February 1983: Isotopic Composition of Snow*. *Journal of Atmospheric Sciences*, *46*, 1637–1649.

Harper, J. T., & Bradford, J. H. (2003). Snow stratigraphy over a uniform depositional surface: spatial variability and measurement tools. *Cold Regions Science and Technology*, *37*, 289–298.

Hooper, R. P., & Shoemaker, C. A. (1986). A Comparison of Chemical and Isotopic Hydrograph Separation. *Water Resources Research*, *22*(10), 1444–1454.

Jasechko, S., Gibson, J. J., & Edwards, T. W. D. (2014). Stable isotope mass balance of the Laurentian Great Lakes. *Journal of Great Lakes Research*, *40*, 336–346.

Jasechko, S., Birks, S. J., Gleeson, T., Wada, Y., Fawcett, P. J., Sharp, Z. D., … Welker, J. M. (2014). The pronounced seasonality of global groundwater recharge. *Water Resources Research*, *50*(11).

Jasperson, J. L., Gran, K. B., & Magner, J. A. (2018). Seasonal and Flood-Induced Variations in Groundwater-Surface Water Exchange in a Northern Coldwater Fishery. *Journal of the American Water Resources Association*, 1–18.

Jouzel, J., Delaygue, G., Landais, A., Masson-Delmotte, V., Risi, C., and Vimeux, F. (2013). Water isotopes as tools to document oceanic sources of precipitation. *Water Resources Research*, *49*(11).

Katsuyama, M., Yoshioka, T., & Konohira, E. (2015). Spatial distribution of oxygen-18 and deuterium in stream waters. *Hydrology and Earth System Sciences*, *19*(2009), 1577–1588.

Kendall, C., & Coplen, T. B. (2001). Distribution of oxygen-18 and deuteriun in river waters across the United States. *Hydrological Processes*, *15*(7), 1363–1393.

Kendall, C., and McDonnell, J. J. (1998). Isotope Tracers in Catchment Hydrology. Amsterdam, Netherlands: Elsevier.

Klaus, J., & McDonnell, J. J. (2013). Hydrograph separation using stable isotopes: Review and evaluation. *Journal of Hydrology*, *505*, 47–64.

Kong, Y., & Pang, Z. (2012). Evaluating the sensitivity of glacier rivers to climate change based on hydrograph separation of discharge. *Journal of Hydrology*, *434*, 121–129.

Kunkel, K. E., Westcott, N. E., and Kristovich, D. A. R. (2000). Climate Change and Lake-Effect Snow. Preparing for a Changing Climate: The Potential Consequences of Climate Variability and Change, 25–28.

Lakesuperiorstreams. (2009). LakeSuperiorStreams: Community Partnerships For Understanding Water Quality and Stormwater Impacts at the Head of the Great Lakes (http://lakesuperiorstreams.org). University of Minnesota-Duluth, Duluth, MN 55812.

Lawrence, J. R., Gedzelman, S. D., White, J. W. C., Smiley, D., & Lazov, P. (1982). Storm trajectories in eastern US D/H isotopic composition of precipitation. *Nature*, *296*(April), 638–640.

Leach, J. A., & Moore, R. D. (2011). Stream temperature dynamics in two hydrogeomorphically distinct reaches. *Hydrological Processes*, *25*(September 2010), 679–690.

Machavaram, M. V, & Krishnamurthy, R. V. (1995). Earth surface evaporative process: A case study from the Great Lakes region of the United States based on deuterium excess in precipitation. *Geochimica et Cosmochimica Acta*, *9*(20), 4279–4283.

Magnuson, J. J., Webster, K. E., Assel, R. A., Bowser, C. J., Dillon, P. J., Eaton, J. G., … Quinn, F. H. (1997). Potential effects of climate changes on aquatic systems: laurentian great lakes and precambrian shield region. *Hydrological Processes*, *11*, 825–871.

Massone, H., Martinez, D., Vich, A., Londoño, M. Q., Trombotto, D., & Grondona, S. (2016). Snowmelt contribution to the sustainability of the irrigated Mendoza's Oasis, Argentina: an isotope study. *Environmental Earth Sciences*, *75*(6).

Minnesota Department of Natural Resources. (2018). The Minnesota Department of Natural Resources Website (online). Accessed Jun. 8, 2018 at mndnr.gov/copyright

Minnesota Department of Natural Resources. (2019). Site Report Lester River nr Duluth, CSAH10 (02036003) [Data file]. Retrieved from https://www.dnr.state.mn.us/waters/csg/site_report.html?mode=get_site_report&site=02036003

Neff, B., and Nicholas, J. (2005). Uncertainty in the Great Lakes Water Balance Scientific Investigations Report 2004-5100. *Water*, *42*.

National Oceanic and Atmospheric Administration (NOAA). Department of Commerce. (2018). *Summary of Annual Normals 1981-2010*. Accessed May 15, 2018 at https://www.ncdc.noaa.gov/cdo-web/datatools/findstation

National Weather Service (NWS). Department of Commerce. (2018). *National Weather Service Glossary*. Accessed August 23, 2018 at https://w1.weather.gov/glossary/

Novotny, E. V, & Stefan, H. G. (2007). Stream flow in Minnesota: Indicator of climate change. *Journal of Hydrology*, *334*, 319–333.

Oki, T., & Kanae, S. (2006). Global Hydrological Cycles and World Water Resources. *Science*, *313*(August), 1068–1073.

Pearce, A. J., Stewart, M. K., & Sklash, M. G. (1986). Storm Runoff Generation in Humid Headwater Catchments: 1. Where Does the Water Come From? *Water Resources Research*, *22*(8), 1263–1272.

Plummer, L. N. (2005). Dating of young groundwater. In *Isotopes in the Water Cycle* (pp. 193-218). Springer, Dordrecht.

Rozanski, K., L. Araguas-Araguas, and R. Gonfiantini. 1993. "Isotopic Patterns in Modern Global Precipitation." Climate Change in Continental Isotopic Records, American Geophysical Union, Geophysical Monograph 78: 1–36.

Schmieder, J., Hanzer, F., Marke, T., Garvelmann, J., Warscher, M., Kunstmann, H., and Strasser, U. (2016). The importance of snowmelt spatiotemporal variability for isotope-based hydrograph separation in a high-elevation catchment. *Hydrology and Earth System Sciences*, *20*, 5015–5033.

Schweizer, J., Kronholm, K., Jamieson, J. B., & Birkeland, K. W. (2008). Review of spatial variability of snowpack properties and its importance for avalanche formation. *Cold Regions Science and Technology, 51,* 253–272.

Scott, R. W., and Huff, F. a. (1996). Impacts of the Great Lakes on regional climate conditions. *Journal of Great Lakes Research, 22*(4), 845–863.

Scholl, M. A., Ingebritsen, S. E., Janik, C. J., & Kauahikaua, J. P. (1996). Use of precipitation and groundwater isotopes to interpret regional hydrology on a tropical volcanic island: Kilauea volcano area, Hawaii. *Water Resources Research*, *32*(12), 3525–3537.

Sklash, M. G. & Farvolden, R. N. (1979). The role of groundwater in storm runoff. *Developments in Water Science*, *43,* 45–65.

Sims, P. K., & Morey, G. B. (1972). Geology of Minnesota: A centennial volume. Minnesota Geological Survey.

Soil Survey Staff, Natural Resources Conservation Service, United States Department of Agriculture. Web Soil Survey. Available online at the following link: https://websoilsurvey.sc.egov.usda.gov/. Accessed [May/15/2018]

Strauch, G. (2014). Isotope methods for dating old groundwater.

Tukey, J. W. (1949). Comparing individual means in the analysis of variance. Biometrics, 5(2), 99-114.

U.S. Geological Survey. (2016). The StreamStats program, online at http://streamstats.usgs.gov, Accessed [5/15/2018]

Van Hise, C. R., and Leith, C. K. (1909). Pre-Cambrian geology of North America., 106–402. Retrieved from http://hdl.handle.net/2027/uiug.30112026956844

Wright, D. M., Posselt, D. J., & Steiner, A. L. (2013). Sensitivity of Lake-Effect Snowfall to Lake Ice Cover and Temperature in the Great Lakes Region. *Monthly Weather Review*, *141*(2), 670–689.

Wu, H., Wu, J., Sakiev, K., Liu, J., Li, J., He, B., … Shen, B. (2019). Spatial and temporal variability of stable isotopes ($\delta^{18}O$ & $\delta^{2}H$) in surface waters of arid, mountainous Central Asia. *Hydrological Processes*, (October 2018), 1–12.

Yeh, H. F., Lin, H. I., Lee, C. H., Hsu, K. C., & Wu, C. S. (2014). Identifying seasonal groundwater recharge using environmental stable isotopes. *Water (Switzerland)*, *6*(10).

Zhou, S., Nakawo, M., Hashimoto, S., & Sakai, A. (2008). The effect of refreezing on the isotopic composition of melting snowpack. *Hydrological Processes*, *22*, 873–882.

APPENDIX 1. STABLE ISOTOPE LAB ANALYIS RESULTS: NORTH SHORE, MN

Table A1) Stable Isotope values of $\delta^{18}O$ and $\delta^{2}H$ from the Picarro L2130-i water isotope analyzer across all site locations along the north shore of Lake Superior.

Date	Site Location	$\delta^{18}O$ (‰)	$\delta^{2}H$ (‰)	Type
9/25/2017	Brule	-9.17	-69.53	stream
9/25/2017	Poplar	-9.48	-70.06	stream
9/25/2017	Baptism	-9.54	-64.15	stream
9/25/2017	Knife	-9.26	-62.73	stream
9/25/2017	Lester	-8.92	-60.26	stream
12/9/2017	Brule	-29.11	-221.79	snow
12/9/2017	Poplar	-26.98	-204.58	snow
12/9/2017	Baptism	-24.72	-183.03	snow
12/9/2017	Knife	-24.62	-173.17	snow
12/9/2017	Lester	-22.00	-156.92	snow
12/15/2017	Brule	-22.95	-157.78	snow
12/15/2017	Poplar	-20.90	-139.50	snow
12/15/2017	Baptism	-19.45	-132.47	snow
12/15/2017	Knife	-20.19	-142.46	snow
12/15/2017	Lester	-19.75	-135.69	snow
1/12/2018	Brule	-21.33	-157.27	snow
1/12/2018	Poplar	-21.55	-160.72	snow
1/12/2018	Baptism	-26.27	-198.17	snow
1/12/2018	Knife	-28.68	-217.12	snow
1/12/2018	Lester	-27.72	-210.55	snow
2/21/2018	Brule	-22.01	-163.23	snow
2/21/2018	Poplar	-20.19	-146.35	snow
2/21/2018	Baptism	-19.95	-145.30	snow
2/21/2018	Knife	-20.07	-147.08	snow
2/21/2018	Lester	-19.58	-141.78	snow
3/31/2018	Baptism	-15.45	-114.70	snow
3/31/2018	Knife	-29.68	-231.45	snow
3/31/2018	Lester	-30.60	-234.21	snow
4/28/2018	Brule	-14.35	-105.47	snowmelt
4/28/2018	Poplar	-14.04	-101.83	snowmelt
4/28/2018	Baptism	-14.83	-106.77	snowmelt
4/28/2018	Knife	-14.11	-102.48	snowmelt
4/28/2018	Lester	-14.04	-102.66	snowmelt
5/24/2018	Brule	-11.19	-83.65	stream
5/24/2018	Poplar	-10.98	-81.41	stream
5/24/2018	Baptism	-11.85	-84.58	stream
5/24/2018	Knife	-10.83	-76.76	stream
5/24/2018	Lester	-10.76	-77.25	stream
6/25/2018	Brule	-9.50	-72.95	stream
6/25/2018	Poplar	-9.62	-72.53	stream
6/25/2018	Baptism	-10.02	-71.41	stream
6/25/2018	Knife	-9.00	-61.26	stream
6/25/2018	Lester	-8.74	-62.37	stream
7/25/2018	Brule	-8.16	-65.85	stream
7/25/2018	Poplar	-8.52	-66.86	stream
7/25/2018	Baptism	-9.26	-67.75	stream
7/25/2018	Knife	-9.35	-65.03	stream
7/25/2018	Lester	-8.27	-58.40	stream

APPENDIX 2: ANOVA RESULTS FROM *STATS* IN R FOR THE DATA COLLECTED ALONG THE NORTH SHORE OF LAKE SUPERIOR.

Table A2: ANOVA results from Tukey's HSD in R comparing site locations testing for significance with a α=0.005.

Comparisons Between Site Locations				
Sites	**difference**	**lower**	**upper**	**p adjusted**
Baptism and Brule	-1.84	-11.426	7.74956	0.9786101
Baptism and Knife	-2.78	-11.922	6.3617	0.8943479
Baptism and Lester	-2.17	-11.312	6.9717	0.954032
Baptism and Poplar	-0.62	-10.208	8.96756	0.999677
Brule and Knife	-0.94	-10.53	8.64622	0.998329
Brule and Lester	-0.33	-9.9196	9.25622	0.9999732
Brule and Poplar	1.22	-8.7962	11.2322	0.9961642
Knife and Lester	0.61	-8.5317	9.7517	0.9996351
Knife and Poplar	2.16	-7.4282	11.7476	0.9617678
Lester and Poplar	1.55	-8.0382	11.1376	0.9886553

Table A3: ANOVA results from Tukey's HSD in R comparing mean $\delta^{18}O$ values from sampling dates for significance with a α=0.005. (*= significant difference)

Comparisons Between Dates				
Dates	**difference**	**lower**	**upper**	**p adjusted**
2017-12-09-2017-09-25	-16.212	-21.443	-10.981	0*
2017-12-15-2017-09-25	-11.374	-16.605	-6.1427	0.0000002*
2018-01-12-2017-09-25	-15.836	-21.067	-10.605	0*
2018-02-21-2017-09-25	-11.086	-16.317	-5.8547	0.0000004*
2018-03-31-2017-09-25	-15.969333	-22.01	-9.9288	0*
2018-04-28-2017-09-25	-5	-10.231	0.23129	0.0720892
2018-05-24-2017-09-25	-1.848	-7.0793	3.38329	0.9788321
2018-06-25-2017-09-25	-0.102	-5.3333	5.12929	1
2018-07-25-2017-09-25	0.562	-4.6693	5.79329	0.9999994
2018-08-22-2017-09-25	0.492	-4.7393	5.72329	0.9999998
2017-12-15-2017-12-09	4.838	-0.3933	10.0693	0.0921972
2018-01-12-2017-12-09	0.376	-4.8553	5.60729	1
2018-02-21-2017-12-09	5.126	-0.1053	10.3573	0.0591828
2018-03-31-2017-12-09	0.2426667	-5.7979	6.28324	1
2018-04-28-2017-12-09	11.212	5.98071	16.4433	0.0000003*
2018-05-24-2017-12-09	14.364	9.13271	19.5953	0*

Table A3 (cont.)

Dates	difference	lower	upper	p adjusted
2018-06-25-2017-12-09	16.11	10.8787	21.3413	0*
2018-07-25-2017-12-09	16.774	11.5427	22.0053	0*
2018-08-22-2017-12-09	16.704	11.4727	21.9353	0*
2018-01-12-2017-12-15	-4.462	-9.6933	0.76929	0.1574006
2018-02-21-2017-12-15	0.288	-4.9433	5.51929	1
2018-03-31-2017-12-15	-4.5953333	-10.636	1.44524	0.2872494
2018-04-28-2017-12-15	6.374	1.14271	11.6053	0.0066909
2018-05-24-2017-12-15	9.526	4.29471	14.7573	0.0000106*
2018-06-25-2017-12-15	11.272	6.04071	16.5033	0.0000003*
2018-07-25-2017-12-15	11.936	6.70471	17.1673	0.0000001*
2018-08-22-2017-12-15	11.866	6.63471	17.0973	0.0000001*
2018-02-21-2018-01-12	4.75	-0.4813	9.98129	0.1049825
2018-03-31-2018-01-12	-0.1333333	-6.1739	5.90724	1
2018-04-28-2018-01-12	10.836	5.60471	16.0673	0.0000007*
2018-05-24-2018-01-12	13.988	8.75671	19.2193	0*
2018-06-25-2018-01-12	15.734	10.5027	20.9653	0*
2018-07-25-2018-01-12	16.398	11.1667	21.6293	0*
2018-08-22-2018-01-12	16.328	11.0967	21.5593	0*
2018-03-31-2018-02-21	-4.8833333	-10.924	1.15724	0.2131624
2018-04-28-2018-02-21	6.086	0.85471	11.3173	0.0114124
2018-05-24-2018-02-21	9.238	4.00671	14.4693	0.0000195*
2018-06-25-2018-02-21	10.984	5.75271	16.2153	0.0000005*
2018-07-25-2018-02-21	11.648	6.41671	16.8793	0.0000001*
2018-08-22-2018-02-21	11.578	6.34671	16.8093	0.0000001*
2018-04-28-2018-03-31	10.9693333	4.92876	17.0099	0.0000112*
2018-05-24-2018-03-31	14.1213333	8.08076	20.1619	0*
2018-06-25-2018-03-31	15.8673333	9.82676	21.9079	0*
2018-07-25-2018-03-31	16.5313333	10.4908	22.5719	0*
2018-08-22-2018-03-31	16.4613333	10.4208	22.5019	0*
2018-05-24-2018-04-28	3.152	-2.0793	8.38329	0.6173025
2018-06-25-2018-04-28	4.898	-0.33329	10.12929	0.0842543
2018-07-25-2018-04-28	5.562	0.33071	10.79329	0.0288436
2018-08-22-2018-04-28	5.492	0.26071	10.72329	0.0324856
2018-06-25-2018-05-24	1.746	-3.48529	6.97729	0.9859185
2018-07-25-2018-05-24	2.41	-2.82129	7.64129	0.8869847
2018-08-22-2018-05-24	2.34	-2.89129	7.57129	0.9041678
2018-07-25-2018-06-25	0.664	-4.56729	5.89529	0.999997
2018-08-22-2018-06-25	0.594	-4.63729	5.82529	0.999999
2018-08-22-2018-07-25	-0.07	-5.30129	5.16129	1

APPENDIX 3. STABLE ISOTOPE LAB ANALYIS RESULTS: LESTER RIVER, DULUTH, MN

Table A4: Stable Isotope values of $\delta^{18}O$ and $\delta^{2}H$ from the Picarro L2130-i water isotope analyzer given in per mil ($^{0}/_{00}$) across stream sites in the Lester River collected weekly. Temperatures collected as snapshot data. (Geology, SDC= Supraglacial Drift Complex)

Date	Site ID	$\delta^{18}O$	$\delta^{2}H$	Geology	D-excess	T (°C)
5/21/2018	1	-10.92	-79.70	Igneous	7.67	n/a
5/21/2018	2	-10.90	-79.67	Till plain	7.52	10.79
5/21/2018	3	-10.96	-80.06	Till plain	7.63	n/a
5/21/2018	4	-10.65	-76.93	SDC	8.29	10.23
5/21/2018	5	-10.95	-79.93	SDC	7.66	11.39
5/21/2018	6.1	-10.69	-77.72	Undifferentiated	7.79	14.23
5/21/2018	6.2	-10.70	-77.95	Undifferentiated	7.63	14.23
5/21/2018	6.3	-10.75	-78.20	Undifferentiated	7.79	14.23
5/21/2018	7	-11.07	-79.79	Ice Contact	8.77	13.66
5/21/2018	8	-10.97	-80.26	Ice Contact	7.51	13.38
5/21/2018	9.1	-10.44	-74.87	SDC	8.62	9.04
5/21/2018	9.2	-10.87	-77.96	SDC	9.02	9.04
5/21/2018	10.1	-11.22	-79.93	SDC	9.80	9.31
5/21/2018	10.2	-11.16	-79.42	SDC	9.83	9.31
5/21/2018	11	-10.53	-77.10	SDC	7.11	15.87
5/21/2018	12.1	-10.76	-78.12	SDC	7.94	12.64
5/21/2018	12.2	-10.63	-76.19	SDC	8.81	12.6
5/21/2018	13	-10.94	-80.73	Outwash	6.77	16.5
5/21/2018	14	-10.64	-77.64	SDC	7.48	13.86
5/21/2018	15	-10.93	-78.69	SDC	8.76	14.01
5/29/2018	1	-10.33	-75.36	Igneous	7.30	n/a
5/29/2018	2	-10.49	-74.98	Till plain	8.96	n/a
5/29/2018	3	-10.44	-75.65	Till plain	7.87	n/a
5/29/2018	4	-9.88	-72.42	SDC	6.62	n/a
5/29/2018	5	-10.56	-75.32	SDC	9.12	n/a
5/29/2018	6.1	-10.05	-73.96	Undifferentiated	6.48	n/a
5/29/2018	6.3	-10.21	-73.64	Undifferentiated	8.04	n/a
5/29/2018	7	-10.55	-75.96	Ice Contact	8.48	n/a
5/29/2018	8	-10.46	-74.86	Ice Contact	8.81	n/a
5/29/2018	9.1	-9.94	-71.54	SDC	7.98	n/a
5/29/2018	9.2	-10.58	-75.08	SDC	9.59	n/a
5/29/2018	10.1	-10.85	-76.97	SDC	9.87	n/a
5/29/2018	10.2	-10.90	-76.26	SDC	10.92	n/a
5/29/2018	11	-10.16	-74.36	SDC	6.93	n/a

Table A4 (cont.)

Date	Site ID	$\delta^{18}O$	$\delta^{2}H$	Geology	D-excess	T (°C)
5/29/2018	12.1	-10.37	-74.74	SDC	8.19	n/a
5/29/2018	12.2	-10.15	-71.85	SDC	9.33	n/a
5/29/2018	13	-10.53	-75.65	Outwash	8.55	n/a
5/29/2018	14	-10.42	-74.42	SDC	8.97	n/a
5/29/2018	15	-10.14	-71.80	SDC	9.36	n/a
6/4/2018	1	-10.17	-70.72	Igneous	10.61	n/a
6/4/2018	2	-10.16	-70.80	Till plain	10.48	n/a
6/4/2018	3	-10.08	-71.27	Till plain	9.34	n/a
6/4/2018	4	-9.91	-70.57	SDC	8.73	n/a
6/4/2018	5	-10.24	-71.19	SDC	10.72	n/a
6/4/2018	6.1	-10.31	-71.25	Undifferentiated	11.26	n/a
6/4/2018	6.2	-10.23	-71.73	Undifferentiated	10.13	n/a
6/4/2018	6.3	-10.34	-71.42	Undifferentiated	11.27	n/a
6/4/2018	7	-10.36	-72.18	Ice Contact	10.72	n/a
6/4/2018	8	-10.02	-70.96	Ice Contact	9.24	n/a
6/4/2018	9.1	-9.78	-68.85	SDC	9.39	n/a
6/4/2018	9.2	-10.71	-74.16	SDC	11.50	n/a
6/4/2018	10.1	-10.28	-71.47	SDC	10.79	n/a
6/4/2018	10.2	-10.23	-71.37	SDC	10.46	n/a
6/4/2018	11	-10.18	-70.75	SDC	10.72	n/a
6/4/2018	12.1	-10.17	-70.74	SDC	10.58	n/a
6/4/2018	12.2	-10.07	-68.79	SDC	11.79	n/a
6/4/2018	13	-10.19	-71.60	Outwash	9.89	n/a
6/4/2018	14	-10.16	-70.93	SDC	10.38	n/a
6/4/2018	15	-9.77	-68.08	SDC	10.06	n/a
6/12/2018	1	-9.96	-71.12	Igneous	8.55	n/a
6/12/2018	2	-9.99	-71.04	Till plain	8.86	n/a
6/12/2018	3	-9.87	-71.52	Till plain	7.45	n/a
6/12/2018	4	-9.49	-69.30	SDC	6.62	n/a
6/12/2018	5	-9.96	-70.70	SDC	9.00	n/a
6/12/2018	6.1	-9.98	-69.84	Undifferentiated	9.98	n/a
6/12/2018	6.2	-9.91	-69.25	Undifferentiated	10.02	n/a
6/12/2018	6.2	-10.14	-74.24	Undifferentiated	6.91	n/a
6/12/2018	6.3	-9.86	-69.87	Undifferentiated	9.05	n/a
6/12/2018	7	-9.78	-70.12	Ice Contact	8.14	n/a
6/12/2018	8	-9.91	-71.06	Ice Contact	8.25	n/a
6/12/2018	9.1	-9.58	-67.96	SDC	8.65	n/a
6/12/2018	9.2	-10.32	-72.66	SDC	9.90	n/a
6/12/2018	10.1	-10.12	-70.22	SDC	10.72	n/a

Table A4 (cont.)

Date	Site ID	$\delta^{18}O$	$\delta^{2}H$	Geology	D-excess	T (°C)
6/12/2018	10.2	-10.19	-69.72	SDC	11.82	n/a
6/12/2018	11	-9.82	-69.08	SDC	9.47	n/a
6/12/2018	12.1	-9.86	-70.46	SDC	8.43	n/a
6/12/2018	12.2	-9.52	-68.06	SDC	8.13	n/a
6/12/2018	13	-9.95	-71.79	Outwash	7.78	n/a
6/12/2018	14	-9.82	-70.06	SDC	8.49	n/a
6/12/2018	15	-9.77	-68.76	SDC	9.43	n/a
6/19/2018	1	-8.75	-59.54	Igneous	10.47	16.8
6/19/2018	2	-8.55	-57.64	Till plain	10.79	17.2
6/19/2018	3	-8.70	-58.62	Till plain	10.96	17.6
6/19/2018	4	-8.39	-58.43	SDC	8.70	17.9
6/19/2018	5	-8.68	-58.54	SDC	10.92	17.1
6/19/2018	6.1	-8.56	-57.13	Undifferentiated	11.36	18
6/19/2018	6.2	-8.56	-56.96	Undifferentiated	11.49	18
6/19/2018	6.3	-8.51	-56.56	Undifferentiated	11.54	18
6/19/2018	7	-8.64	-58.56	Ice Contact	10.58	17.9
6/19/2018	8	-8.60	-57.93	Ice Contact	10.87	17.6
6/19/2018	9.1	-8.67	-58.32	SDC	11.04	17.3
6/19/2018	9.2	-8.91	-59.38	SDC	11.86	17.3
6/19/2018	10.1	-8.55	-56.23	SDC	12.20	16.9
6/19/2018	10.2	-8.39	-55.10	SDC	12.05	16.9
6/19/2018	11	-8.34	-55.03	SDC	11.69	18.8
6/19/2018	12.1	-8.76	-58.80	SDC	11.26	18.2
6/19/2018	12.2	-8.50	-56.72	SDC	11.30	18.2
6/19/2018	13	-8.53	-57.49	Outwash	10.76	18.2
6/19/2018	14	-8.55	-57.27	SDC	11.12	18.7
6/19/2018	15	-8.43	-56.80	SDC	10.64	18.1
6/26/2018	1	-8.86	-62.71	Igneous	8.15	14.6
6/26/2018	2	-9.56	-68.02	Till plain	8.45	14.7
6/26/2018	4	-8.76	-62.29	SDC	7.77	15.4
6/26/2018	5	-9.04	-63.68	SDC	8.65	13.2
6/26/2018	6.1	-8.64	-60.18	Undifferentiated	8.91	15.3
6/26/2018	6.2	-8.40	-57.79	Undifferentiated	9.38	16.4
6/26/2018	6.3	-8.70	-60.41	Undifferentiated	9.19	16.4
6/26/2018	6.3	-8.95	-63.34	Undifferentiated	8.30	16.4
6/26/2018	7	-8.79	-61.06	Ice Contact	9.26	19
6/26/2018	8	-8.71	-62.30	Ice Contact	7.37	16.4
6/26/2018	9.1	-8.78	-60.05	SDC	10.17	15.4
6/26/2018	9.2	-8.53	-57.99	SDC	10.27	15.4

Table A4 (cont.)

Date	Site ID	$\delta^{18}O$	$\delta^{2}H$	Geology	D-excess	T (°C)
6/26/2018	10.1	-8.66	-57.08	SDC	12.20	14.8
6/26/2018	10.2	-8.72	-58.01	SDC	11.71	14.8
6/26/2018	11	-8.47	-58.34	SDC	9.39	17.1
6/26/2018	12.1	-8.86	-61.37	SDC	9.49	15.1
6/26/2018	12.2	-8.42	-58.23	SDC	9.13	16.1
6/26/2018	13	-8.80	-63.01	Outwash	7.42	16.1
6/26/2018	14	-8.83	-61.30	SDC	9.35	17.9
6/26/2018	15	-8.72	-59.93	SDC	9.81	15.7
7/2/2018	1	-8.93	-60.63	Igneous	10.83	n/a
7/2/2018	2	-8.92	-60.09	Till plain	11.26	n/a
7/2/2018	3	-9.03	-61.14	Till plain	11.07	n/a
7/2/2018	4	-8.80	-60.30	SDC	10.07	n/a
7/2/2018	5	-8.98	-61.05	SDC	10.77	n/a
7/2/2018	6.1	-9.33	-63.29	Undifferentiated	11.36	n/a
7/2/2018	6.2	-8.90	-60.39	Undifferentiated	10.83	n/a
7/2/2018	6.3	-8.89	-60.41	Undifferentiated	10.75	n/a
7/2/2018	7	-8.96	-60.84	Ice Contact	10.86	n/a
7/2/2018	8	-8.96	-60.69	Ice Contact	11.03	n/a
7/2/2018	9.1	-8.86	-60.16	SDC	10.74	n/a
7/2/2018	9.2	-8.96	-60.16	SDC	11.55	n/a
7/2/2018	10.1	-9.39	-63.62	SDC	11.53	n/a
7/2/2018	10.2	-8.88	-59.35	SDC	11.68	n/a
7/2/2018	11	-8.99	-61.38	SDC	10.57	n/a
7/2/2018	12.1	-9.00	-61.38	SDC	10.64	n/a
7/2/2018	12.2	-9.11	-61.26	SDC	11.65	n/a
7/2/2018	13	-9.02	-61.58	Outwash	10.55	n/a
7/2/2018	14	-9.06	-62.03	SDC	10.41	n/a
7/2/2018	15	-9.22	-62.22	SDC	11.51	n/a
7/10/2018	1	-7.74	-50.16	Igneous	11.75	19.2
7/10/2018	2	-7.83	-51.18	Till plain	11.47	19.2
7/10/2018	3	-7.80	-50.87	Till plain	11.52	19.1
7/10/2018	4	-7.74	-50.41	SDC	11.48	18.9
7/10/2018	5	-7.84	-51.24	SDC	11.51	19.1
7/10/2018	6.1	-7.66	-48.81	Undifferentiated	12.47	19.4
7/10/2018	6.2	-7.74	-49.61	Undifferentiated	12.33	19.4
7/10/2018	6.3	-7.81	-49.96	Undifferentiated	12.55	19.4
7/10/2018	7	-7.91	-51.67	Ice Contact	11.61	20
7/10/2018	8	-7.70	-49.96	Ice Contact	11.61	19.5
7/10/2018	9.1	-7.92	-51.53	SDC	11.79	19.1

Table A4 (cont.)

Date	Site ID	$\delta^{18}O$	$\delta^{2}H$	Geology	D-excess	T (°C)
7/10/2018	9.2	-7.83	-51.24	SDC	11.36	19.1
7/10/2018	10.1	-7.37	-46.09	SDC	12.90	18.4
7/10/2018	10.2	-7.44	-46.62	SDC	12.89	18.4
7/10/2018	11	-7.44	-47.26	SDC	12.34	20.3
7/10/2018	12.1	-7.50	-47.90	SDC	12.09	20.1
7/10/2018	12.2	-7.52	-48.27	SDC	11.89	20.1
7/10/2018	13	-7.61	-49.47	Outwash	11.38	20.4
7/10/2018	14	-7.62	-49.01	SDC	11.97	20
7/10/2018	15	-8.07	-52.75	SDC	11.83	19.4
7/16/2018	1	-8.39	-57.65	Igneous	9.51	18.4
7/16/2018	2	-8.12	-55.44	Till plain	9.51	18.5
7/16/2018	3	-8.42	-57.97	Till plain	9.41	18.8
7/16/2018	4	-8.37	-57.76	SDC	9.20	17.8
7/16/2018	5	-8.03	-55.06	SDC	9.17	19.2
7/16/2018	6.1	-7.82	-51.72	Undifferentiated	10.81	19.2
7/16/2018	6.2	-8.05	-53.35	Undifferentiated	11.01	19.2
7/16/2018	6.3	-7.80	-51.56	Undifferentiated	10.84	19.2
7/16/2018	7	-7.91	-53.13	Ice Contact	10.14	21.8
7/16/2018	8	-8.01	-55.07	Ice Contact	9.02	19.8
7/16/2018	9.1	-8.04	-53.37	SDC	10.95	19.2
7/16/2018	9.2	-7.77	-50.80	SDC	11.34	19.2
7/16/2018	10.1	-7.64	-48.44	SDC	12.67	18.8
7/16/2018	10.2	-7.69	-48.99	SDC	12.53	18.8
7/16/2018	11	-7.94	-52.77	SDC	10.77	21.8
7/16/2018	12.1	-7.85	-52.26	SDC	10.54	20.1
7/16/2018	12.2	-7.50	-49.78	SDC	10.20	20.8
7/16/2018	13	-7.78	-53.94	Outwash	8.29	20.8
7/16/2018	14	-7.84	-52.11	SDC	10.58	21.9
7/16/2018	15	-8.46	-56.72	SDC	10.95	20.5
7/24/2018	1	-8.43	-59.20	Igneous	8.23	18.8
7/24/2018	2	-8.34	-58.47	Till plain	8.25	18.5
7/24/2018	3	-8.37	-58.84	Till plain	8.14	18.4
7/24/2018	4	-8.60	-60.02	SDC	8.82	17.1
7/24/2018	5	-8.33	-58.18	SDC	8.44	18.4
7/24/2018	6.1	-7.58	-52.15	Undifferentiated	8.48	20.6
7/24/2018	6.2	-7.60	-52.32	Undifferentiated	8.46	20.6
7/24/2018	6.3	-7.54	-52.04	Undifferentiated	8.30	20.6
7/24/2018	7	-7.78	-53.37	Ice Contact	8.87	22.9
7/24/2018	8	-8.22	-58.29	Ice Contact	7.44	19.1

Table A4 (cont.)

Date	Site ID	$\delta^{18}O$	$\delta^{2}H$	Geology	D-excess	T (°C)
7/24/2018	9.1	-7.89	-52.92	SDC	10.24	18.1
7/24/2018	9.2	-7.89	-52.85	SDC	10.30	18.1
7/24/2018	10.1	-7.87	-50.75	SDC	12.20	17.1
7/24/2018	10.2	-7.79	-50.08	SDC	12.28	17.1
7/24/2018	11	-8.16	-56.44	SDC	8.85	20.2
7/24/2018	12.1	-8.26	-56.62	SDC	9.45	20.6
7/24/2018	12.2	-7.49	-51.40	SDC	8.48	20.6
7/24/2018	13	-8.17	-58.28	Outwash	7.10	21.2
7/24/2018	14	-8.49	-58.83	SDC	9.09	19.7
7/24/2018	15	-8.28	-56.62	SDC	9.60	19.1
7/31/2018	1	-8.36	-59.64	Igneous	7.24	19.5
7/31/2018	2	-8.43	-60.05	Till plain	7.42	18.6
7/31/2018	3	-8.52	-60.45	Till plain	7.72	18.4
7/31/2018	4	-8.97	-62.61	SDC	9.15	17.4
7/31/2018	5	-8.63	-61.19	SDC	7.86	18.3
7/31/2018	6.1	-7.01	-51.10	Undifferentiated	5.01	19.1
7/31/2018	6.2	-7.12	-51.46	Undifferentiated	5.46	19.1
7/31/2018	6.3	-7.18	-51.98	Undifferentiated	5.48	19.1
7/31/2018	7	-7.50	-52.62	Ice Contact	7.37	22.2
7/31/2018	8	-8.24	-59.08	Ice Contact	6.88	17.1
7/31/2018	9.1	-7.80	-52.83	SDC	9.59	17.1
7/31/2018	9.2	-7.82	-53.24	SDC	9.28	17.1
7/31/2018	10.1	-7.92	-51.35	SDC	12.00	16
7/31/2018	10.2	-8.01	-52.35	SDC	11.77	16
7/31/2018	11	-8.56	-61.02	SDC	7.45	19
7/31/2018	12.1	-8.71	-62.00	SDC	7.70	20.5
7/31/2018	12.2	-7.18	-50.27	SDC	7.16	20.5
7/31/2018	13	-8.16	-58.90	Outwash	6.37	21.3
7/31/2018	14	-8.75	-62.25	SDC	7.75	18.3
7/31/2018	15	-7.68	-55.21	SDC	6.27	19
8/7/2018	1	-8.52	-59.64	Igneous	8.54	17.1
8/7/2018	2	-8.55	-60.41	Till plain	8.00	16.6
8/7/2018	3	-8.78	-62.30	Till plain	7.94	16.4
8/7/2018	4	-8.98	-62.90	SDC	8.95	15.4
8/7/2018	5	-9.07	-64.02	SDC	8.56	16.4
8/7/2018	6.1	-7.30	-52.17	Undifferentiated	6.23	18.4
8/7/2018	6.2	-7.21	-51.40	Undifferentiated	6.31	18.4
8/7/2018	6.3	-7.38	-52.49	Undifferentiated	6.55	18.4
8/7/2018	7	-7.61	-54.10	Ice Contact	6.78	20.6

Table A4 (cont.)

Date	Site ID	$\delta^{18}O$	$\delta^{2}H$	Geology	D-excess	T (°C)
8/7/2018	8	-9.10	-64.89	Ice Contact	7.87	16.6
8/7/2018	9.1	-8.03	-54.68	SDC	9.57	16.5
8/7/2018	9.2	-7.79	-53.00	SDC	9.35	16.5
8/7/2018	10.1	-8.21	-53.41	SDC	12.28	15.7
8/7/2018	10.2	-8.07	-53.05	SDC	11.51	15.7
8/7/2018	11	-8.89	-63.54	SDC	7.62	16.1
8/7/2018	12.1	-9.04	-64.12	SDC	8.23	19.2
8/7/2018	12.2	-7.47	-52.92	SDC	6.87	19.2
8/7/2018	13	-8.60	-61.08	Outwash	7.68	n/a
8/7/2018	14	-8.99	-64.15	SDC	7.78	16.7
8/7/2018	15	-8.33	-57.51	SDC	9.12	16.5
8/13/2018	1	-8.63	-61.78	Igneous	7.25	21.2
8/13/2018	3	-8.96	-63.34	Till plain	8.34	20.4
8/13/2018	4	-8.96	-63.74	SDC	7.94	19.5
8/13/2018	4	-9.30	-65.13	SDC	9.23	20.2
8/13/2018	6.1	-7.36	-54.04	Undifferentiated	4.84	21.1
8/13/2018	6.2	-7.02	-51.74	Undifferentiated	4.42	21.1
8/13/2018	6.3	-7.18	-52.54	Undifferentiated	4.87	21.1
8/13/2018	7	-7.25	-52.60	Ice Contact	5.38	24.7
8/13/2018	8	-8.77	-62.97	Ice Contact	7.15	21.4
8/13/2018	9.1	-7.85	-54.18	SDC	8.64	19.6
8/13/2018	10.1	-8.27	-54.46	SDC	11.71	19.6
8/13/2018	10.2	-8.26	-54.35	SDC	11.75	19.6
8/13/2018	11	-8.95	-63.68	SDC	7.93	22.6
8/13/2018	12.1	-9.22	-65.75	SDC	7.97	22.6
8/13/2018	12.2	-9.14	-65.44	SDC	7.65	22.6
8/13/2018	13	-8.52	-61.84	Outwash	6.33	23.8
8/13/2018	14	-9.41	-66.77	SDC	8.52	21.8
8/13/2018	15	-7.77	-55.67	SDC	6.50	22.8
8/21/2018	1	-8.87	-63.62	Igneous	7.32	18.2
8/21/2018	2	-9.17	-65.41	Till plain	7.95	17.4
8/21/2018	3	-9.86	-70.25	Till plain	8.64	17.1
8/21/2018	4	-9.26	-64.38	SDC	9.72	16.2
8/21/2018	5	-9.19	-65.57	SDC	7.92	17
8/21/2018	6.1	-6.72	-51.57	Undifferentiated	2.16	18
8/21/2018	6.2	-6.86	-52.32	Undifferentiated	2.60	18
8/21/2018	6.3	-7.25	-54.64	Undifferentiated	3.37	18
8/21/2018	7	-7.17	-52.70	Ice Contact	4.64	20.4
8/21/2018	8	-8.79	-63.60	Ice Contact	6.72	17.3

Table A4 (cont.)

Date	Site ID	$\delta^{18}O$	$\delta^{2}H$	Geology	D-excess	T (°C)
8/21/2018	9.1	-8.17	-56.83	SDC	8.51	19.8
8/21/2018	9.2	-7.86	-54.69	SDC	8.23	19.8
8/21/2018	10.1	-8.71	-57.84	SDC	11.87	16.4
8/21/2018	10.2	-9.12	-60.67	SDC	12.27	16.4
8/21/2018	11	-9.27	-66.49	SDC	7.65	17.5
8/21/2018	12.1	-9.61	-68.59	SDC	8.29	18.8
8/21/2018	12.2	-7.59	-55.49	SDC	5.21	18.8
8/21/2018	13	-8.84	-64.94	Outwash	5.74	28.8
8/21/2018	14	-9.29	-66.63	SDC	7.72	17.4
8/21/2018	15	-8.33	-59.78	SDC	6.83	n/a
8/28/2018	1	-9.00	-64.04	Igneous	7.98	n/a
8/28/2018	2	-8.97	-63.51	Till plain	8.27	n/a
8/28/2018	3	-8.88	-63.63	Till plain	7.42	n/a
8/28/2018	4	-9.18	-64.58	SDC	8.85	n/a
8/28/2018	5	-9.11	-64.56	SDC	8.31	n/a
8/28/2018	6.1	-6.54	-50.04	Undifferentiated	2.28	n/a
8/28/2018	6.2	-6.62	-50.49	Undifferentiated	2.45	n/a
8/28/2018	6.3	-7.54	-55.21	Undifferentiated	5.09	n/a
8/28/2018	7	-6.96	-51.92	Ice Contact	3.73	n/a
8/28/2018	8	-8.89	-63.40	Ice Contact	7.70	n/a
8/28/2018	9.1	-7.81	-54.31	SDC	8.18	n/a
8/28/2018	9.2	-7.62	-52.91	SDC	8.01	n/a
8/28/2018	10.1	-8.22	-54.93	SDC	10.86	n/a
8/28/2018	10.2	-8.49	-56.21	SDC	11.70	n/a
8/28/2018	11	-9.49	-67.99	SDC	7.91	n/a
8/28/2018	12.1	-9.51	-67.50	SDC	8.57	n/a
8/28/2018	12.2	-7.99	-57.98	SDC	5.94	n/a
8/28/2018	13	-8.87	-64.11	Outwash	6.83	n/a
8/28/2018	14	-9.71	-69.00	SDC	8.64	n/a
8/28/2018	15	-7.83	-56.31	SDC	6.30	n/a
9/3/2018	1	-8.49	-60.28	Igneous	7.66	15.7
9/3/2018	2	-8.88	-62.50	Till plain	8.57	15.2
9/3/2018	3	-8.59	-60.97	Till plain	7.74	15.3
9/3/2018	4	-8.30	-57.49	SDC	8.88	15
9/3/2018	5	-8.95	-62.96	SDC	8.65	15.4
9/3/2018	6.1	-7.31	-52.47	Undifferentiated	5.99	16.7
9/3/2018	6.2	-7.48	-52.61	Undifferentiated	7.24	16.7
9/3/2018	6.3	-7.36	-52.53	Undifferentiated	6.33	16.7
9/3/2018	7	-7.93	-56.60	Ice Contact	6.82	19.5

Table A4 (cont.)

Date	Site ID	$\delta^{18}O$	$\delta^{2}H$	Geology	D-excess	T (°C)
9/3/2018	8	-8.58	-61.24	Ice Contact	7.36	15.3
9/3/2018	9.1	-7.81	-53.06	SDC	9.39	15.4
9/3/2018	9.2	-7.74	-53.11	SDC	8.80	15.4
9/3/2018	10.1	-7.92	-52.44	SDC	10.95	14.5
9/3/2018	10.2	-8.05	-53.45	SDC	10.92	14.5
9/3/2018	11	-8.97	-63.84	SDC	7.93	16.3
9/3/2018	12.1	-9.15	-64.54	SDC	8.63	17.1
9/3/2018	12.2	-9.06	-63.33	SDC	9.15	17.1
9/3/2018	13	-8.52	-61.35	Outwash	6.81	16.9
9/3/2018	14	-9.07	-64.46	SDC	8.13	15.4
9/3/2018	15	-7.80	-53.04	SDC	9.36	14.8
9/11/2018	1	-8.59	-61.35	Igneous	7.40	17.6
9/11/2018	2	-9.03	-63.74	Till plain	8.46	19.4
9/11/2018	3	-8.95	-63.20	Till plain	8.43	18.8
9/11/2018	4	-8.44	-59.06	SDC	8.45	16.4
9/11/2018	5	-8.69	-62.18	SDC	7.32	17.3
9/11/2018	6.1	-7.43	-53.13	Undifferentiated	6.35	18.8
9/11/2018	6.2	-7.47	-53.46	Undifferentiated	6.31	18.8
9/11/2018	6.3	-7.24	-52.35	Undifferentiated	5.58	18.8
9/11/2018	7	-8.08	-57.28	Ice Contact	7.36	20
9/11/2018	8	-8.32	-60.46	Ice Contact	6.13	18
9/11/2018	9.1	-7.99	-54.55	SDC	9.37	16.4
9/11/2018	9.2	-7.98	-54.73	SDC	9.15	16.4
9/11/2018	10.1	-8.04	-53.52	SDC	10.79	15.3
9/11/2018	10.2	-8.21	-53.81	SDC	11.90	15.3
9/11/2018	11	-9.39	-67.19	SDC	7.96	18.7
9/11/2018	12.1	-9.24	-65.82	SDC	8.06	19
9/11/2018	12.2	-8.46	-60.56	SDC	7.14	19
9/11/2018	13	-8.31	-60.35	Outwash	6.17	20.6
9/11/2018	14	-9.25	-66.04	SDC	7.97	16.7
9/11/2018	15	-7.77	-54.08	SDC	8.09	18.3
9/18/2018	1	-8.44	-57.41	Igneous	10.10	16.1
9/18/2018	2	-8.63	-58.19	Till plain	10.84	16.1
9/18/2018	3	-8.58	-57.89	Till plain	10.77	16.1
9/18/2018	4	-8.22	-55.44	SDC	10.34	14.9
9/18/2018	5	-8.55	-57.67	SDC	10.77	15.9
9/18/2018	6.1	-7.95	-53.89	Undifferentiated	9.70	16.2
9/18/2018	6.2	-8.01	-54.38	Undifferentiated	9.67	16.2
9/18/2018	6.3	-8.33	-56.05	Undifferentiated	10.57	16.2

Table A4 (cont.)

Date	Site ID	$\delta^{18}O$	$\delta^{2}H$	Geology	D-excess	T (°C)
9/18/2018	7	-8.11	-55.87	Ice Contact	9.03	17.8
9/18/2018	8	-8.55	-56.96	Ice Contact	11.42	16.3
9/18/2018	9.1	-8.26	-55.24	SDC	10.86	15.7
9/18/2018	9.2	-8.27	-55.18	SDC	10.95	15.7
9/18/2018	10.1	-8.13	-53.36	SDC	11.67	15.8
9/18/2018	10.2	-8.12	-52.95	SDC	11.98	15.8
9/18/2018	11	-9.07	-60.70	SDC	11.87	16.9
9/18/2018	12.1	-8.83	-58.87	SDC	11.79	16.4
9/18/2018	12.2	-8.58	-57.77	SDC	10.83	16.4
9/18/2018	13	-8.31	-56.69	Outwash	9.81	16.9
9/18/2018	14	-8.60	-57.87	SDC	10.90	16.5
9/18/2018	15	-8.42	-55.55	SDC	11.79	16.4
9/25/2018	1	-8.58	-58.25	Igneous	10.40	12.5
9/25/2018	2	-8.46	-57.13	Till plain	10.57	12.4
9/25/2018	3	-8.70	-59.13	Till plain	10.50	12.3
9/25/2018	4	-8.64	-58.61	SDC	10.50	11.7
9/25/2018	5	-8.62	-58.55	SDC	10.41	12.1
9/25/2018	6.1	-8.52	-56.45	Undifferentiated	11.75	n/a
9/25/2018	6.2	-8.46	-56.03	Undifferentiated	11.67	n/a
9/25/2018	6.3	-8.47	-55.87	Undifferentiated	11.86	n/a
9/25/2018	7	-8.32	-55.97	Ice Contact	10.63	n/a
9/25/2018	8	-8.46	-57.92	Ice Contact	9.79	n/a
9/25/2018	9.1	-8.39	-55.42	SDC	11.68	n/a
9/25/2018	9.2	-8.91	-58.21	SDC	13.07	n/a
9/25/2018	10.1	-8.40	-56.02	SDC	11.21	n/a
9/25/2018	10.2	-8.58	-56.30	SDC	12.33	n/a
9/25/2018	11	-8.87	-59.97	SDC	11.01	n/a
9/25/2018	12.1	-8.76	-58.57	SDC	11.51	n/a
9/25/2018	12.2	-8.67	-57.84	SDC	11.50	n/a
9/25/2018	13	-8.36	-57.96	Outwash	8.93	n/a
9/25/2018	14	-8.79	-59.25	SDC	11.06	n/a
9/25/2018	15	-8.72	-57.01	SDC	12.78	n/a
10/2/2018	1	-8.89	-61.74	Igneous	9.41	n/a
10/2/2018	2	-9.03	-62.81	Till plain	9.44	n/a
10/2/2018	3	-9.05	-62.72	Till plain	9.65	n/a
10/2/2018	4	-8.51	-58.85	SDC	9.24	n/a
10/2/2018	5	-8.49	-58.48	SDC	9.42	n/a
10/2/2018	6.1	-8.73	-58.28	Undifferentiated	11.53	n/a
10/2/2018	6.2	-8.76	-58.97	Undifferentiated	11.09	n/a

Table A4 (cont.)

Date	Site ID	$\delta^{18}O$	$\delta^{2}H$	Geology	D-excess	T (°C)
10/2/2018	6.3	-8.58	-57.11	Undifferentiated	11.49	n/a
10/2/2018	7	-8.62	-58.92	Ice Contact	10.04	n/a
10/2/2018	8	-8.50	-59.90	Ice Contact	8.09	n/a
10/2/2018	9.1	-8.71	-58.33	SDC	11.33	n/a
10/2/2018	9.2	-8.60	-57.78	SDC	11.05	n/a
10/2/2018	10.1	-8.75	-57.88	SDC	12.15	n/a
10/2/2018	10.2	-8.50	-55.56	SDC	12.45	n/a
10/2/2018	11	-8.77	-59.90	SDC	10.30	n/a
10/2/2018	12.1	-8.95	-60.79	SDC	10.84	n/a
10/2/2018	12.2	-9.40	-64.29	SDC	10.94	n/a
10/2/2018	13	-8.39	-59.55	Outwash	7.59	n/a
10/2/2018	14	-9.30	-63.98	SDC	10.42	n/a
10/2/2018	15	-9.07	-60.29	SDC	12.28	n/a
10/9/2018	1	-9.39	-63.04	Igneous	12.07	8
10/9/2018	2	-9.47	-63.40	Till plain	12.36	7.9
10/9/2018	3	-9.26	-61.65	Till plain	12.42	7.7
10/9/2018	4	-9.72	-65.55	SDC	12.18	7.6
10/9/2018	5	-9.22	-61.38	SDC	12.42	7.5
10/9/2018	6.1	-9.47	-61.74	Undifferentiated	14.00	7.3
10/9/2018	6.2	-9.92	-66.04	Undifferentiated	13.33	7.3
10/9/2018	6.3	-9.88	-65.61	Undifferentiated	13.44	7.3
10/9/2018	7	-9.28	-61.96	Ice Contact	12.28	7.6
10/9/2018	8	-9.73	-66.22	Ice Contact	11.58	7.4
10/9/2018	9.1	-9.19	-60.34	SDC	13.16	7.3
10/9/2018	9.2	-9.40	-61.73	SDC	13.49	7.3
10/9/2018	10.1	-9.07	-59.10	SDC	13.47	7.2
10/9/2018	10.2	-9.23	-60.53	SDC	13.29	7.2
10/9/2018	11	-9.20	-61.64	SDC	11.99	7.3
10/9/2018	12.1	-9.43	-63.42	SDC	11.98	7.2
10/9/2018	12.2	-9.55	-64.44	SDC	11.93	7.2
10/9/2018	13	-9.30	-63.65	Outwash	10.74	7.4
10/9/2018	14	-9.16	-61.54	SDC	11.77	7.3
10/9/2018	15	-9.45	-61.73	SDC	13.84	7.3
10/18/2018	1	-9.38	-63.51	Igneous	11.54	6.8
10/18/2018	2	-9.44	-64.39	Till plain	11.09	6.3
10/18/2018	4	-9.62	-64.59	SDC	12.35	5.1
10/18/2018	5	-9.70	-67.23	SDC	10.40	5.3
10/18/2018	6.1	-9.96	-66.99	Undifferentiated	12.69	5
10/18/2018	6.2	-9.78	-65.07	Undifferentiated	13.15	5.8

Table A4 (cont.)

Date	Site ID	$\delta^{18}O$	$\delta^{2}H$	Geology	D-excess	T (°C)
10/18/2018	6.3	-9.70	-65.88	Undifferentiated	11.75	5.8
10/18/2018	8	-9.37	-64.67	Ice Contact	10.33	4.7
10/18/2018	9.2	-9.67	-64.94	SDC	12.42	4.1
10/18/2018	14	-9.43	-64.47	SDC	10.99	4
10/24/2018	3	-9.46	-65.50	Till plain	10.16	4.2
10/24/2018	4	-9.96	-68.61	SDC	11.06	3.4
10/24/2018	5	-9.61	-66.66	SDC	10.25	3.4
10/24/2018	7	-9.77	-65.76	Ice Contact	12.37	4.6
10/24/2018	8	-9.07	-62.50	Ice Contact	10.03	4.1
10/24/2018	9.2	-9.53	-63.51	SDC	12.71	4.2
10/24/2018	10.1	-9.56	-63.70	SDC	12.77	2.9
10/24/2018	10.2	-9.55	-63.88	SDC	12.53	2.9
10/24/2018	11	-9.48	-65.60	SDC	10.20	4.8
10/24/2018	13	-9.13	-64.40	Outwash	8.63	5.1
10/24/2018	14	-9.69	-67.28	SDC	10.26	4.3
10/31/2018	1	-9.72	-67.04	Igneous	10.73	5
10/31/2018	4	-10.18	-69.47	SDC	11.93	4.7
10/31/2018	5	-9.59	-66.46	SDC	10.27	4.7
10/31/2018	6.1	-10.53	-72.28	Undifferentiated	12.00	4
10/31/2018	6.2	-10.56	-72.45	Undifferentiated	12.02	4
10/31/2018	6.3	-10.08	-68.44	Undifferentiated	12.22	4
10/31/2018	7	-10.19	-69.08	Ice Contact	12.45	5.1
10/31/2018	8	-9.69	-68.47	Ice Contact	9.04	4.6
10/31/2018	9.1	-10.08	-68.72	SDC	11.92	3.8
10/31/2018	9.2	-10.05	-67.91	SDC	12.47	3.8
10/31/2018	10.1	-9.92	-66.62	SDC	12.72	3.9
10/31/2018	10.2	-10.25	-70.17	SDC	11.81	3.9
10/31/2018	11	-10.28	-71.85	SDC	10.41	4.7
10/31/2018	12.1	-9.99	-68.55	SDC	11.40	4.3
10/31/2018	12.2	-10.11	-69.36	SDC	11.52	4.3
10/31/2018	14	-10.08	-69.84	SDC	10.84	4.5
11/7/2018	1	-10.54	-72.42	Igneous	11.86	3.1
11/7/2018	2	-10.59	-72.76	Till plain	11.97	2.9
11/7/2018	3	-10.47	-71.94	Till plain	11.84	2.7
11/7/2018	4	-11.25	-76.75	SDC	13.28	2.3
11/7/2018	5	-10.51	-72.17	SDC	11.94	2.5
11/7/2018	6.1	-11.11	-75.23	Undifferentiated	13.67	1.7
11/7/2018	6.2	-11.16	-75.78	Undifferentiated	13.52	1.7
11/7/2018	6.3	-11.07	-74.93	Undifferentiated	13.66	1.7

Table A4 (cont.)

Date	Site ID	$\delta^{18}O$	$\delta^{2}H$	Geology	D-excess	T (°C)
11/7/2018	7	-10.83	-73.95	Ice Contact	12.71	3
11/7/2018	8	-10.31	-71.07	Ice Contact	11.43	2.3
11/7/2018	9.1	-10.78	-73.64	SDC	12.61	2.2
11/7/2018	9.2	-10.77	-73.08	SDC	13.08	2.2
11/7/2018	10.1	-10.61	-71.62	SDC	13.30	1.8
11/7/2018	10.2	-10.58	-71.28	SDC	13.39	1.8
11/7/2018	11	-10.53	-72.70	SDC	11.55	2.5
11/7/2018	12.1	-10.63	-73.26	SDC	11.78	2.3
11/7/2018	12.2	-10.70	-73.73	SDC	11.87	2.3
11/7/2018	13	-9.99	-69.61	Outwash	10.33	2.3
11/7/2018	14	-10.60	-73.59	SDC	11.24	2.5
11/7/2018	15	-11.19	-76.59	SDC	12.92	1.8
11/13/2018	1	-10.45	-71.87	Igneous	11.71	0.1
11/13/2018	2	-10.38	-71.80	Till plain	11.22	n/a
11/13/2018	3	-10.32	-71.31	Till plain	11.22	n/a
11/13/2018	4	-10.93	-74.07	SDC	13.34	0.1
11/13/2018	5	-10.30	-70.97	SDC	11.45	n/a
11/13/2018	7	-10.82	-73.49	Ice Contact	13.07	n/a
11/13/2018	8	-10.21	-71.14	Ice Contact	10.57	n/a
11/13/2018	10.1	-10.62	-71.71	SDC	13.28	n/a
11/13/2018	11	-10.51	-72.74	SDC	11.31	n/a
11/13/2018	13	-9.81	-68.49	Outwash	9.98	n/a
11/20/2018	1	-10.37	-71.67	Igneous	11.25	n/a
11/20/2018	2	-10.34	-71.52	Till plain	11.18	n/a
11/20/2018	3	-10.22	-70.80	Till plain	10.92	n/a
11/20/2018	4	-10.89	-74.23	SDC	12.86	n/a
11/20/2018	5	-10.28	-71.00	SDC	11.26	n/a
11/20/2018	7	-10.87	-73.65	Ice Contact	13.31	n/a
11/20/2018	10.1	-10.73	-72.13	SDC	13.67	n/a
11/20/2018	13	-9.99	-70.24	Outwash	9.69	n/a
11/27/2018	1	-10.92	-75.46	Igneous	11.86	n/a
11/27/2018	2	-10.95	-74.99	Till plain	12.61	n/a
11/27/2018	3	-10.89	-75.14	Till plain	12.01	n/a
11/27/2018	4	-11.51	-78.75	SDC	13.34	n/a
11/27/2018	5	-10.93	-75.51	SDC	11.95	n/a
11/27/2018	7	-11.26	-76.37	Ice Contact	13.69	n/a
11/27/2018	10.1	-11.10	-74.88	SDC	13.89	n/a
11/27/2018	13	-10.49	-73.20	Outwash	10.68	n/a
12/4/2018	1	-10.69	-73.69	Igneous	11.80	n/a

Table A4 (cont.)

Date	Site ID	$\delta^{18}O$	$\delta^{2}H$	Geology	D-excess	T (°C)
12/4/2018	2	-10.69	-73.47	Till plain	12.06	n/a
12/4/2018	3	-10.58	-72.50	Till plain	12.16	n/a
12/4/2018	4	-11.07	-75.60	SDC	12.97	n/a
12/4/2018	5	-10.67	-73.50	SDC	11.86	n/a
12/4/2018	7	-11.18	-76.02	Ice Contact	13.40	n/a
12/4/2018	10.1	-10.99	-74.09	SDC	13.84	n/a
12/4/2018	13	-10.42	-72.45	Outwash	10.89	n/a
12/11/2018	1	-10.63	-73.40	Igneous	11.68	n/a
12/11/2018	2	-10.64	-73.55	Till plain	11.54	n/a
12/11/2018	3	-10.61	-73.47	Till plain	11.42	n/a
12/11/2018	5	-10.62	-73.30	SDC	11.66	n/a
12/11/2018	7	-11.29	-76.58	Ice Contact	13.71	n/a
12/11/2018	10.1	-11.03	-74.19	SDC	14.05	n/a
12/11/2018	13	-10.42	-72.79	Outwash	10.61	n/a
12/18/2018	1	-10.66	-73.84	Igneous	11.47	n/a
12/18/2018	7	-11.25	-76.38	Ice Contact	13.64	n/a
12/18/2018	10.1	-11.00	-74.08	SDC	13.89	n/a
12/18/2018	13	-10.48	-73.21	Outwash	10.64	n/a

Table A5: Stable Isotope values of $\delta^{18}O$ and $\delta^{2}H$ from the Picarro L2130-i water isotope analyzer given in per mil ($^{0}/_{00}$) across precipitation sites near the Lester River.

Date	Site ID	$\delta^{18}O$	$\delta^{2}H$	Type	D-excess
7/31/2018	16	-11.47	-89.096	precipitation	2.66266
8/2/2018	16	-11.006	-82.146	precipitation	5.90381
8/5/2018	16	-5.4569	-29.808	precipitation	13.847
8/28/2018	16	-7.9957	-56.167	precipitation	7.79888
8/28/2018	17	-6.4415	-43.921	precipitation	7.61177
8/29/2018	17	-9.7793	-61.456	precipitation	16.779
9/1/2018	17	-8.4433	-54.087	precipitation	13.4594
9/3/2018	16	-7.3595	-45.657	precipitation	13.2191
9/15/2018	17	-9.3046	-60.072	precipitation	14.3652
9/18/2018	16	-7.2539	-47.964	precipitation	10.0679
9/21/2018	19	-12.05	-82.728	gw	13.6683
9/21/2018	19	-11.849	-80.888	gw	13.9037
9/21/2018	19	-11.966	-81.779	gw	13.9489
9/21/2018	19	-11.827	-80.916	gw	13.6978
9/22/2018	16	-9.5877	-60.418	precipitation	16.2834
9/26/2018	17	-10.438	-68.635	precipitation	14.8721
10/4/2018	17	-6.921	-40.132	precipitation	15.2361
10/8/2018	17	-12.884	-81.201	precipitation	21.8718
10/9/2018	16	-11.466	-75.084	precipitation	16.6406
10/9/2018	17	-11.456	-74.451	precipitation	17.1947
10/10/2018	17	-12.536	-81.469	precipitation	18.8169
10/11/2018	17	-11.319	-71.909	precipitation	18.6442
10/26/2018	17	-17.379	-131.77	precipitation	7.26103
10/27/2018	17	-21.839	-152.86	precipitation	21.8536
10/28/2018	17	-17.611	-128.7	precipitation	12.1826
10/30/2018	17	-12.813	-92.025	precipitation	10.4783
10/31/2018	16	-12.825	-97.048	precipitation	5.54906
11/4/2018	17	-25.202	-176.8	snow	24.8142
11/4/2018	18	-21.435	-152.92	precipitation	18.5561
11/11/2018	17	-25.914	-187.33	snow	19.9823
11/19/2018	17	-24.164	-173.46	snow	19.8506
11/24/2018	17	-20.673	-144.78	snow	20.6076
11/29/2018	17	-22.665	-168.5	snow	12.8271

APPENDIX 4: TEMPERATURE RESULTS IN THE LESTER RIVER WATERSHED, DULUTH, MN.

Table A6: Stream Temperature data collected from Onset HOBO tidbit v2 Water Temperature Data Loggers. The amount of time that the stream experienced specific conditions related to trout living conditions is listed as the percent of time. The percentage is taken over June, July, and August.

	Average Temperatures (°C)				Percent of Time		
Site ID	**June**	**July**	**August**	**Summer**	**% Growth**	**% Stress**	**% Lethal**
2	16.8	20.7	20.1	19.2	62.2	32.8	5
4	15.3	18.6	17.1	17	90.6	0.094	0
5	16.5	19.9	18.6	18.3	73.2	26.8	0
6	18.1	21.4	19.5	19.7	55.3	42.3	2.4
8	17.2	20.3	18.7	18.8	67.6	32.2	0.2
10	15	18	16.5	16.5	97.8	2.2	0
11	17.8	20.8	19.1	19.3	60.6	39.2	0.2
15	16	19.3	18.6	18	76.7	23.3	0

APPENDIX 5: ANOVA RESULTS FROM *STATS* IN R FOR THE DATA COLLECTED IN THE LESTER RIVER WATERSHED, DULUTH, MN.

Table A7: ANOVA results from Tukey's HSD in R comparing mean $\delta^{18}O$ values from sampling dates for significance with a α=0.005. (*= significant difference)

Comparisons between Dates				
Dates	**diff**	**lwr**	**upr**	**p adj**
2018-05-29-2018-05-21	0.4765	-0.0583	1.01133	0.17193
2018-06-04-2018-05-21	0.666	0.13117	1.20083	0.00127*
2018-06-12-2018-05-21	0.951	0.41617	1.48583	0*
2018-06-19-2018-05-21	2.2555	1.72067	2.79033	0*
2018-06-26-2018-05-21	2.074	1.53917	2.60883	0*
2018-07-02-2018-05-21	1.8245	1.28967	2.35933	0*
2018-07-10-2018-05-21	3.1045	2.56967	3.63933	0*
2018-07-16-2018-05-21	2.887	2.35217	3.42183	0*
2018-07-24-2018-05-21	2.78	2.24517	3.31483	0*
2018-07-31-2018-05-21	2.8065	2.27167	3.34133	0*
2018-08-07-2018-05-21	2.538	2.00317	3.07283	0*
2018-08-13-2018-05-21	2.45511	1.90563	3.00459	0*
2018-08-21-2018-05-21	2.3375	1.80267	2.87233	0*
2018-08-28-2018-05-21	2.4725	1.93767	3.00733	0*
2018-09-03-2018-05-21	2.536	2.00117	3.07083	0*
2018-09-11-2018-05-21	2.49	1.95517	3.02483	0*
2018-09-18-2018-05-21	2.436	1.90117	2.97083	0*
2018-09-25-2018-05-21	2.25	1.71517	2.78483	0*
2018-10-02-2018-05-21	2.054	1.51917	2.58883	0*
2018-10-09-2018-05-21	1.418	0.88317	1.95283	0*
2018-10-18-2018-05-21	1.22862	0.57359	1.88364	0*
2018-10-24-2018-05-21	1.30712	0.67225	1.94199	0*
2018-10-31-2018-05-21	0.75231	0.18505	1.31958	0.0003*
2018-11-07-2018-05-21	0.123	-0.4118	0.65783	1
2018-11-13-2018-05-21	0.399	-0.256	1.05403	0.8986
2018-11-20-2018-05-21	0.37275	-0.3348	1.08026	0.98136
2018-11-27-2018-05-21	-0.1723	-0.8798	0.53526	1
2018-12-04-2018-05-21	0.04775	-0.6598	0.75526	1
2018-12-11-2018-05-21	0.08543	-0.6573	0.82816	1
2018-12-18-2018-05-21	-0.0135	-0.9398	0.91285	1
2018-06-04-2018-05-29	0.1895	-0.3453	0.72433	0.99998
2018-06-12-2018-05-29	0.4745	-0.0603	1.00933	0.17843

Table A7 (cont.)

Dates	diff	lwr	upr	p adj
2018-06-19-2018-05-29	1.779	1.24417	2.31383	0*
2018-06-26-2018-05-29	1.5975	1.06267	2.13233	0*
2018-07-02-2018-05-29	1.348	0.81317	1.88283	0*
2018-07-10-2018-05-29	2.628	2.09317	3.16283	0*
2018-07-16-2018-05-29	2.4105	1.87567	2.94533	0*
2018-07-24-2018-05-29	2.3035	1.76867	2.83833	0*
2018-07-31-2018-05-29	2.33	1.79517	2.86483	0*
2018-08-07-2018-05-29	2.0615	1.52667	2.59633	0*
2018-08-13-2018-05-29	1.97861	1.42913	2.52809	0*
2018-08-21-2018-05-29	1.861	1.32617	2.39583	0*
2018-08-28-2018-05-29	1.996	1.46117	2.53083	0*
2018-09-03-2018-05-29	2.0595	1.52467	2.59433	0*
2018-09-11-2018-05-29	2.0135	1.47867	2.54833	0*
2018-09-18-2018-05-29	1.9595	1.42467	2.49433	0*
2018-09-25-2018-05-29	1.7735	1.23867	2.30833	0*
2018-10-02-2018-05-29	1.5775	1.04267	2.11233	0*
2018-10-09-2018-05-29	0.9415	0.40667	1.47633	0*
2018-10-18-2018-05-29	0.75212	0.09709	1.40714	0.00619
2018-10-24-2018-05-29	0.83062	0.19575	1.46549	0.00042*
2018-10-31-2018-05-29	0.27581	-0.2915	0.84308	0.9941
2018-11-07-2018-05-29	-0.3535	-0.8883	0.18133	0.79034
2018-11-13-2018-05-29	-0.0775	-0.7325	0.57753	1
2018-11-20-2018-05-29	-0.1038	-0.8113	0.60376	1
2018-11-27-2018-05-29	-0.6488	-1.3563	0.05876	0.13149
2018-12-04-2018-05-29	-0.4288	-1.1363	0.27876	0.90368
2018-12-11-2018-05-29	-0.3911	-1.1338	0.35166	0.98151
2018-12-18-2018-05-29	-0.49	-1.4163	0.43635	0.98034
2018-06-12-2018-06-04	0.285	-0.2498	0.81983	0.97832
2018-06-19-2018-06-04	1.5895	1.05467	2.12433	0*
2018-06-26-2018-06-04	1.408	0.87317	1.94283	0*
2018-07-02-2018-06-04	1.1585	0.62367	1.69333	0*
2018-07-10-2018-06-04	2.4385	1.90367	2.97333	0*
2018-07-16-2018-06-04	2.221	1.68617	2.75583	0*
2018-07-24-2018-06-04	2.114	1.57917	2.64883	0*
2018-07-31-2018-06-04	2.1405	1.60567	2.67533	0*
2018-08-07-2018-06-04	1.872	1.33717	2.40683	0*
2018-08-13-2018-06-04	1.78911	1.23963	2.33859	0*
2018-08-21-2018-06-04	1.6715	1.13667	2.20633	0*
2018-08-28-2018-06-04	1.8065	1.27167	2.34133	0*

Table A7 (cont.)

Dates	diff	lwr	upr	p adj
2018-09-03-2018-06-04	1.87	1.33517	2.40483	0*
2018-09-11-2018-06-04	1.824	1.28917	2.35883	0*
2018-09-18-2018-06-04	1.77	1.23517	2.30483	0*
2018-09-25-2018-06-04	1.584	1.04917	2.11883	0*
2018-10-02-2018-06-04	1.388	0.85317	1.92283	0*
2018-10-09-2018-06-04	0.752	0.21717	1.28683	6.8E-05*
2018-10-18-2018-06-04	0.56262	-0.0924	1.21764	0.23339
2018-10-24-2018-06-04	0.64112	0.00625	1.27599	0.04412
2018-10-31-2018-06-04	0.08631	-0.481	0.65358	1
2018-11-07-2018-06-04	-0.543	-1.0778	-0.0082	0.04114
2018-11-13-2018-06-04	-0.267	-0.922	0.38803	0.99971
2018-11-20-2018-06-04	-0.2933	-1.0008	0.41426	0.9996
2018-11-27-2018-06-04	-0.8383	-1.5458	-0.1307	0.00348*
2018-12-04-2018-06-04	-0.6183	-1.3258	0.08926	0.20311
2018-12-11-2018-06-04	-0.5806	-1.3233	0.16216	0.43286
2018-12-18-2018-06-04	-0.6795	-1.6058	0.24685	0.58077
2018-06-19-2018-06-12	1.3045	0.76967	1.83933	0*
2018-06-26-2018-06-12	1.123	0.58817	1.65783	0*
2018-07-02-2018-06-12	0.8735	0.33867	1.40833	6E-07*
2018-07-10-2018-06-12	2.1535	1.61867	2.68833	0*
2018-07-16-2018-06-12	1.936	1.40117	2.47083	0*
2018-07-24-2018-06-12	1.829	1.29417	2.36383	0*
2018-07-31-2018-06-12	1.8555	1.32067	2.39033	0*
2018-08-07-2018-06-12	1.587	1.05217	2.12183	0*
2018-08-13-2018-06-12	1.50411	0.95463	2.05359	0*
2018-08-21-2018-06-12	1.3865	0.85167	1.92133	0*
2018-08-28-2018-06-12	1.5215	0.98667	2.05633	0*
2018-09-03-2018-06-12	1.585	1.05017	2.11983	0*
2018-09-11-2018-06-12	1.539	1.00417	2.07383	0*
2018-09-18-2018-06-12	1.485	0.95017	2.01983	0*
2018-09-25-2018-06-12	1.299	0.76417	1.83383	0*
2018-10-02-2018-06-12	1.103	0.56817	1.63783	0*
2018-10-09-2018-06-12	0.467	-0.0678	1.00183	0.20439
2018-10-18-2018-06-12	0.27762	-0.3774	0.93264	0.9994
2018-10-24-2018-06-12	0.35612	-0.2787	0.99099	0.95876
2018-10-31-2018-06-12	-0.1987	-0.766	0.36858	0.99999
2018-11-07-2018-06-12	-0.828	-1.3628	-0.2932	3.8E-06*
2018-11-13-2018-06-12	-0.552	-1.207	0.10303	0.26952
2018-11-20-2018-06-12	-0.5783	-1.2858	0.12926	0.3327

Table A7 (cont.)

Dates	diff	lwr	upr	p adj
2018-11-27-2018-06-12	-1.1233	-1.8308	-0.4157	1.6E-06*
2018-12-04-2018-06-12	-0.9033	-1.6108	-0.1957	0.00074*
2018-12-11-2018-06-12	-0.8656	-1.6083	-0.1228	0.00474*
2018-12-18-2018-06-12	-0.9645	-1.8908	-0.0382	0.02923
2018-06-26-2018-06-19	-0.1815	-0.7163	0.35333	0.99999
2018-07-02-2018-06-19	-0.431	-0.9658	0.10383	0.36353
2018-07-10-2018-06-19	0.849	0.31417	1.38383	1.6E-06*
2018-07-16-2018-06-19	0.6315	0.09667	1.16633	0.00371*
2018-07-24-2018-06-19	0.5245	-0.0103	1.05933	0.0635
2018-07-31-2018-06-19	0.551	0.01617	1.08583	0.03383
2018-08-07-2018-06-19	0.2825	-0.2523	0.81733	0.98071
2018-08-13-2018-06-19	0.19961	-0.3499	0.74909	0.99997
2018-08-21-2018-06-19	0.082	-0.4528	0.61683	1
2018-08-28-2018-06-19	0.217	-0.3178	0.75183	0.99973
2018-09-03-2018-06-19	0.2805	-0.2543	0.81533	0.98247
2018-09-11-2018-06-19	0.2345	-0.3003	0.76933	0.99891
2018-09-18-2018-06-19	0.1805	-0.3543	0.71533	0.99999
2018-09-25-2018-06-19	-0.0055	-0.5403	0.52933	1
2018-10-02-2018-06-19	-0.2015	-0.7363	0.33333	0.99994
2018-10-09-2018-06-19	-0.8375	-1.3723	-0.3027	2.6E-06*
2018-10-18-2018-06-19	-1.0269	-1.6819	-0.3719	2.5E-06*
2018-10-24-2018-06-19	-0.9484	-1.5832	-0.3135	1.2E-05*
2018-10-31-2018-06-19	-1.5032	-2.0705	-0.9359	0*
2018-11-07-2018-06-19	-2.1325	-2.6673	-1.5977	0*
2018-11-13-2018-06-19	-1.8565	-2.5115	-1.2015	0*
2018-11-20-2018-06-19	-1.8828	-2.5903	-1.1752	0*
2018-11-27-2018-06-19	-2.4278	-3.1353	-1.7202	0*
2018-12-04-2018-06-19	-2.2078	-2.9153	-1.5002	0*
2018-12-11-2018-06-19	-2.1701	-2.9128	-1.4273	0*
2018-12-18-2018-06-19	-2.269	-3.1953	-1.3427	0*
2018-07-02-2018-06-26	-0.2495	-0.7843	0.28533	0.99692
2018-07-10-2018-06-26	1.0305	0.49567	1.56533	0*
2018-07-16-2018-06-26	0.813	0.27817	1.34783	6.8E-06*
2018-07-24-2018-06-26	0.706	0.17117	1.24083	0.00034*
2018-07-31-2018-06-26	0.7325	0.19767	1.26733	0.00014*
2018-08-07-2018-06-26	0.464	-0.0708	0.99883	0.21549
2018-08-13-2018-06-26	0.38111	-0.1684	0.93059	0.7018
2018-08-21-2018-06-26	0.2635	-0.2713	0.79833	0.9928
2018-08-28-2018-06-26	0.3985	-0.1363	0.93333	0.54471

Table A7 (cont.)

Dates	diff	lwr	upr	p adj
2018-09-03-2018-06-26	0.462	-0.0728	0.99683	0.22311
2018-09-11-2018-06-26	0.416	-0.1188	0.95083	0.44433
2018-09-18-2018-06-26	0.362	-0.1728	0.89683	0.74881
2018-09-25-2018-06-26	0.176	-0.3588	0.71083	1
2018-10-02-2018-06-26	-0.02	-0.5548	0.51483	1
2018-10-09-2018-06-26	-0.656	-1.1908	-0.1212	0.00175*
2018-10-18-2018-06-26	-0.8454	-1.5004	-0.1904	0.00058*
2018-10-24-2018-06-26	-0.7669	-1.4017	-0.132	0.00238*
2018-10-31-2018-06-26	-1.3217	-1.889	-0.7544	0*
2018-11-07-2018-06-26	-1.951	-2.4858	-1.4162	0*
2018-11-13-2018-06-26	-1.675	-2.33	-1.02	0*
2018-11-20-2018-06-26	-1.7013	-2.4088	-0.9937	0*
2018-11-27-2018-06-26	-2.2463	-2.9538	-1.5387	0*
2018-12-04-2018-06-26	-2.0263	-2.7338	-1.3187	0*
2018-12-11-2018-06-26	-1.9886	-2.7313	-1.2458	0*
2018-12-18-2018-06-26	-2.0875	-3.0138	-1.1612	0*
2018-07-10-2018-07-02	1.28	0.74517	1.81483	0*
2018-07-16-2018-07-02	1.0625	0.52767	1.59733	0*
2018-07-24-2018-07-02	0.9555	0.42067	1.49033	0*
2018-07-31-2018-07-02	0.982	0.44717	1.51683	0*
2018-08-07-2018-07-02	0.7135	0.17867	1.24833	0.00026*
2018-08-13-2018-07-02	0.63061	0.08113	1.18009	0.00625*
2018-08-21-2018-07-02	0.513	-0.0218	1.04783	0.08205
2018-08-28-2018-07-02	0.648	0.11317	1.18283	0.00224*
2018-09-03-2018-07-02	0.7115	0.17667	1.24633	0.00028*
2018-09-11-2018-07-02	0.6655	0.13067	1.20033	0.00129*
2018-09-18-2018-07-02	0.6115	0.07667	1.14633	0.00668
2018-09-25-2018-07-02	0.4255	-0.1093	0.96033	0.39237
2018-10-02-2018-07-02	0.2295	-0.3053	0.76433	0.99926
2018-10-09-2018-07-02	-0.4065	-0.9413	0.12833	0.49832
2018-10-18-2018-07-02	-0.5959	-1.2509	0.05914	0.14192
2018-10-24-2018-07-02	-0.5174	-1.1522	0.11749	0.33895
2018-10-31-2018-07-02	-1.0722	-1.6395	-0.5049	0*
2018-11-07-2018-07-02	-1.7015	-2.2363	-1.1667	0*
2018-11-13-2018-07-02	-1.4255	-2.0805	-0.7705	0*
2018-11-20-2018-07-02	-1.4518	-2.1593	-0.7442	0*
2018-11-27-2018-07-02	-1.9968	-2.7043	-1.2892	0*
2018-12-04-2018-07-02	-1.7768	-2.4843	-1.0692	0*
2018-12-11-2018-07-02	-1.7391	-2.4818	-0.9963	0*

Table A7 (cont.)

Dates	diff	lwr	upr	p adj
2018-12-18-2018-07-02	-1.838	-2.7643	-0.9117	0*
2018-07-16-2018-07-10	-0.2175	-0.7523	0.31733	0.99972
2018-07-24-2018-07-10	-0.3245	-0.8593	0.21033	0.9025
2018-07-31-2018-07-10	-0.298	-0.8328	0.23683	0.96194
2018-08-07-2018-07-10	-0.5665	-1.1013	-0.0317	0.02285
2018-08-13-2018-07-10	-0.6494	-1.1989	-0.0999	0.00365*
2018-08-21-2018-07-10	-0.767	-1.3018	-0.2322	3.9E-05*
2018-08-28-2018-07-10	-0.632	-1.1668	-0.0972	0.00365*
2018-09-03-2018-07-10	-0.5685	-1.1033	-0.0337	0.0217
2018-09-11-2018-07-10	-0.6145	-1.1493	-0.0797	0.00612
2018-09-18-2018-07-10	-0.6685	-1.2033	-0.1337	0.00118*
2018-09-25-2018-07-10	-0.8545	-1.3893	-0.3197	1.3E-06*
2018-10-02-2018-07-10	-1.0505	-1.5853	-0.5157	0*
2018-10-09-2018-07-10	-1.6865	-2.2213	-1.1517	0*
2018-10-18-2018-07-10	-1.8759	-2.5309	-1.2209	0*
2018-10-24-2018-07-10	-1.7974	-2.4322	-1.1625	0*
2018-10-31-2018-07-10	-2.3522	-2.9195	-1.7849	0*
2018-11-07-2018-07-10	-2.9815	-3.5163	-2.4467	0*
2018-11-13-2018-07-10	-2.7055	-3.3605	-2.0505	0*
2018-11-20-2018-07-10	-2.7318	-3.4393	-2.0242	0*
2018-11-27-2018-07-10	-3.2768	-3.9843	-2.5692	0*
2018-12-04-2018-07-10	-3.0568	-3.7643	-2.3492	0*
2018-12-11-2018-07-10	-3.0191	-3.7618	-2.2763	0*
2018-12-18-2018-07-10	-3.118	-4.0443	-2.1917	0*
2018-07-24-2018-07-16	-0.107	-0.6418	0.42783	1
2018-07-31-2018-07-16	-0.0805	-0.6153	0.45433	1
2018-08-07-2018-07-16	-0.349	-0.8838	0.18583	0.81089
2018-08-13-2018-07-16	-0.4319	-0.9814	0.11759	0.42012
2018-08-21-2018-07-16	-0.5495	-1.0843	-0.0147	0.03511
2018-08-28-2018-07-16	-0.4145	-0.9493	0.12033	0.45274
2018-09-03-2018-07-16	-0.351	-0.8858	0.18383	0.80189
2018-09-11-2018-07-16	-0.397	-0.9318	0.13783	0.55345
2018-09-18-2018-07-16	-0.451	-0.9858	0.08383	0.26824
2018-09-25-2018-07-16	-0.637	-1.1718	-0.1022	0.00314*
2018-10-02-2018-07-16	-0.833	-1.3678	-0.2982	3.1E-06*
2018-10-09-2018-07-16	-1.469	-2.0038	-0.9342	0*
2018-10-18-2018-07-16	-1.6584	-2.3134	-1.0034	0*
2018-10-24-2018-07-16	-1.5799	-2.2147	-0.945	0*
2018-10-31-2018-07-16	-2.1347	-2.702	-1.5674	0*

Table A7 (cont.)

Dates	diff	lwr	upr	p adj
2018-11-07-2018-07-16	-2.764	-3.2988	-2.2292	0*
2018-11-13-2018-07-16	-2.488	-3.143	-1.833	0*
2018-11-20-2018-07-16	-2.5143	-3.2218	-1.8067	0*
2018-11-27-2018-07-16	-3.0593	-3.7668	-2.3517	0*
2018-12-04-2018-07-16	-2.8393	-3.5468	-2.1317	0*
2018-12-11-2018-07-16	-2.8016	-3.5443	-2.0588	0*
2018-12-18-2018-07-16	-2.9005	-3.8268	-1.9742	0*
2018-07-31-2018-07-24	0.0265	-0.5083	0.56133	1
2018-08-07-2018-07-24	-0.242	-0.7768	0.29283	0.99814
2018-08-13-2018-07-24	-0.3249	-0.8744	0.22459	0.92531
2018-08-21-2018-07-24	-0.4425	-0.9773	0.09233	0.30676
2018-08-28-2018-07-24	-0.3075	-0.8423	0.22733	0.94506
2018-09-03-2018-07-24	-0.244	-0.7788	0.29083	0.99786
2018-09-11-2018-07-24	-0.29	-0.8248	0.24483	0.97285
2018-09-18-2018-07-24	-0.344	-0.8788	0.19083	0.83244
2018-09-25-2018-07-24	-0.53	-1.0648	0.00483	0.05597
2018-10-02-2018-07-24	-0.726	-1.2608	-0.1912	0.00017*
2018-10-09-2018-07-24	-1.362	-1.8968	-0.8272	0*
2018-10-18-2018-07-24	-1.5514	-2.2064	-0.8964	0*
2018-10-24-2018-07-24	-1.4729	-2.1077	-0.838	0*
2018-10-31-2018-07-24	-2.0277	-2.595	-1.4604	0*
2018-11-07-2018-07-24	-2.657	-3.1918	-2.1222	0*
2018-11-13-2018-07-24	-2.381	-3.036	-1.726	0*
2018-11-20-2018-07-24	-2.4073	-3.1148	-1.6997	0*
2018-11-27-2018-07-24	-2.9523	-3.6598	-2.2447	0*
2018-12-04-2018-07-24	-2.7323	-3.4398	-2.0247	0*
2018-12-11-2018-07-24	-2.6946	-3.4373	-1.9518	0*
2018-12-18-2018-07-24	-2.7935	-3.7198	-1.8672	0*
2018-08-07-2018-07-31	-0.2685	-0.8033	0.26633	0.9905
2018-08-13-2018-07-31	-0.3514	-0.9009	0.19809	0.84059
2018-08-21-2018-07-31	-0.469	-1.0038	0.06583	0.19722
2018-08-28-2018-07-31	-0.334	-0.8688	0.20083	0.87122
2018-09-03-2018-07-31	-0.2705	-0.8053	0.26433	0.98943
2018-09-11-2018-07-31	-0.3165	-0.8513	0.21833	0.92461
2018-09-18-2018-07-31	-0.3705	-0.9053	0.16433	0.70422
2018-09-25-2018-07-31	-0.5565	-1.0913	-0.0217	0.02949
2018-10-02-2018-07-31	-0.7525	-1.2873	-0.2177	6.7E-05*
2018-10-09-2018-07-31	-1.3885	-1.9233	-0.8537	0*
2018-10-18-2018-07-31	-1.5779	-2.2329	-0.9229	0*

Table A7 (cont.)

Dates	diff	lwr	upr	p adj
2018-10-24-2018-07-31	-1.4994	-2.1342	-0.8645	0*
2018-10-31-2018-07-31	-2.0542	-2.6215	-1.4869	0*
2018-11-07-2018-07-31	-2.6835	-3.2183	-2.1487	0*
2018-11-13-2018-07-31	-2.4075	-3.0625	-1.7525	0*
2018-11-20-2018-07-31	-2.4338	-3.1413	-1.7262	0*
2018-11-27-2018-07-31	-2.9788	-3.6863	-2.2712	0*
2018-12-04-2018-07-31	-2.7588	-3.4663	-2.0512	0*
2018-12-11-2018-07-31	-2.7211	-3.4638	-1.9783	0*
2018-12-18-2018-07-31	-2.82	-3.7463	-1.8937	0*
2018-08-13-2018-08-07	-0.0829	-0.6324	0.46659	1
2018-08-21-2018-08-07	-0.2005	-0.7353	0.33433	0.99994
2018-08-28-2018-08-07	-0.0655	-0.6003	0.46933	1
2018-09-03-2018-08-07	-0.002	-0.5368	0.53283	1
2018-09-11-2018-08-07	-0.048	-0.5828	0.48683	1
2018-09-18-2018-08-07	-0.102	-0.6368	0.43283	1
2018-09-25-2018-08-07	-0.288	-0.8228	0.24683	0.97515
2018-10-02-2018-08-07	-0.484	-1.0188	0.05083	0.1491
2018-10-09-2018-08-07	-1.12	-1.6548	-0.5852	0*
2018-10-18-2018-08-07	-1.3094	-1.9644	-0.6544	0*
2018-10-24-2018-08-07	-1.2309	-1.8657	-0.596	0*
2018-10-31-2018-08-07	-1.7857	-2.353	-1.2184	0*
2018-11-07-2018-08-07	-2.415	-2.9498	-1.8802	0*
2018-11-13-2018-08-07	-2.139	-2.794	-1.484	0*
2018-11-20-2018-08-07	-2.1653	-2.8728	-1.4577	0*
2018-11-27-2018-08-07	-2.7103	-3.4178	-2.0027	0*
2018-12-04-2018-08-07	-2.4903	-3.1978	-1.7827	0*
2018-12-11-2018-08-07	-2.4526	-3.1953	-1.7098	0*
2018-12-18-2018-08-07	-2.5515	-3.4778	-1.6252	0*
2018-08-21-2018-08-13	-0.1176	-0.6671	0.43187	1
2018-08-28-2018-08-13	0.01739	-0.5321	0.56687	1
2018-09-03-2018-08-13	0.08089	-0.4686	0.63037	1
2018-09-11-2018-08-13	0.03489	-0.5146	0.58437	1
2018-09-18-2018-08-13	-0.0191	-0.5686	0.53037	1
2018-09-25-2018-08-13	-0.2051	-0.7546	0.34437	0.99995
2018-10-02-2018-08-13	-0.4011	-0.9506	0.14837	0.59179
2018-10-09-2018-08-13	-1.0371	-1.5866	-0.4876	0*
2018-10-18-2018-08-13	-1.2265	-1.8935	-0.5594	0*
2018-10-24-2018-08-13	-1.148	-1.7953	-0.5007	0*
2018-10-31-2018-08-13	-1.7028	-2.2839	-1.1217	0*

Table A7 (cont.)

Dates	diff	lwr	upr	p adj
2018-11-07-2018-08-13	-2.3321	-2.8816	-1.7826	0*
2018-11-13-2018-08-13	-2.0561	-2.7232	-1.3891	0*
2018-11-20-2018-08-13	-2.0824	-2.801	-1.3637	0*
2018-11-27-2018-08-13	-2.6274	-3.346	-1.9087	0*
2018-12-04-2018-08-13	-2.4074	-3.126	-1.6887	0*
2018-12-11-2018-08-13	-2.3697	-3.123	-1.6163	0*
2018-12-18-2018-08-13	-2.4686	-3.4035	-1.5337	0*
2018-08-28-2018-08-21	0.135	-0.3998	0.66983	1
2018-09-03-2018-08-21	0.1985	-0.3363	0.73333	0.99995
2018-09-11-2018-08-21	0.1525	-0.3823	0.68733	1
2018-09-18-2018-08-21	0.0985	-0.4363	0.63333	1
2018-09-25-2018-08-21	-0.0875	-0.6223	0.44733	1
2018-10-02-2018-08-21	-0.2835	-0.8183	0.25133	0.97978
2018-10-09-2018-08-21	-0.9195	-1.4543	-0.3847	1E-07*
2018-10-18-2018-08-21	-1.1089	-1.7639	-0.4539	2E-07*
2018-10-24-2018-08-21	-1.0304	-1.6652	-0.3955	7E-07*
2018-10-31-2018-08-21	-1.5852	-2.1525	-1.0179	0*
2018-11-07-2018-08-21	-2.2145	-2.7493	-1.6797	0*
2018-11-13-2018-08-21	-1.9385	-2.5935	-1.2835	0*
2018-11-20-2018-08-21	-1.9648	-2.6723	-1.2572	0*
2018-11-27-2018-08-21	-2.5098	-3.2173	-1.8022	0*
2018-12-04-2018-08-21	-2.2898	-2.9973	-1.5822	0*
2018-12-11-2018-08-21	-2.2521	-2.9948	-1.5093	0*
2018-12-18-2018-08-21	-2.351	-3.2773	-1.4247	0*
2018-09-03-2018-08-28	0.0635	-0.4713	0.59833	1
2018-09-11-2018-08-28	0.0175	-0.5173	0.55233	1
2018-09-18-2018-08-28	-0.0365	-0.5713	0.49833	1
2018-09-25-2018-08-28	-0.2225	-0.7573	0.31233	0.99958
2018-10-02-2018-08-28	-0.4185	-0.9533	0.11633	0.43042
2018-10-09-2018-08-28	-1.0545	-1.5893	-0.5197	0*
2018-10-18-2018-08-28	-1.2439	-1.8989	-0.5889	0*
2018-10-24-2018-08-28	-1.1654	-1.8002	-0.5305	0*
2018-10-31-2018-08-28	-1.7202	-2.2875	-1.1529	0*
2018-11-07-2018-08-28	-2.3495	-2.8843	-1.8147	0*
2018-11-13-2018-08-28	-2.0735	-2.7285	-1.4185	0*
2018-11-20-2018-08-28	-2.0998	-2.8073	-1.3922	0*
2018-11-27-2018-08-28	-2.6448	-3.3523	-1.9372	0*
2018-12-04-2018-08-28	-2.4248	-3.1323	-1.7172	0*
2018-12-11-2018-08-28	-2.3871	-3.1298	-1.6443	0*

Table A7 (cont.)

Dates	diff	lwr	upr	p adj
2018-12-18-2018-08-28	-2.486	-3.4123	-1.5597	0*
2018-09-11-2018-09-03	-0.046	-0.5808	0.48883	1
2018-09-18-2018-09-03	-0.1	-0.6348	0.43483	1
2018-09-25-2018-09-03	-0.286	-0.8208	0.24883	0.9773
2018-10-02-2018-09-03	-0.482	-1.0168	0.05283	0.15495
2018-10-09-2018-09-03	-1.118	-1.6528	-0.5832	0*
2018-10-18-2018-09-03	-1.3074	-1.9624	-0.6524	0*
2018-10-24-2018-09-03	-1.2289	-1.8637	-0.594	0*
2018-10-31-2018-09-03	-1.7837	-2.351	-1.2164	0*
2018-11-07-2018-09-03	-2.413	-2.9478	-1.8782	0*
2018-11-13-2018-09-03	-2.137	-2.792	-1.482	0*
2018-11-20-2018-09-03	-2.1633	-2.8708	-1.4557	0*
2018-11-27-2018-09-03	-2.7083	-3.4158	-2.0007	0*
2018-12-04-2018-09-03	-2.4883	-3.1958	-1.7807	0*
2018-12-11-2018-09-03	-2.4506	-3.1933	-1.7078	0*
2018-12-18-2018-09-03	-2.5495	-3.4758	-1.6232	0*
2018-09-18-2018-09-11	-0.054	-0.5888	0.48083	1
2018-09-25-2018-09-11	-0.24	-0.7748	0.29483	0.99838
2018-10-02-2018-09-11	-0.436	-0.9708	0.09883	0.33822
2018-10-09-2018-09-11	-1.072	-1.6068	-0.5372	0*
2018-10-18-2018-09-11	-1.2614	-1.9164	-0.6064	0*
2018-10-24-2018-09-11	-1.1829	-1.8177	-0.548	0*
2018-10-31-2018-09-11	-1.7377	-2.305	-1.1704	0*
2018-11-07-2018-09-11	-2.367	-2.9018	-1.8322	0*
2018-11-13-2018-09-11	-2.091	-2.746	-1.436	0*
2018-11-20-2018-09-11	-2.1173	-2.8248	-1.4097	0*
2018-11-27-2018-09-11	-2.6623	-3.3698	-1.9547	0*
2018-12-04-2018-09-11	-2.4423	-3.1498	-1.7347	0*
2018-12-11-2018-09-11	-2.4046	-3.1473	-1.6618	0*
2018-12-18-2018-09-11	-2.5035	-3.4298	-1.5772	0*
2018-09-25-2018-09-18	-0.186	-0.7208	0.34883	0.99999
2018-10-02-2018-09-18	-0.382	-0.9168	0.15283	0.64024
2018-10-09-2018-09-18	-1.018	-1.5528	-0.4832	0*
2018-10-18-2018-09-18	-1.2074	-1.8624	-0.5524	0*
2018-10-24-2018-09-18	-1.1289	-1.7637	-0.494	0*
2018-10-31-2018-09-18	-1.6837	-2.251	-1.1164	0*
2018-11-07-2018-09-18	-2.313	-2.8478	-1.7782	0*
2018-11-13-2018-09-18	-2.037	-2.692	-1.382	0*
2018-11-20-2018-09-18	-2.0633	-2.7708	-1.3557	0*

Table A7 (cont.)

Dates	diff	lwr	upr	p adj
2018-11-27-2018-09-18	-2.6083	-3.3158	-1.9007	0*
2018-12-04-2018-09-18	-2.3883	-3.0958	-1.6807	0*
2018-12-11-2018-09-18	-2.3506	-3.0933	-1.6078	0*
2018-12-18-2018-09-18	-2.4495	-3.3758	-1.5232	0*
2018-10-02-2018-09-25	-0.196	-0.7308	0.33883	0.99996
2018-10-09-2018-09-25	-0.832	-1.3668	-0.2972	3.2E-06*
2018-10-18-2018-09-25	-1.0214	-1.6764	-0.3664	3E-06*
2018-10-24-2018-09-25	-0.9429	-1.5777	-0.308	1.4E-05*
2018-10-31-2018-09-25	-1.4977	-2.065	-0.9304	0*
2018-11-07-2018-09-25	-2.127	-2.6618	-1.5922	0*
2018-11-13-2018-09-25	-1.851	-2.506	-1.196	0*
2018-11-20-2018-09-25	-1.8773	-2.5848	-1.1697	0*
2018-11-27-2018-09-25	-2.4223	-3.1298	-1.7147	0*
2018-12-04-2018-09-25	-2.2023	-2.9098	-1.4947	0*
2018-12-11-2018-09-25	-2.1646	-2.9073	-1.4218	0*
2018-12-18-2018-09-25	-2.2635	-3.1898	-1.3372	0*
2018-10-09-2018-10-02	-0.636	-1.1708	-0.1012	0.00324*
2018-10-18-2018-10-02	-0.8254	-1.4804	-0.1704	0.00099*
2018-10-24-2018-10-02	-0.7469	-1.3817	-0.112	0.00397*
2018-10-31-2018-10-02	-1.3017	-1.869	-0.7344	0*
2018-11-07-2018-10-02	-1.931	-2.4658	-1.3962	0*
2018-11-13-2018-10-02	-1.655	-2.31	-1	0*
2018-11-20-2018-10-02	-1.6813	-2.3888	-0.9737	0*
2018-11-27-2018-10-02	-2.2263	-2.9338	-1.5187	0*
2018-12-04-2018-10-02	-2.0063	-2.7138	-1.2987	0*
2018-12-11-2018-10-02	-1.9686	-2.7113	-1.2258	0*
2018-12-18-2018-10-02	-2.0675	-2.9938	-1.1412	0*
2018-10-18-2018-10-09	-0.1894	-0.8444	0.46564	1
2018-10-24-2018-10-09	-0.1109	-0.7457	0.52399	1
2018-10-31-2018-10-09	-0.6657	-1.233	-0.0984	0.00417*
2018-11-07-2018-10-09	-1.295	-1.8298	-0.7602	0*
2018-11-13-2018-10-09	-1.019	-1.674	-0.364	3.2E-06*
2018-11-20-2018-10-09	-1.0453	-1.7528	-0.3377	1.6E-05*
2018-11-27-2018-10-09	-1.5903	-2.2978	-0.8827	0*
2018-12-04-2018-10-09	-1.3703	-2.0778	-0.6627	0*
2018-12-11-2018-10-09	-1.3326	-2.0753	-0.5898	0*
2018-12-18-2018-10-09	-1.4315	-2.3578	-0.5052	4E-06*
2018-10-24-2018-10-18	0.0785	-0.6605	0.81747	1
2018-10-31-2018-10-18	-0.4763	-1.1581	0.20547	0.68709

Table A7 (cont.)

Dates	diff	lwr	upr	p adj
2018-11-07-2018-10-18	-1.1056	-1.7606	-0.4506	2E-07*
2018-11-13-2018-10-18	-0.8296	-1.586	-0.0733	0.0134
2018-11-20-2018-10-18	-0.8559	-1.6581	-0.0536	0.02056
2018-11-27-2018-10-18	-1.4009	-2.2031	-0.5986	0*
2018-12-04-2018-10-18	-1.1809	-1.9831	-0.3786	1.8E-05*
2018-12-11-2018-10-18	-1.1432	-1.9767	-0.3097	0.00013*
2018-12-18-2018-10-18	-1.2421	-2.2427	-0.2415	0.00136*
2018-10-31-2018-10-24	-0.5548	-1.2172	0.10762	0.28178
2018-11-07-2018-10-24	-1.1841	-1.819	-0.5493	0*
2018-11-13-2018-10-24	-0.9081	-1.6471	-0.1692	0.00168*
2018-11-20-2018-10-24	-0.9344	-1.7202	-0.1485	0.00325*
2018-11-27-2018-10-24	-1.4794	-2.2652	-0.6935	0*
2018-12-04-2018-10-24	-1.2594	-2.0452	-0.4735	1.2E-06*
2018-12-11-2018-10-24	-1.2217	-2.0394	-0.404	1.2E-05*
2018-12-18-2018-10-24	-1.3206	-2.3081	-0.3331	0.00025*
2018-11-07-2018-10-31	-0.6293	-1.1966	-0.062	0.01115
2018-11-13-2018-10-31	-0.3533	-1.0351	0.32846	0.98511
2018-11-20-2018-10-31	-0.3796	-1.1119	0.35278	0.98509
2018-11-27-2018-10-31	-0.9246	-1.6569	-0.1922	0.00095*
2018-12-04-2018-10-31	-0.7046	-1.4369	0.02778	0.07933
2018-12-11-2018-10-31	-0.6669	-1.4333	0.09953	0.21038
2018-12-18-2018-10-31	-0.7658	-1.7113	0.17963	0.35223
2018-11-13-2018-11-07	0.276	-0.379	0.93103	0.99946
2018-11-20-2018-11-07	0.24975	-0.4578	0.95726	0.99998
2018-11-27-2018-11-07	-0.2953	-1.0028	0.41226	0.99955
2018-12-04-2018-11-07	-0.0753	-0.7828	0.63226	1
2018-12-11-2018-11-07	-0.0376	-0.7803	0.70516	1
2018-12-18-2018-11-07	-0.1365	-1.0628	0.78985	1
2018-11-20-2018-11-13	-0.0263	-0.8285	0.77599	1
2018-11-27-2018-11-13	-0.5713	-1.3735	0.23099	0.64688
2018-12-04-2018-11-13	-0.3513	-1.1535	0.45099	0.99894
2018-12-11-2018-11-13	-0.3136	-1.147	0.51989	0.99994
2018-12-18-2018-11-13	-0.4125	-1.4131	0.58807	0.99964
2018-11-27-2018-11-20	-0.545	-1.3906	0.30063	0.82955
2018-12-04-2018-11-20	-0.325	-1.1706	0.52063	0.99991
2018-12-11-2018-11-20	-0.2873	-1.1626	0.58799	1
2018-12-18-2018-11-20	-0.3863	-1.4219	0.64944	0.99995
2018-12-04-2018-11-27	0.22	-0.6256	1.06563	1
2018-12-11-2018-11-27	0.25768	-0.6176	1.13299	1

Table A7 (cont.)

Dates	diff	lwr	upr	p adj
2018-12-18-2018-11-27	0.15875	-0.8769	1.19444	1
2018-12-11-2018-12-04	0.03768	-0.8376	0.91299	1
2018-12-18-2018-12-04	-0.0613	-1.0969	0.97444	1
2018-12-18-2018-12-11	-0.0989	-1.159	0.96113	1

Table A8: ANOVA results from Tukey's HSD in R comparing mean $\delta^{18}O$ values from site locations in the stream for significance with a α=0.005. (*= significant difference)

Site ID	diff	lwr	upr	p adj
2-1	-0.1987	-1.4943	1.09682	1
3-1	-0.1903	-1.4859	1.10523	1
4-1	0.10169	-1.1827	1.38604	1
5-1	0.09098	-1.2046	1.38654	1
6.1-1	0.69749	-0.6505	2.04553	0.95208
6.2-1	0.69495	-0.6531	2.04299	0.9537
6.3-1	0.66364	-0.67	1.99725	0.96717
7-1	0.15774	-1.116	1.43151	1
8-1	0.43504	-0.8986	1.76865	0.99983
9.1-1	0.39591	-0.9521	1.74395	0.99997
9.2-1	0.58467	-0.7788	1.94817	0.99358
10.1-1	0.06713	-1.2066	1.3409	1
10.2-1	0.3943	-0.9537	1.74234	0.99997
11-1	0.13922	-1.1944	1.47283	1
12.1-1	-0.0714	-1.4194	1.27665	1
12.2-1	0.30724	-1.0408	1.65528	1
13-1	0.08576	-1.188	1.35954	1
14-1	0.25469	-1.0933	1.60273	1
15-1	0.06194	-1.2861	1.40998	1
3-2	0.00842	-1.3086	1.32538	1
4-2	0.30043	-1.0055	1.60637	1
5-2	0.28972	-1.0272	1.60669	1
6.1-2	0.89623	-0.4724	2.26486	0.7107
6.2-2	0.89368	-0.4749	2.26232	0.71544
6.3-2	0.86238	-0.492	2.2168	0.75557
7-2	0.35647	-0.9391	1.65202	0.99999
8-2	0.63378	-0.7206	1.9882	0.98268
9.1-2	0.59464	-0.774	1.96328	0.9925
9.2-2	0.78341	-0.6005	2.16727	0.89465
10.1-2	0.26586	-1.0297	1.56141	1

Table A8 (cont)

Site ID	diff	lwr	upr	p adj
10.2-2	0.59303	-0.7756	1.96166	0.99273
11-2	0.33795	-1.0165	1.69238	1
12.1-2	0.12734	-1.2413	1.49598	1
12.2-2	0.50597	-0.8627	1.87461	0.99903
13-2	0.28449	-1.0111	1.58005	1
14-2	0.45343	-0.9152	1.82206	0.99979
15-2	0.26068	-1.108	1.62931	1
4-3	0.29201	-1.0139	1.59796	1
5-3	0.2813	-1.0357	1.59827	1
6.1-3	0.88781	-0.4808	2.25644	0.72625
6.2-3	0.88527	-0.4834	2.2539	0.73089
6.3-3	0.85396	-0.5005	2.20838	0.77023
7-3	0.34806	-0.9475	1.64361	0.99999
8-3	0.62536	-0.7291	1.97978	0.98503
9.1-3	0.58623	-0.7824	1.95486	0.99366
9.2-3	0.77499	-0.6089	2.15885	0.90354
10.1-3	0.25745	-1.0381	1.553	1
10.2-3	0.58462	-0.784	1.95325	0.99387
11-3	0.32954	-1.0249	1.68396	1
12.1-3	0.11893	-1.2497	1.48756	1
12.2-3	0.49756	-0.8711	1.86619	0.99922
13-3	0.27608	-1.0195	1.57163	1
14-3	0.44501	-0.9236	1.81364	0.99984
15-3	0.25226	-1.1164	1.62089	1
5-4	-0.0107	-1.3167	1.29524	1
6.1-4	0.5958	-0.7622	1.95383	0.9916
6.2-4	0.59326	-0.7648	1.95129	0.992
6.3-4	0.56195	-0.7818	1.90566	0.99525
7-4	0.05605	-1.2283	1.34039	1
8-4	0.33335	-1.0104	1.67706	1
9.1-4	0.29422	-1.0638	1.65225	1
9.2-4	0.48298	-0.8904	1.85636	0.99951
10.1-4	-0.0346	-1.3189	1.24978	1
10.2-4	0.29261	-1.0654	1.65064	1
11-4	0.03753	-1.3062	1.38124	1
12.1-4	-0.1731	-1.5311	1.18495	1
12.2-4	0.20555	-1.1525	1.56358	1
13-4	-0.0159	-1.3003	1.26842	1
14-4	0.153	-1.205	1.51103	1

Table A8 (cont)

Site ID	diff	lwr	upr	p adj
15-4	-0.0397	-1.3978	1.31828	1
6.1-5	0.60651	-0.7621	1.97514	0.99056
6.2-5	0.60396	-0.7647	1.9726	0.99101
6.3-5	0.57266	-0.7818	1.92708	0.99457
7-5	0.06675	-1.2288	1.3623	1
8-5	0.34406	-1.0104	1.69848	1
9.1-5	0.30492	-1.0637	1.67356	1
9.2-5	0.49369	-0.8902	1.87755	0.9994
10.1-5	-0.0239	-1.3194	1.2717	1
10.2-5	0.30331	-1.0653	1.67195	1
11-5	0.04823	-1.3062	1.40266	1
12.1-5	-0.1624	-1.531	1.20626	1
12.2-5	0.21625	-1.1524	1.58489	1
13-5	-0.0052	-1.3008	1.29033	1
14-5	0.16371	-1.2049	1.53234	1
15-5	-0.029	-1.3977	1.33959	1
6.2-6.1	-0.0025	-1.421	1.41587	1
6.3-6.1	-0.0339	-1.4386	1.37086	1
7-6.1	-0.5398	-1.8878	0.80828	0.99723
8-6.1	-0.2625	-1.6672	1.14226	1
9.1-6.1	-0.3016	-1.72	1.11683	1
9.2-6.1	-0.1128	-1.5459	1.3203	1
10.1-6.1	-0.6304	-1.9784	0.71767	0.98281
10.2-6.1	-0.3032	-1.7216	1.11522	1
11-6.1	-0.5583	-1.963	0.84644	0.99748
12.1-6.1	-0.7689	-2.1873	0.64953	0.92685
12.2-6.1	-0.3903	-1.8087	1.02816	0.99999
13-6.1	-0.6117	-1.9598	0.7363	0.98764
14-6.1	-0.4428	-1.8612	0.97561	0.99991
15-6.1	-0.6356	-2.054	0.78287	0.98929
6.3-6.2	-0.0313	-1.436	1.3734	1
7-6.2	-0.5372	-1.8853	0.81083	0.99739
8-6.2	-0.2599	-1.6646	1.1448	1
9.1-6.2	-0.299	-1.7175	1.11938	1
9.2-6.2	-0.1103	-1.5434	1.32284	1
10.1-6.2	-0.6278	-1.9759	0.72022	0.98355
10.2-6.2	-0.3007	-1.7191	1.11776	1
11-6.2	-0.5557	-1.9604	0.84898	0.99763
12.1-6.2	-0.7663	-2.1848	0.65208	0.92895

Table A8 (cont)

Site ID	diff	lwr	upr	p adj
12.2-6.2	-0.3877	-1.8061	1.03071	0.99999
13-6.2	-0.6092	-1.9572	0.73885	0.98821
14-6.2	-0.4403	-1.8587	0.97816	0.99992
15-6.2	-0.633	-2.0514	0.78541	0.98977
7-6.3	-0.5059	-1.8395	0.8277	0.99863
8-6.3	-0.2286	-1.6195	1.16227	1
9.1-6.3	-0.2677	-1.6724	1.13698	1
9.2-6.3	-0.079	-1.4985	1.34058	1
10.1-6.3	-0.5965	-1.9301	0.7371	0.9895
10.2-6.3	-0.2693	-1.6741	1.13537	1
11-6.3	-0.5244	-1.9153	0.86645	0.99873
12.1-6.3	-0.735	-2.1397	0.66968	0.94677
12.2-6.3	-0.3564	-1.7611	1.04831	1
13-6.3	-0.5779	-1.9115	0.75573	0.99273
14-6.3	-0.409	-1.8137	0.99576	0.99997
15-6.3	-0.6017	-2.0064	0.80301	0.99366
8-7	0.27731	-1.0563	1.61092	1
9.1-7	0.23817	-1.1099	1.58621	1
9.2-7	0.42694	-0.9366	1.79043	0.99991
10.1-7	-0.0906	-1.3644	1.18317	1
10.2-7	0.23656	-1.1115	1.5846	1
11-7	-0.0185	-1.3521	1.31509	1
12.1-7	-0.2291	-1.5772	1.11891	1
12.2-7	0.1495	-1.1985	1.49754	1
13-7	-0.072	-1.3458	1.2018	1
14-7	0.09695	-1.2511	1.44499	1
15-7	-0.0958	-1.4438	1.25224	1
9.1-8	-0.0391	-1.4438	1.36558	1
9.2-8	0.14963	-1.2699	1.56918	1
10.1-8	-0.3679	-1.7015	0.9657	0.99999
10.2-8	-0.0407	-1.4455	1.36397	1
11-8	-0.2958	-1.6867	1.09505	1
12.1-8	-0.5064	-1.9111	0.89828	0.99931
12.2-8	-0.1278	-1.5325	1.27691	1
13-8	-0.3493	-1.6829	0.98433	0.99999
14-8	-0.1804	-1.5851	1.22436	1
15-8	-0.3731	-1.7778	1.03161	0.99999
9.2-9.1	0.18877	-1.2444	1.62188	1
10.1-9.1	-0.3288	-1.6768	1.01926	1

Table A8 (cont)

Site ID	diff	lwr	upr	p adj
10.2-9.1	-0.0016	-1.42	1.41681	1
11-9.1	-0.2567	-1.6614	1.14802	1
12.1-9.1	-0.4673	-1.8857	0.95112	0.99981
12.2-9.1	-0.0887	-1.5071	1.32975	1
13-9.1	-0.3101	-1.6582	1.03789	1
14-9.1	-0.1412	-1.5596	1.2772	1
15-9.1	-0.334	-1.7524	1.08445	1
10.1-9.2	-0.5175	-1.881	0.84595	0.99861
10.2-9.2	-0.1904	-1.6235	1.24274	1
11-9.2	-0.4455	-1.865	0.9741	0.99991
12.1-9.2	-0.6561	-2.0892	0.77705	0.98638
12.2-9.2	-0.2774	-1.7105	1.15568	1
13-9.2	-0.4989	-1.8624	0.86458	0.99915
14-9.2	-0.33	-1.7631	1.10313	1
15-9.2	-0.5227	-1.9558	0.91039	0.99919
10.2-10.1	0.32717	-1.0209	1.67521	1
11-10.1	0.07209	-1.2615	1.4057	1
12.1-10.1	-0.1385	-1.4866	1.20952	1
12.2-10.1	0.24011	-1.1079	1.58815	1
13-10.1	0.01863	-1.2551	1.29241	1
14-10.1	0.18756	-1.1605	1.5356	1
15-10.1	-0.0052	-1.3532	1.34285	1
11-10.2	-0.2551	-1.6598	1.14963	1
12.1-10.2	-0.4657	-1.8841	0.95273	0.99982
12.2-10.2	-0.0871	-1.5055	1.33136	1
13-10.2	-0.3085	-1.6566	1.0395	1
14-10.2	-0.1396	-1.558	1.27881	1
15-10.2	-0.3324	-1.7508	1.08606	1
12.1-11	-0.2106	-1.6153	1.1941	1
12.2-11	0.16802	-1.2367	1.57273	1
13-11	-0.0535	-1.3871	1.28015	1
14-11	0.11547	-1.2892	1.52019	1
15-11	-0.0773	-1.482	1.32744	1
12.2-12.1	0.37863	-1.0398	1.79705	0.99999
13-12.1	0.15715	-1.1909	1.50519	1
14-12.1	0.32608	-1.0923	1.7445	1
15-12.1	0.13333	-1.2851	1.55175	1
13-12.2	-0.2215	-1.5695	1.12656	1
14-12.2	-0.0525	-1.471	1.36587	1

Table A8 (cont)

Site ID	diff	lwr	upr	p adj
15-12.2	-0.2453	-1.6637	1.17312	1
14-13	0.16893	-1.1791	1.51697	1
15-13	-0.0238	-1.3719	1.32422	1
15-14	-0.1927	-1.6112	1.22567	1
15-14	-0.1927	-1.6112	1.22567	1

APPENDIX 6: ANOMALOUS DATA REMOVED FROM OVERALL ANALYSES

Table A9: Stream Isotope values for $\delta^{18}O$ and $\delta^{2}H$ that were removed from the overall analysis process given in $^{0}/_{00}$. The values showed lighter than normal signatures and were all run during the same time on the machine. The table is followed by figures created with the data.

Date	Site ID	$\delta^{18}O$	$\delta^{2}H$	Type	Geology	D-excess
10/18/2018	3	-13.475	-92.489	stream	Till plain	15.3133
10/18/2018	7	-14.104	-95.328	stream	Ice Contact	17.5012
10/18/2018	9.1	-13.694	-92.115	stream	SDC	17.4353
10/18/2018	10.1	-13.784	-92.276	stream	SDC	17.9993
10/18/2018	10.2	-13.668	-91.517	stream	SDC	17.8246
10/18/2018	11	-13.545	-93.221	stream	SDC	15.1399
10/18/2018	12.1	-13.662	-93.873	stream	SDC	15.4196
10/18/2018	12.2	-13.777	-94.644	stream	SDC	15.5748
10/18/2018	13	-12.935	-90.402	stream	SDC	13.081
10/18/2018	15	-13.876	-92.807	stream	SDC	18.1969
10/24/2018	1	-13.437	-92.958	stream	Igneous	14.5358
10/24/2018	2	-13.445	-92.767	stream	Till plain	14.7908
10/24/2018	6.1	-13.932	-94.373	stream	Undifferentiated	17.0786
10/24/2018	6.2	-13.906	-94.009	stream	Undifferentiated	17.2369
10/24/2018	6.3	-13.579	-93.053	stream	Undifferentiated	15.5808
10/24/2018	9.1	-13.583	-91.65	stream	SDC	17.0151
10/24/2018	12.1	-13.614	-93.951	stream	SDC	14.9583
10/24/2018	12.2	-13.674	-94.104	stream	SDC	15.2868
10/24/2018	15	-13.756	-92.584	stream	SDC	17.4682
10/31/2018	2	-13.816	-95.788	stream	Till plain	14.7404
10/31/2018	3	-13.692	-95.129	stream	Till plain	14.4033
10/31/2018	13	-13.029	-92.646	stream	Outwash	11.5838
10/31/2018	15	-14.605	-99.934	stream	SDC	16.905

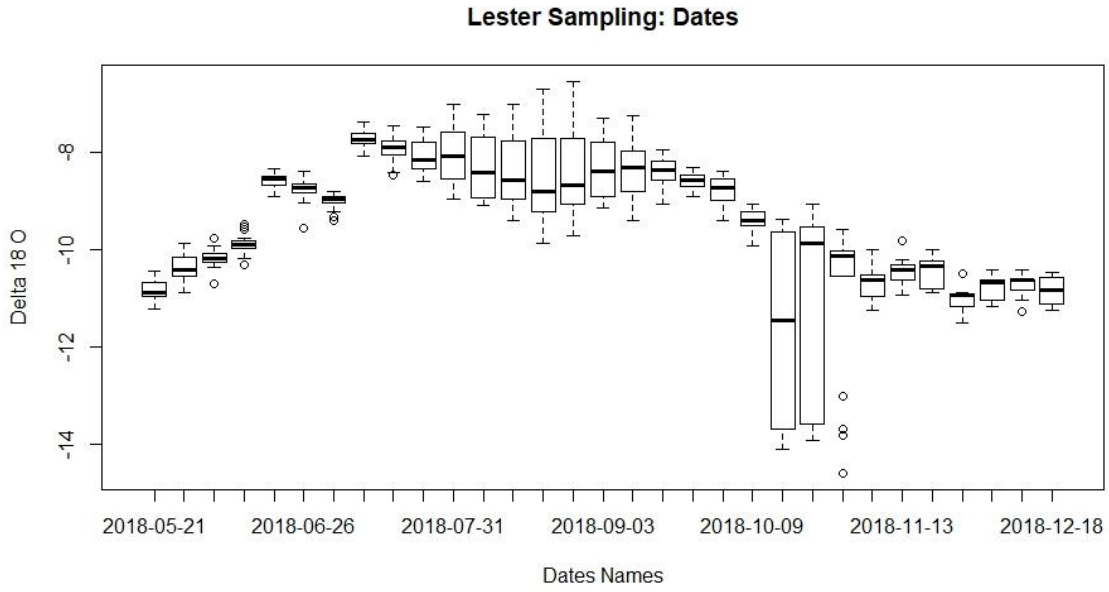
Lester Sampling: Dates
Delta 18 O
-8
-10
-12
-14
2018-05-21
2018-06-26
2018-07-31
2018-09-03
2018-10-09
2018-11-13
2018-12-18
Dates Names

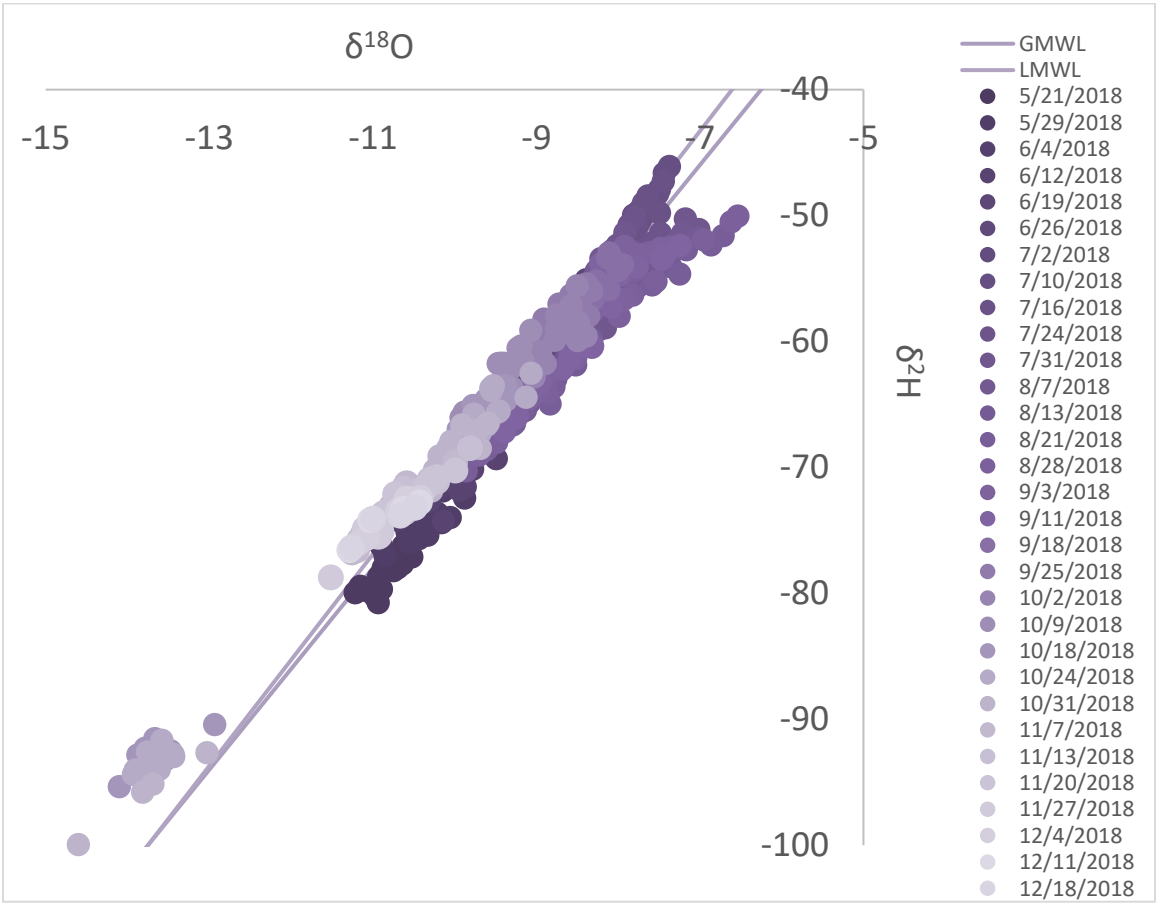
δ18O
-15
-13
-11
-9
-7
-5
δ2H
-40
-50
-60
-70
-80
-90
-100
GMWL
LMWL
5/21/2018
5/29/2018
6/4/2018
6/12/2018
6/19/2018
6/26/2018
7/2/2018
7/10/2018
7/16/2018
7/24/2018
7/31/2018
8/7/2018
8/13/2018
8/21/2018
8/28/2018
9/3/2018
9/11/2018
9/18/2018
9/25/2018
10/2/2018
10/9/2018
10/18/2018
10/24/2018
10/31/2018
11/7/2018
11/13/2018
11/20/2018
11/27/2018
12/4/2018
12/11/2018
12/18/2018

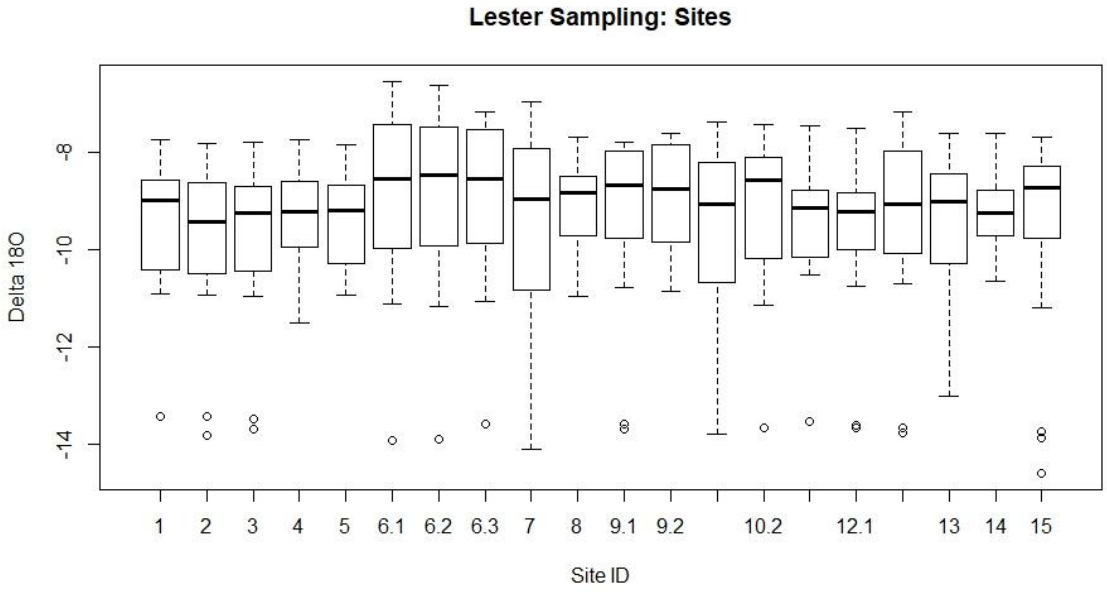
Lester Sampling: Sites
Delta 18O
-8
-10
-12
-14
1
2
3
4
5
6.1
6.2
6.3
7
8
9.1
9.2
10.2
12.1
13
14
15
Site ID

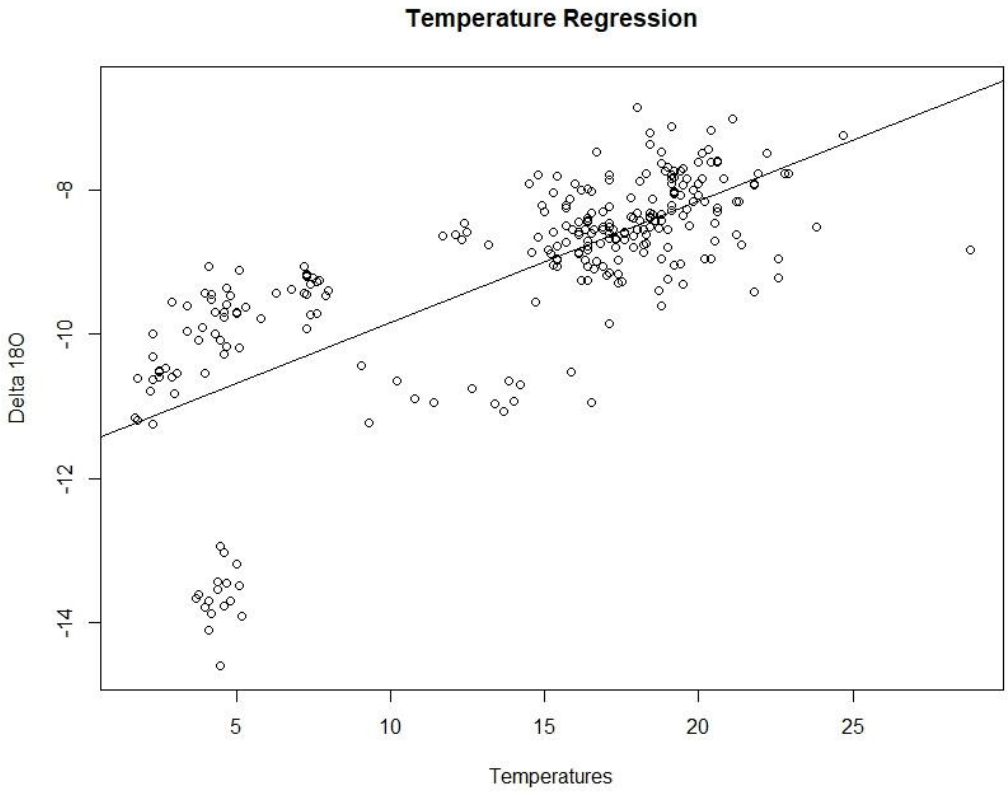
Temperature Regression
Delta 18O
-8
-10
-12
-14
5
10
15
20
25
Temperatures